MODELING OF PLASMA REMEDIATION OF NO_X USING GLOBAL KINETIC MODELS ACCOUNTING FOR HYDROCARBONS

BY

RAJESH DORAI

B.S., Indian Institute Of Technology, Madras, 1998

THESIS

Submitted in partial fulfillment of the requirements
for the degree of Master of Science in Chemical Engineering
in the Graduate College of the
University of Illinois at Urbana-Champaign, 2000

Urbana, Illinois

(RED BORDERED SIGNATURE PAGE HERE)

MODELING OF PLASMA REMEDIATION OF NO_X USING GLOBAL KINETIC MODELS ACCOUNTING FOR HYDROCARBONS

Rajesh Dorai
Department of Chemical Engineering
University of Illinois at Urbana-Champaign, 1999
M. J. Kushner, Advisor

Increasing awareness of pollution and its harmful effects has led to the development of energy efficient methods for remediation. In this study, we have numerically quantified the feasibility of Dielectric Barrier Discharges (DBD) for the remediation of NO_x. Reaction mechanisms for the hydrocarbon (propane and propene) and NO_x system were formulated for diesel exhausts. Parameterizations were performed to determine the optimum operating conditions for NO_x removal.

Remediation of NO_x for automotive emissions should ideally produce N_2 and O_2 through reduction reactions. Most of the NO in DBDs is oxidized to NO_2. In the presence of hydrocarbons, propene and propane, this conversion is increased. Some extra remediation of NO_x is also observed with hydrocarbons through the formation of organic nitrates and nitrites. Increased energy deposition through the application of higher applied voltages, resulted in improved NO_x remediation. Multiple pulse formats have been found to produce different end products. New reactions occur in latter pulses due to the reaction products from previous pulses. Simulation of multiple discharge formats yielded better agreement of the final product concentrations with the experimental data.

ACKNOWLEDGEMENTS

It is with great pleasure and pride that I wish to record my thanks to my advisor, Prof. Mark J. Kushner for his constant and motivating guidance throughout the course of this work. I am indeed indebted to him for his inspiring and timely ideas and discussions without which this work would not have been a success. My interest and appreciation for the subject of plasma sciences has added a new dimension to itself after this project. The zest and zeal with which I worked for completing this project was the result of his enthusiastic support, encouragement and unstinted cooperation.

I am grateful to Mr. John Hoard, Mr. Tim Wallington and Mr. Richard Bretz from Ford Research Laboratories for their invaluable guidance. I am also thankful to them for providing us experimental data for comparison purposes.

I am also thankful to my fellow members in the Computational Optical and Discharge Physics group, Ron Kinder, Dr. Trudy van der Straaten, Da Zhang, Junqing Lu, Kelly Collier, Dan Cronin, Pramod Subramonium and Arvind Sankaran. Special thanks are due to Dr. Xudong "Peter" Xu, Brian Lay and Dan Cronin for their constructive criticisms and timely help on various occasions.

I am most indebted to my parents, Sri. Dorai Krishnamurthy and Smt. Subhalakshmi Dorai for their constant support, love and encouragement throughout the course of my education. Many thanks are also due to my uncles and aunts for their constant motivation and guidance throughout my life. I would also take this opportunity to thank my brother, D. Mahesh and my cousins for all those happy moments that they have afforded me. Finally, this note would go incomplete if I were not to mention that all this would not have been possible without the blessings of my grandmothers and my late grandfathers.

TABLE OF CONTENTS

1. INTRODUCTION

The continual release of toxic gases into the atmosphere from a variety of sources has resulted in the gradual degradation of the environment and this, in turn, has motivated investigations into new methods of reducing and, if possible, preventing these harmful emissions. Increasing awareness of these emissions has resulted in legislation requiring stringent enforcement of new regulations having the goal of improving the quality of environment.

Since 1970, Environment Protection Agency (EPA) has tracked emissions of six major air pollutants – CO, lead, nitrogen oxides (NO_x), particulate matter, sulfur dioxide and volatile organic compounds[1]. Emissions of these pollutants have significantly decreased except for NO_x which has increased approximately 10% over this period. Reducing emissions of NO_x is therefore critical for improving the quality of air in urban regions. Sources of NO_x are shown in Fig. 1.1 and include non-utility boilers, reciprocating internal combustion engines, gas turbines, residential fuel combustion, cement manufacturing industries, ferrous metal processing, wood, pulp and paper manufacturing and agricultural chemical manufacturing industries. NO_x in air is one of the main constituents in the formation of ground-level ozone, which can cause respiratory problems. NO_x also reacts to form nitrate particles, acid aerosols, as well as NO_2, which also cause respiratory problems. NO_x also contributes to the formation of acid rain. Apart from being a greenhouse gas, NO_x also acts as a precursor for the formation of atmospheric particles that cause reduced visibility. NO_x also contributes to nutrient overload that deteriorates water quality.

These economic and health implications have motivated research into abatement techniques for NO_x pollution. One of the methods which are being developed for the control of NO_x is plasma processing. Plasma remediation of toxic gases is a major area of research both in industry and in academia. Plasma remediation of nitrogen oxides (NO and NO_2), in particular, has been the object of many studies in the past decade [2-8].

Non-thermal plasma remediation of NO_x is a highly efficient method in that the operation of the reactor is such that the input energy mostly goes into heating the electrons as opposed to increasing the gas temperature. The remediation technique is also feasible for operating a reactor at atmospheric pressure. Several types of reactors are used for the non-thermal plasma processing, including electron beam (e-beam) or electrical discharges.

In e-beam processing [2-3], electrons are accelerated down a high voltage gradient in vacuum before being injected through a thin foil window that serves as a vacuum seal. The high-energy electrons then collide with neutrals in an atmospheric-pressure chamber producing ions and radicals that trigger the process chemistry. Electrical discharge reactors are typically pulsed corona discharges and dielectric barrier discharges. Pulsed corona discharge reactors, shown schematically in Fig. 1.2, employ short pulses (10s-100s of ns) of high voltage (up to 30 kV) with kilohertz repetition rates, thereby creating short-lived discharges which produce the radicals responsible for the decomposition of the undesired molecules. The reactor consists of a point to plane or wire coaxial electrode configuration. These reactors are characterized by low gas temperatures (300 K) and high electron temperatures (3-6 eV). Several studies have been performed to evaluate these reactors for the plasma remediation of pollutant gases. [3-7].

Dielectric barrier discharge reactors (DBD's), shown schematically in Fig. 1.3, consist of planar electrodes or concentric cylindrical tubes with either one or both of the electrodes being covered with dielectric layers, separating them from the gas. DBDs are known for their high-energy efficiency, reliability, and, more importantly, their low cost [8]. DBDs also have the added advantage of operating at high pressure (atmospheric and above) resulting in higher reaction rates and larger reactor throughputs.

Many studies have been performed to analyze the importance of reactor design, choice of packing material, voltage, frequency and gas composition on the removal of NO_x from automotive exhausts [9-10]. The results indicate that voltage and frequency do not affect the overall energy efficiency in certain ranges of operation. However, gas composition and choice of packing material have been found to significantly change the process outputs. The possibility of using downstream or an upstream catalytic converters with plasma remediation has been investigated. The results indicate that with the plasma reactor upstream of the catalytic converter, more NO_x conversion was achieved [11-12]. Computer modeling and simulation of the plasma remediation of toxic gases have been extensively performed and all studies point towards the positive role played by plasma process [13-16].

The present study applies a global kinetics model to the study of the plasma remediation of NO_x with the goal of quantifying the effects of hydrocarbons in the gas stream. Hydrocarbons are unavoidably present in the emissions and have been found to play an important role in the reaction pathways [12,15,16]. With the improvement in the knowledge base for the underlying reactions that are responsible for the NO_x chemistry, simulations have been able to more closely predict the actual process outputs and thus have been very much useful in process design. Comparisons have been made to available experimental data wherever applicable. Several hydrocarbon species have been investigated to determine their role in the NO_x remediation process. The global kinetics model is described in Chapter 2. The effects of energy deposition and initial gas temperature have been parameterized. The effect of varying the hydrocarbon concentration in the inlet gas stream on the remediation of NO_x is discussed in Chapter 3. The results of the simulations with the inclusion of propane in the system are discussed in Chapter 4. Multiple pulsing of the plasma has been found to yield significantly different results which are discussed in Chapter 5. The list of species considered in simulations is included in Appendix A and their corresponding reactions are in Appendix B.

In general, it was found that with increasing energy deposition into the system, NO_x remediation improved but the energy efficiency decreased. Increasing the amount of hydrocarbons in the inlet stream significantly affected the NO decomposition but the NO_x conversion remained almost unaffected. Variation of the temperature of the reactor resulted in an initial improvement in NO_x reduction but for temperatures greater than 400 K, the NO_x conversion remained at an almost constant level. Comparison to experimental data has been performed wherever possible and the overall results indicate good agreement between modeling and experiments.

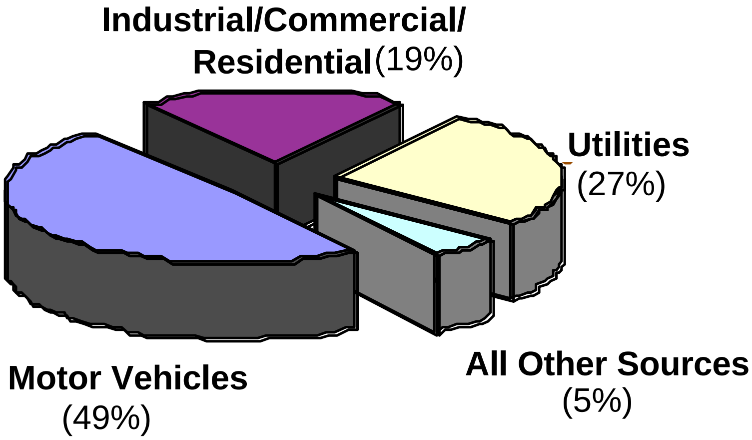

Fig 1.1 : Sources of NO_x emissions [1]

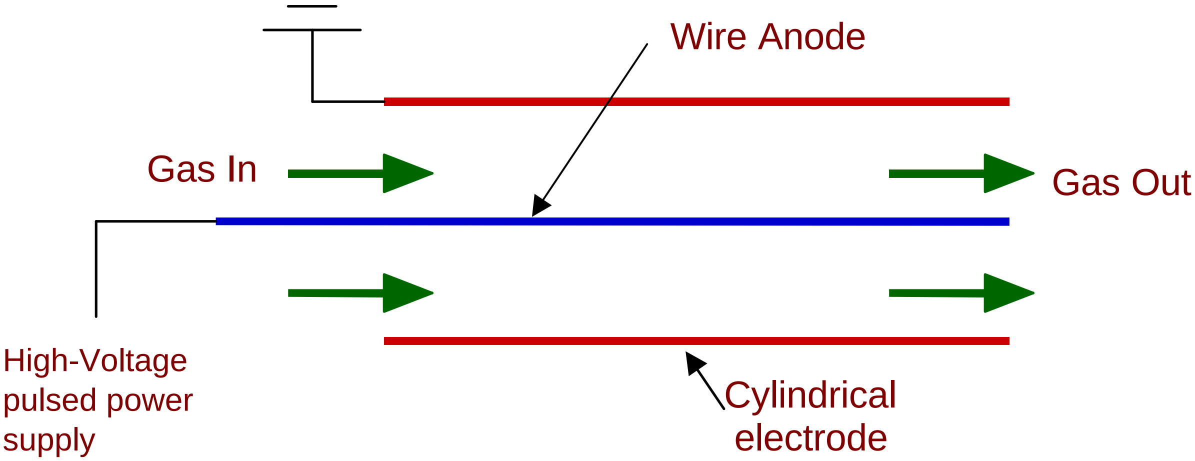

Fig 1.2 : Schematic of the pulsed corona discharge reactor.

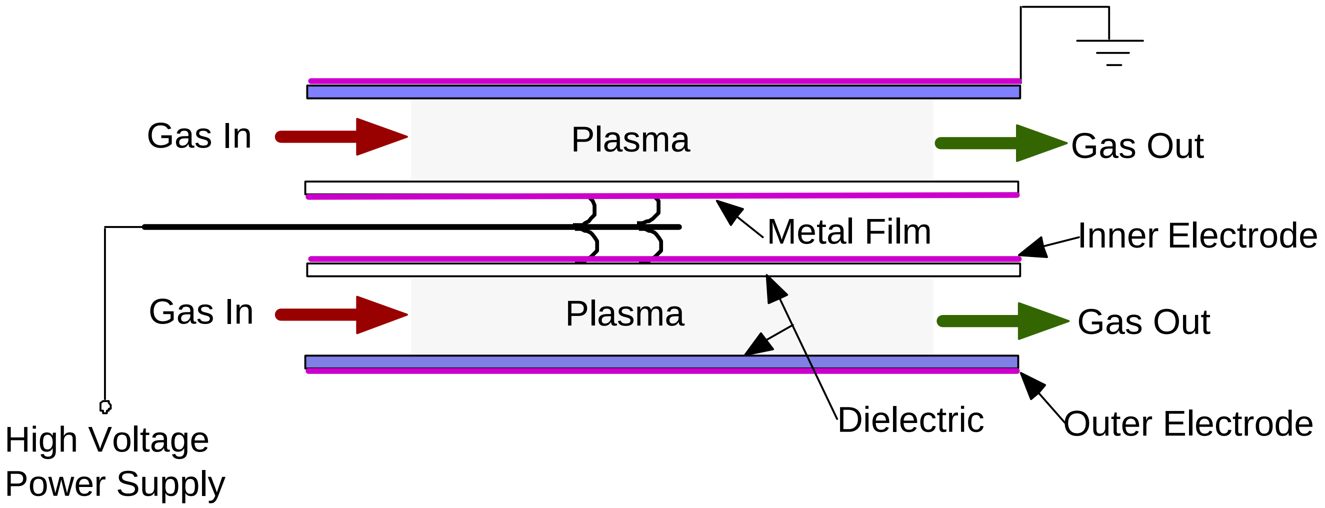

Fig. 1.3. Schematic of a typical Dielectric Barrier Discharge reactor

1.1 References

1. United States Environmental Protection Agency, “NO_x – How nitrogen oxides affect the way we live and breathe”, EPA-456/F-98-005, September 1998.
2. Frank, N.W., et al. (1986), “Integrated SO_x and NO_x removal process”, Integrated Environmental Control Symposium, Pittsburgh, Pa.
3. Fuch, P., et al. (1987), “Removal of SO_2 and NO_x by electron beam process”, presented at the 6th International Meeting on Radiation Processing, Ontario, Canada.
4. S.Masuda and H.Nakao, “Control of NO_x by positive and negative pulsed corona discharges,” IEEE Trans. Ind. Applicat., vol. 26, pp. 374-383, Mar./Apr. 1990.
5. R.H. Amirov, E.I.Asinovsky, I.S.Samoilov, and A.V. Shepelin, “Experimental studies on NO removal from methane combustion products using nanosecond corona discharge,” in Non-Thermal Plasma Techniques for Pollution Control, Part B, B. M. Penetrante and S.E.Schultheis, Eds. Berlin, Germany: Springer-Verlag, 1993, pp.149-164.
6. A.Mizuno, K.Shimizu,K, A.Chakrabarti, L.Dascalescu, and S.Furuta, “NO_x removal process using pulsed discharge plasma,” IEEE Trans. Ind. Applicat., vol. 31, pp. 957-964, Sept./Oct, 1995.
7. Y.S.Mok and S.W.Ham, “Conversion of NO to NO_2 in air by a pulsed corona discharge process,” Chem. Eng. Sci., vol. 53, no. 9, pp. 1667-1678, 1998.
8. Eliasson, B. and Kogelschatz, U. (1991), “Non-equilibrium volume plasma chemical processing,” IEEE Transactions on Plasma Science **19**, 1065-1077.
9. McLarnon,C.R., and Penetrante, B.M., “Effect of Reactor Design on the Plasma Treatment of NO_x”, SAE Paper 982434 (1998).

10. McLarnon, C.R., and Penetrante, B.M., "Effect of Gas Composition on the NO_x Conversion Chemistry in a Plasma", SAE Paper 982433 (1998).
11. Hoard, J.W., and Balmer, M.L., "Analysis of Plasma Catalysis for Diesel NO_x Remediatoin", SAE Paper 982429 (1998).
12. Penetrante, B.M., Brusasco, R.M., Merritt, B.T., Pitz, W.J., Vogtlin, G.E., Kung, M.C., Kung, H.H., Wan, C.,Z., and Voss, K.E., "Plasma-Assisted Catalytic Reduction of NO_x", SAE Paper 982508 (1998).
13. Braun, D., Gibalov, V., and Pietsch, G., "Two-dimensional modeling of the dielectric barrier discharge in air." Plasma Sources Science and Technology, **1,** (1963-0252), 166-174 (1992).
14. Gentile, A.C., and Kushner, M.J., "Microstreamer dynamics during plasma remediation of NO using atmospheric pressure dielectric barrier discharges", J. Appl. Phys., **79**(8) (1996).
15. Niessen, W., Wolf, O., Schruft, R., and Neiger, M., "The influence of ethene on the conversion of NO_x in a dielectric barrier discharge", J. Phys. D:Appl. Phys. **31**, 542-550 (1998).
16. "Non-Thermal Plasma for Exhaust Emission Control", *Proceedings of the 1999 SAE International Fall Fuels and Lubricants Meeting*, Toronto, Ontario, Canada.

2. DESCRIPTION OF THE MODEL

2.1 Overview

The model used to study the volumetric plasma kinetics of NO_x plasma remediation is a zero-dimensional, plug flow simulation where the spatial variations are not considered and the reactor is assumed to be completely mixed and homogenous. The generalized representation of the reaction mechanism is discussed in Section 2.2. Descriptions of the 0-D model, called GLOBAL_KIN, used to investigate NO_x chemistry in propene and propane mixtures are in Section 2.3.

2.2 Reaction Network Equations

When dealing with a large number of reactions, it is beneficial to have a generalized reaction network equation that represents all the reactions. The generalized reaction network equation can be written as

$$\frac{dN_i}{dt} = \sum_{j=1}^{R} a_{ji} k_j \prod_{l=1}^{S} \left(N_l \right)^{b_{jl}} ,$$

where,

$\frac{dN_i}{dt}$	represents the rate of change of species density N_i with respect to time,
N_i	represents the number density of species i at any given time t,
j	spans reactions in the network,
l	spans the species in the system,
k_j	is the reaction rate coefficient of reaction j,
R	is the total number of reactions occurring in the system

S	is the total number of species participating in the reactions
$b_{jl} = 1$	if species l appears on the L.H.S of reaction j
$= 0$	otherwise
$a_{jl} = 0$	if species l does not appear on the L.H.S of reaction j,
$= -1$	if species l appears on the L.H.S of reaction j,
$= +1$	if species l appears on the R.H.S of reaction j.

2.3 Description of the Zero-Dimensional Model

GLOBAL_KIN consists of an offline Boltzmann solver module for the electron energy distribution, a circuit module and a plasma chemistry module. A schematic of the modules used in GLOBAL_KIN is in Fig. 2.1 and that for the device modeled is in Fig. 2.2.

In the 0-D model, a uniform concentration of species is assumed in the reactor. Since the quantities of interest, temperature, species densities, electric field/number density (E/N) in the plasma, are continually changing in the system with time, the rate equations representing these quantities have to be constantly updated. The plasma chemistry module performs the operations of setting up the differential equations for the time evolution of the various species in the reactor at different points in time. The circuit module provides the E/N in the plasma which is further used to obtain the rate coefficients of electron impact reactions based on the electron temperature. In order to do this, an offline lookup table is initially generated using the Boltzmann solver module for the representative gas composition and temperature. The entire set of differential equations for species densities along with the circuit equations are integrated over time to obtain the temporal evolution of the species present in the reactor. This integration in time is accomplished by using the LSODE/ODE solver [1]. The time steps chosen for integration are such that they are much less compared to the dynamics of the system in that time period and are allowed to vary with time. The magnitudes of the initial time steps for recording results are chosen to be of the order of ns in order to capture the rapid dynamics of the system in the initial phase. With time, the time-step at which results are recorded is increased by a fixed multiplication factor.

For validation purposes, the initial conditions for the reactor were chosen to closely match those for the experiments conducted at Ford Research Laboratories [2]. The following procedure was adopted in choosing reactions for the simulation. First, all the reactions of species initially present in the reactor with the products of the electron impact reactions are considered. Of these, only those reactions that occur at appreciable rates at the conditions of operation are considered. Then, all the appreciable reactions of the products of these reactions with all other species present in the system are considered and this process is repeated until the products along every given pathway are found to be stable. For the study of NO_x processing in the absence of hydrocarbons, 76 electron impact reactions and 360 heavy particle reactions are considered. With propene included, the total number of reactions was 752 with the electron impact reactions remaining the same. Including propane in the model added another 54 heavy particle reactions. The reaction mechanism is given in Appendix B.

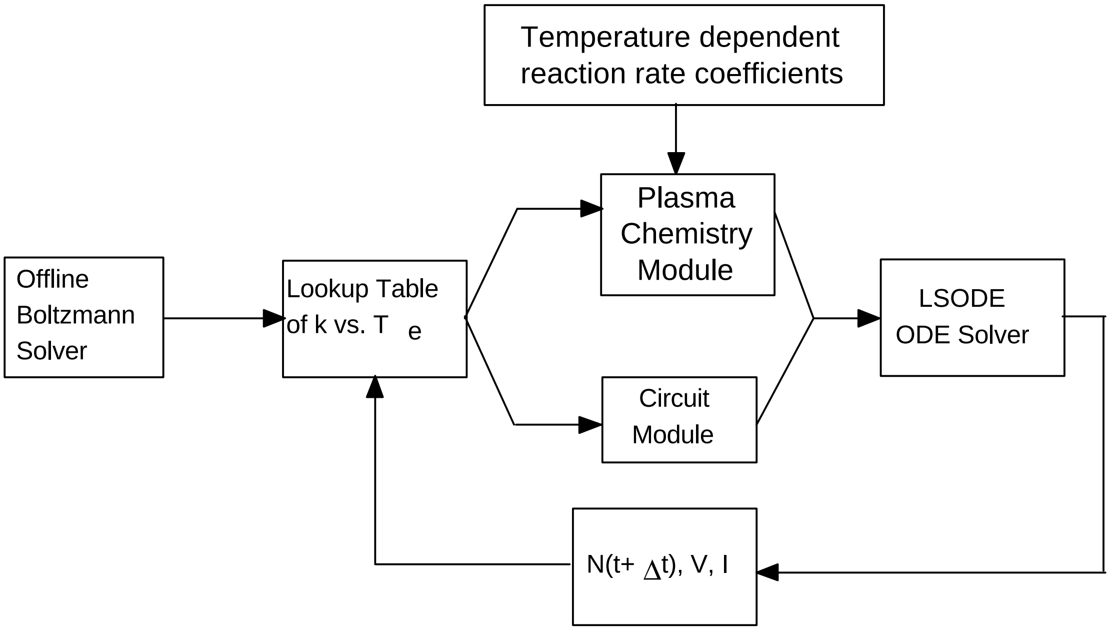

Fig 2.1 Block diagram of the model

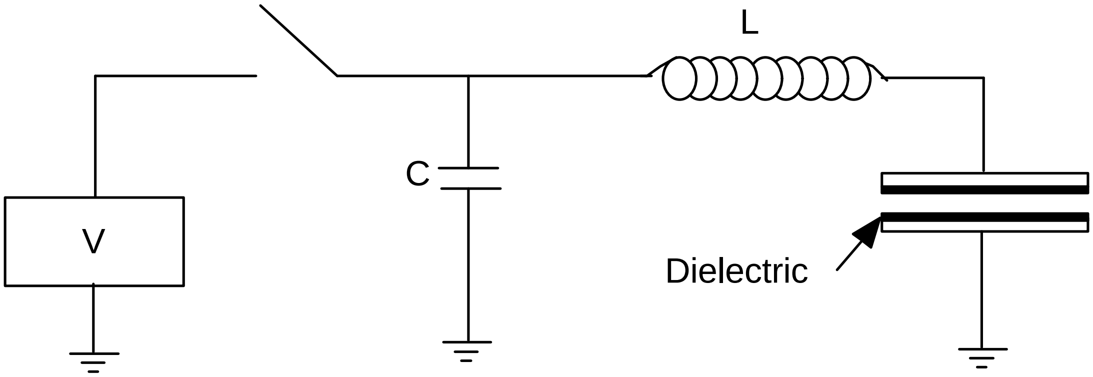

Fig. 2.2 Schematic of the DBD modeled

2.4 References

1. A.C. Hindmarsh, “Livermore Solver for Ordinary Differential Equations”, Lawrence Livermore Laboratories, 1987.
2. John Hoard, “Plasma Aftertreatment Program Data”, Ford Motor Company.

3. EFFECT OF PROPENE ON THE CONVERSION OF NO_x

3.1 Overview

Most of the previous studies of NO_x remediation were performed with gas mixtures predominantly containing N_2, O_2, NO and one or more of NO_2 and H_2O. In real exhausts, hydrocarbons are inevitably part of the emissions. The effect of ethene on the conversion of NO_x in a dielectric barrier discharge reactor has been modeled by Niessen *et. al*. and the results indicate a significant role played by hydrocarbons in the overall reaction chemistry [1]. Their findings showed that the energy requirement for NO remediation reduced from 60 eV/NO molecule to 10 eV/molecule when 2000 ppmv of C_2H_4 (ethene) was added to the inlet gas. However, most of the NO that was converted went into forming NO_2. Hence, it is important to consider the effect of hydrocarbons on the plasma remediation of NO_x. In this chapter, results from GLOBAL_KIN with and without the inclusion of propene as a model hydrocarbon will be discussed. The reaction mechanisms for NO_x in the absence of hydrocarbon are discussed in Section 3.2 and the effects of energy deposition are described in Section 3.3. The reaction mechanisms for NO_x in the presence of propene are discussed in Section 3.4. The results of the parameterizations of energy density, inlet hydrocarbon concentration and reaction temperature are discussed in Section 3.5, Section 3.6 and Section 3.7 respectively. The conclusions are given in Section 3.8.

3.2 Reaction Mechanisms in NO_x Remediation in the Absence of C_3H_6

It is beneficial to study NO_x processing in the absence of hydrocarbons to provide a base-case for comparison. Hence, simulations were initially performed with gas mixtures containing N_2, NO, H_2O, O_2, CO and CO_2 (See Table 3.1). In the absence of propene, the reaction mechanism for NO_x remediation is given in Fig. 3.1. The initial compounds and major end products are in bold. The reactor is operated at atmospheric pressure and at a temperature of 453 K (180 ^{o}C). The gas gap is 2.5 mm unless otherwise indicated. All the results presented in this chapter are for a single discharge pulse. In order to validate model against experimental data, simulations were performed with the initial conditions of the experiments conducted at Ford Research Laboratories. It is known that, for the typical operating conditions of dielectric barrier discharge reactors, radical reactions dominate over ionic reactions for remediation. However, the ion reactions have been included for completeness. During the initial current pulse period [0-100 ns], electron impact reactions produce radicals. Important electron impact reactions include,

$$e + O_2 \rightarrow O + O + e \qquad [\ 3.1\ ]$$

$$e + N_2 \rightarrow N + N + e \qquad [\ 3.2\ ]$$

$$e + H_2O \rightarrow OH + H + e \qquad [\ 3.3\ ]$$

As regards NO, there are two main pathways for effective removal,

$$NO + N \rightarrow N_2 + O, \qquad k = 3.41\times10^{-11}\exp\left(-\frac{24}{T}\right)cm^3\,s^{-1} \qquad [\ 3.4\ ]$$

$$NO + O + M \rightarrow NO_2 + M, \qquad k = 1.03\times10^{-30}\left(\frac{T}{300}\right)^{-2.87}\exp\left(-\frac{781}{T}\right)cm^6\,s^{-1} \qquad [\ 3.5a\ ]$$

$$NO_2 + OH + M \rightarrow HNO_3 + M, \qquad k = 4.62\times10^{-29}\left(\frac{T}{300}\right)^{-5.49}\exp\left(-\frac{1183}{T}\right)cm^6\,s^{-1} \qquad [\ 3.5b\ ]$$

Reaction 3.4 is a reduction and 3.5(a) and 3.5(b) are oxidation channels. Though reaction 3.4 is the most preferred of the three with respect to plasma remediation of automotive emissions, it is the one that occurs with the lowest probability because the concentration of O atoms are at least an order of magnitude higher than N atoms. This is because the bond energy in O_2 is smaller to that in N_2. O_2 has a double bond and N_2 has a triple bond, which is stronger. For example, the concentrations of O and N atoms in a typical DBD are shown in Fig. 3.2. The concentrations of O atoms are at least an order of magnitude greater in comparison with N atoms at the conditions of interest. Hence reaction 3.5(a) occurs with a higher rate as compared to reaction 3.4. Reaction 3.5(b) cannot be avoided since OH radicals are produced due to electron impact dissociation of H_2O. Depending on the nature of the NO_x source, different channels may be preferred for plasma remediation. For stationary sources such as coal-fired power plants, production of HNO_3 could be an acceptable option, since the effluent can then be treated with base solutions to produce salts and water which then can be easily removed. For mobile sources, Reaction 3.4 is more favorable as the harmful gas is converted into pure N_2. The products of the reduction reaction would result in the generation of ozone (O_3) through the reaction with O_2.

$$\mathrm{O + O_2 + M \rightarrow O_3 + M}, \qquad k = 6.90\times10^{-34}\left(\frac{T}{300}\right)^{-1.25} cm^3 s^{-1} \qquad [\ 3.6\ ]$$

Ozone by itself participates in the NO remediation through the reaction,

$$\mathrm{O_3 + NO \rightarrow NO_2 + O_2}, \qquad k = 4.3\times10^{-12}\exp\left(-\frac{1598}{T}\right) cm^3 s^{-1} \qquad [\ 3.7\ ]$$

Since NO_x includes NO and NO_2, conversion of NO to NO_2 does not result in its remediation. Hence, NO_2 is also an unwanted byproduct of this processing.

The time evolution of electrons, ions and certain radicals are shown for a typical current pulse in Fig. 3.3. Electron densities peak at around 100 ns wherein the circuit is switched off. Near around the point where the electron densities peak, one also sees a rise in the concentration of the radicals, O and OH in the system. These radicals then react with other species in the system to initiate the plasma chemistry.

3.3 Effect of Input Energy Density on the Remediation of NO_x in the Absence of C_3H_6

The energy input to the system is typically varied by the voltage applied to the DBD reactor. The variation in the NO, NO_2 and NO_x levels after 0.2 seconds is shown in Fig. 3.4 for a single discharge pulse in the absence of propene for various input energies. At the highest energy deposition (60 J/L), only about 20 ppm of NO_x is removed while 130 ppm of NO is remediated. The remaining NO removed is mostly converted into NO_2. Acids such as HNO_2 and HNO_3 are also produced, though in smaller quantities (≈15 ppm) compared to NO_2 or NO_x. In the absence of propene, about 10% of NO_x is remediated at 60 J/L whereas the NO conversion is around 50%. As will be discussed in later chapters, the effect of multiple discharges pulse could significantly alter the product distribution by changing the composition of the gas during the inter pulse-period. The presence of CO_2 in the system, through e-impact dissociation, produces CO.

$$e + CO_2 \rightarrow CO + O^- \qquad [\ 3.8\ ]$$

$$e + CO_2 \rightarrow CO + O + e \qquad [\ 3.9\ ]$$

The production levels of CO as a function of energy input are shown in Fig. 3.5. In the absence of propene, as much as 60 ppm of CO is produced with the maximum energy input of 60 J/L.

The energy efficiency of the process is measured in terms of W-values [eV/molecule NO_x remediated]. Higher W-values indicate lesser efficient processes. The W-values for the NO_x remediation in the absence of propene are shown in Fig. 3.6. At lower values of energy deposition, the W-value for NO_x is 520 eV/molecule and for NO is 80 eV/molecule. Although higher energy deposition results in increased NO_x remediation, the processes become less efficient. At high energy inputs [60 J/L], W-values are as high as 770 eV/molecule NO_x and 190 eV/molecule NO.

3.4 Reaction Mechanisms for NO_x in the Presence of Propene

In presence of a hydrocarbon (propene), the reaction mechanism has additional pathways as shown in Fig. 3.7. The channel that has a major influence on NO remediation is initiated by the reaction of propene with OH. OH is dominantly produced either by electron impact of H_2O or by the reaction of $O(^1D)$ with H_2O.

$$O(^1D) + H_2O \rightarrow OH + OH \qquad k = 2.2\times10^{-10}\ cm^3\ s^{-1} \qquad [\ 3.10\ ]$$

The reaction of OH with propene results in the formation of *b*-hydroxyalkyl radicals (CH_3CHCH_2OH, $CH_3CH(OH)CH_2$) which then react rapidly with O_2 to form the *b*-hydroxylalkyl peroxy radicals ($CH_3CH(OO)CH_2OH$, $CH_3CH(OH)CH_2OO$). The peroxy radicals are the major reactants as they react with NO to form NO_2. The resulting alkoxy radicals ($CH_3CH(O)CH_2OH$, $CH_3CH(OH)CH_2O$) can then undergo reaction with O_2, decompose or isomerize. It has been experimentally observed that decomposition of alkoxy radicals is the dominant process of the three channels [2,3]. The decomposition of alkoxy radicals results in the production of α-hydroxyl alkyl radicals and aldehydes namely, formaldehyde (HCHO) and acetaldehyde (CH_3CHO). The *a*-hydroxy alkyl radicals react with O_2 to again produce aldehydes and HO_2 radical. Propene is also subject to attack by $O(^3P)$. Products of this reaction include methyl oxirane, propionaldehyde (C_2H_5CHO), ethyl radical (C_2H_5) , methyl (CH_3) and vinoxy (CH_2CHO) radical. Inclusion of these species initiate other reactions such as,

$$CH_3 + O_2 + M \rightarrow CH_3O_2 + M, \qquad k = 7.56\times10^{-31}\left(\frac{T}{300}\right)^{-3.64} cm^6\ s^{-1} \qquad [\ 3.11\ ]$$

$$CH_2CHO + O_2 \rightarrow CHO\text{-}CHO + OH \qquad k = 2.2\times10^{-13}\ cm^3\ s^{-1} \qquad [\ 3.12\ ]$$

$$CH2CHO + O2 \rightarrow HCHO + CO + OH \qquad k = 3.0\times10^{-14}\ cm^3\ s^{-1} \qquad [\ 3.13\ ]$$

3.5 Effect of Varying Input Energy Density on the Conversion of NO_x in the Presence of Propene

The effect of input energy in the presence of propene was investigated. The same gas composition given in Table 3.1 was used with 500 ppm of propene. Species densities after 0.2 s as a function of input energy are shown in Fig. 3.8(a) and the results indicate a significant change in the final NO_x conversion. NO conversion is almost 100% at higher energy inputs [60 J/L]. However, a major portion of the converted NO goes into forming NO_2 thereby limiting the total NO_x conversion. As much as 60 ppm of NO_x is remediated at an energy input of 60 J/L. The removed NO_x is mainly converted to nitrous acid (HNO_2), nitric acid (HNO_3) and 2-nitroso ethanal ($ONCH_2CHO$) and to some smaller extent, nitrogen. The final NO and NO_x conversions with and without propene are summarized in Fig. 3.8(b). NO_x remediation is nearly tripled [6.4% to 18.6%] with propene as compared to the case with no propene at an energy deposition of 30 J/L. There is a larger difference in the NO conversion levels. At 60 J/L, NO conversion is 99.6% with propene as compared to 50% without propene, primarily due to the reaction of NO with the peroxy radical to form NO_2. The efficiency of the remediation process is shown in terms of W-values in Fig. 3.9. The W-value for NO_x remediation decreases from 770 eV/molecule NO_x without propene to 325 eV/molecule NO_x with propene, and for NO remediation, the reduction is from 190 eV/molecule NO to 90 eV/molecule.

The time integrated contributions from each of the reactions for the production and consumption of NO are shown in Fig. 3.10. NO is mainly remediated through the reactions,

$$NO + HO_2 \rightarrow NO_2 + OH \qquad k = 3.7\times10^{-12}\exp\left(\frac{240}{T}\right)cm^3s^{-1} \qquad [\ 3.14\ ]$$

$$CH_3CH(OH)CH_2OO + NO \rightarrow CH_3CH(OH)CH_2O + NO_2 \qquad [\ 3.15\ ]$$

$$k_{3.15} = 2.7\times10^{-12}\exp\left(+\frac{360}{T}\right)cm^3s^{-1} \qquad [\ 3.15a\ ]$$

$$CH_3CH(OO)CH_2OH + NO \rightarrow CH_3CH(O)CH_2OH + NO_2 \qquad [\ 3.16\ ]$$

$$k_{3.16} = 2.7\times10^{-12}\exp\left(+\frac{360}{T}\right)cm^3s^{-1} \qquad [\ 3.16a\ ]$$

The inclusion of propene increases the generation of CO. This is expected since CO is the end product of many hydrocarbon induced reactions such as,

$$HCO + O_2 \rightarrow CO + HO_2, \qquad k = 8.5\times10^{-11}\exp\left(-\frac{850}{T}\right)cm^3s^{-1} \qquad [\ 3.17\ ]$$

$$CH_2CHO + O_2 \rightarrow HCHO + CO + OH, \qquad k=3.0\times10^{-14}\ cm^3\ s^{-1} \qquad [\ 3.18\ ]$$

The individual contributions of the major CO producing and consuming reactions are shown in Fig. 3.11. The majority of CO is produced by reactions 3.9 and 3.17.

The end product concentrations as a function of input energy density are shown in Fig. 3.12. The density of formaldehyde [HCHO] saturates at higher energy inputs (> 40

J/L). In the initial stages of the process [0-200 ns], HCHO is primarily produced by the reaction of O atoms with methyl (CH_3) and ethyl radicals (C_2H_5).

$$CH_3 + O \rightarrow HCHO + H, \quad k = 1.4\times10^{-10}\ cm^3\ s^{-1} \quad [\ 3.19\ ]$$

$$C_2H_5 + O \rightarrow HCHO + CH_3, \quad k = 2.67\times10^{-10}\ cm^3\ s^{-1} \quad [\ 3.20\ ]$$

The production of radicals such as CH_3O and CH_2CHO induce new channels for the formation of HCHO.

$$CH_3O + O \rightarrow HCHO + OH, \quad k = 1.0\times10^{-11}\left(\frac{T}{300}\right)^{0.5} cm^3 s^{-1} \quad [\ 3.21\ ]$$

$$CH_3O + O_2 \rightarrow HCHO + HO_2, \quad k = 1.1\times10^{-13}\exp\left(-\frac{1310}{T}\right) cm^3 s^{-1} \quad [\ 3.22\ ]$$

$$CH_3O + OH \rightarrow HCHO + H_2O, \quad k = 3.0\times10^{-11}\left(\frac{T}{300}\right)^{0.5} cm^3 s^{-1} \quad [\ 3.23\ ]$$

$$CH_3O + CH_3O \rightarrow CH_3OH + HCHO, \quad k = 1.0\times10^{-10}\left(\frac{T}{300}\right)^{0.5} cm^3 s^{-1} \quad [\ 3.24\ ]$$

$$CH_3O + NO \rightarrow HCHO + HNO, \quad k = 4.0\times10^{-12}\left(\frac{\mathrm{T}}{300}\right)^{-0.7} cm^3 s^{-1} \quad [\ 3.25\ ]$$

$$CH_2CHO + O_2 \rightarrow HCHO + CO + OH, \quad k = 3.0\times10^{-14}\ cm^3 s^{-1} \quad [\ 3.26\ ]$$

With the formation of CH_2OH and $CH_3CH(OH)CH_2O$, new pathways for the production of HCHO are introduced.

$$CH_2OH + O_2 \rightarrow HCHO + HO_2, \quad k = 1.06\times10^{-10}\left(\frac{T}{300}\right)^{-1.58}\exp\left(-\frac{801.2}{T}\right) cm^3 s^{-1} \quad [\ 3.27\ ]$$

$$CH_3CH(OH)CH_2O \rightarrow CH_3CHOH + HCHO, \quad k = 7.94\times10^{13}\exp\left(-\frac{10520}{T}\right) s^{-1} \quad [\ 3.28\ ]$$

The main pathway for the consumption of HCHO is the reaction of HCHO with OH.

$$\text{HCHO + OH} \rightarrow \text{HCO + H2O}, \quad k = 4.74\times10^{-12}\left(\frac{T}{300}\right)^{1.18}\exp\left(\frac{225}{T}\right)cm^3s^{-1} \quad [\ 3.29]$$

HCHO removal also occurs by the reaction of HCHO with O.

$$\text{HCHO + O} \rightarrow \text{HCO + OH}, \quad k = 2.99\times10^{-11}\exp\left(-\frac{1543}{T}\right)cm^3s^{-1} \quad [\ 3.30\ ]$$

This reaction accounts for about 12% of the overall consumption of HCHO, whereas the reaction with OH contributes to around 87% of the total removal. The contributions from the various reactions towards the production and consumption of HCHO are shown in Fig. 3.13.

With increasing energy deposition, more OH and HO_2 are produced. The reaction of NO with HO_2 accounts for a major portion of the NO remediated.

$$NO + HO_2 \rightarrow NO_2 + OH \quad [\ 3.31\ ]$$

Hence, as more energy is deposited, the amount of NO available for reaction with the peroxy radicals decreases and so, CH_2OH, $CH_3CH(OH)CH_2O$ and CH_3CHO, which are the products of the peroxy-initiated reactions, are generated in smaller quantities.

$$CH_3CH(OH)CH_2OO + NO \rightarrow CH_3CH(OH)CH_2O + NO_2 \quad [\ 3.15\ ]$$

$$CH_3CH(O)CH_2OH + M \rightarrow CH_2OH + CH_3CHO + M, \quad k_{3.32} = 1.0\times10^{-11}\ cm^3s^{-1} \quad [\ 3.32\ ]$$

Hence, one sees a reduction in the production level of acetaldehyde in the system. However, the same is not the case with HCHO, since the channels for the formation of HCHO are more numerous compared to CH_3CHO. With increasing energy deposition, the reactions of O radicals with the first generation products (CH_3, CH_3O) are accelerated due to the increased production of these radicals. This increase in the formation of HCHO keeps the final production almost a constant at higher energy inputs in spite of the decrease in its formation from CH_2OH. As a result one sees a saturation in the production of HCHO. With increase in energy deposition, more HCHO is produced by channels B, C, D and F. However, the contributions from the major reactions channels, E and G, decrease with increasing energy deposition, this decrease being more than the increase due to the channels B, C, D and F.

3.6 Effect of Varying Inlet Hydrocarbon Concentration on the Conversion of NO_x

One of the key factors that determine the NO conversion to NO_2 is the quantity of the peroxy radical. This is in turn dependent on the amount of propene. Simulations were performed with the same base gas composition shown in Table 3.2 and the base case operating conditions while varying the propene concentration with the input energy fixed at 18.7 J/L.

The variation in NO, NO_2, NO_x, HNO_2, HNO_3 concentrations following 0.2 seconds as a function of inlet propene concentration are shown in Fig. 3.14(a). Increasing the inlet hydrocarbon has little effect on the NO_x conversion though the effects on NO conversion and NO_2 production are noticeable. Increasing the inlet hydrocarbon results in increased production of the peroxy radicals which then convert more NO to NO_2 while keeping the NO_x unchanged. Increasing the inlet hydrocarbon also produces more rapid reactions of O and OH with the hydrocarbons as compared to the reactions with other competing species. Therefore, the availability of the radicals for reactions with non-hydrocarbon species becomes more limited. This is shown in the concentrations of HNO_2 and HNO_3 that result from the reaction of OH with NO_x. The decrease in concentration of acids is due to the depletion of OH. The fractional remediation of NO_x

and conversion of C_3H_6 are shown in Fig. 3.14(b) as a function of inlet C_3H_6. The radicals that are involved in the initial reactions with propene are produced in fixed amounts with fixed energy deposition and hence these are the rate-limiting species. Therefore, higher concentrations of propene in feed result in lower percentages of conversion. NO remediation increases due to the increased production of peroxy radicals. CO production almost remains the same. CO is produced mainly by the electron impact dissociation of CO_2 and by the reactions with hydrocarbons [Reactions 3.9 and 3.13].

Although the hydrocarbons are present in higher quantities, the rate limiting reactions are constrained by the radicals. The end-product concentrations as a function of inlet hydrocarbon concentration are shown in Fig. 3.15. As anticipated, increases in the inlet hydrocarbon results in increased production of the final products. Major end products include acetaldehyde (CH_3CHO), methyl oxirane and formaldehyde. Acetaldehyde and methyl oxirane are produced mainly by,

$$C_3H_6 + O \rightarrow \text{Methyl Oxirane} \qquad [\ 3.33\ ]$$

$$CH_3CHOH + O2 \rightarrow CH_3CHO + HO_2 \qquad [\ 3.34\ ]$$

W-values are shown as a function of inlet propene concentration in Fig. 3.16. With more propene in the inlet, the efficiency of the process decreases since more NO is converted to NO_2 by the hydrocarbon. However, the efficiency for NO remediation increases. At 1100 ppm of propene, the W-value for NO_x is 240 eV/molecule and that for NO is 30 eV/molecule.

3.7 Effect of Reactor Temperature on the Conversion of NO_x in the Presence of Propene

The gas temperature has an important effect on the reaction characteristics through the Arrhenius dependence of reaction rate coefficients.

$$k = A\left(\frac{T}{300}\right)^{n}\exp\left(-\frac{E_a}{T}\right) \qquad [3.35]$$

where,

k = reaction rate constant,

A = frequency factor,

T = temperature of the gas,

E_a = activation energy in K.

Simulations were performed to quantify the effect of temperature on NO_x remediation. All the results discussed in this section are for the inlet gas mixture in Table. 3.1 with 500 ppm of propene and an energy deposition of 30.9 J/L. Product concentrations are shown in Fig 3.17 as a function of initial temperature. Increasing temperature has little effect on total NO_x conversion, although the effect on NO and NO_2 is quite significant. This is because the rate coefficients for the reaction of the peroxy radicals with NO increases with temperature. Therefore, at higher temperatures more NO gets converted into NO_2. The maxima in the concentrations of HNO_2 and HNO_3 are a result of the inherent complex non-linear kinetics associated with the temperature dependence of the reaction rate coefficients. The main reactions responsible for the production of HNO_2 are,

$$\text{NO} + \text{OH} + \text{M} \rightarrow \text{HNO}_2 + \text{M}, \quad k = 7.4\times10^{-31}\left(\frac{T}{300}\right)^{-2.4} cm^3 s^{-1} \qquad [\ 3.36]$$

$$HO_2 + NO_2 \rightarrow HNO_2 + O_2, \qquad k = 1.2\times10^{-13}\left(\frac{T}{300}\right)^{0.5} cm^3 s^{-1} \qquad [\,3.37]$$

Consumption of HNO_2 mainly occurs by the reaction with OH,

$$OH + HNO_2 \rightarrow NO_2 + H_2O, \qquad k = 1.8\times10^{-11}\exp\left(-\frac{390}{T}\right) cm^3 s^{-1} \qquad [\,3.38\,]$$

On the whole, increasing temperature reduces the production of HNO_2 and HNO_3. The conversion levels of NO, propene and NO_x are shown in Fig. 3.18. At higher temperatures, a larger proportion of propene is converted due to the overall positive temperature dependence of the propene-initiated reactions.

$$C_3H_6 + OH \rightarrow Products, \qquad k = 4.86\times10^{-12}\left(\frac{T}{300}\right)^{0.5}\exp\left(+\frac{504}{T}\right) cm^3 s^{-1} \qquad [\,3.39\,]$$

$$C_3H_6 + O \rightarrow Products, \qquad k = 1.25\times10^{-12}\left(\frac{T}{300}\right)^{2.15}\exp\left(+\frac{400}{T}\right) cm^3 s^{-1} \qquad [\,3.40]$$

Of the two reactions 3.39 and 3.40, $k_{3.39}$ decreases with increasing temperature and $k_{3.40}$ increases with increasing temperature. Also, at the temperatures of interest, $k_{3.40} > k_{3.39}$. Since the concentration of O radicals is greater than [OH], the rate of reaction 3.40 is greater than the rate of the reaction 3.39. Hence, with an increase in temperature, there is an increased consumption of propene. Increasing amounts of CO are also produced, again due to the increased production of the radicals at higher temperatures.

$$CH_2CHO + O_2 \rightarrow HCHO + CO + OH, \qquad k = 3.0\times10^{-14}\left(\frac{T}{300}\right)^{0.5} cm^3 s^{-1} \qquad [\,3.41\,]$$

NO conversion increases at higher temperatures due to the increased production of the peroxies, though the NO converted mostly goes into forming NO_2, keeping the level of NO_x unaltered. The effect of temperature on the concentration of end products is summarized in Fig. 3.19. In general, more aldehydes are produced. The increased rate of the initiator reaction with propene by O increases the production of oxirane and $ONCH_2CHO$. In general, higher temperatures result in the formation of a conducive environment for the breakdown of NO, but this breakdown unfortunately results in the production of NO_2 rather than in the conversion to N_2, nitric or nitrous acids.

3.8 Concluding Remarks

Hydrocarbons play a significant role in modifying the overall reaction chemistry of NO_x. There is a significant change in NO_x conversion when including the effects of hydrocarbons. Increasing energy deposition with gas mixtures containing hydrocarbons showed increased conversion levels of NO_x. Typical products with propene include formaldehyde, acetaldehyde, propionaldehye, methyl oxirane, glyoxal and CO. Increasing the hydrocarbon concentration resulted in decreased conversion levels of hydrocarbons for the same input energy density. However, NO_x conversion remained the same when the inlet propene concentration was varied. With increasing reactor temperatures, NO_x conversion remained at an almost constant level. However, NO conversion and NO_2 production levels increased with increase in temperature. End products generally showed an increase in concentration with increasing reactor temperature.

Species	Inlet Concentration
O_2	8%
CO_2	7%
H_2O	6%
CO	400 ppm
NO	260 ppm
H_2	133 ppm
N_2	Balance

Table 3.1 Inlet concentration of species for the DBD reactor

Species	Inlet Concentration
O_2	8%
CO_2	7%
H_2O	6%
CO	400 ppm
NO	260 ppm
H_2	133 ppm
C_3H_6	0-1100 ppm
N_2	Balance

Table 3.2 Inlet concentration of species for the DBD reactor with hydrocarbons added

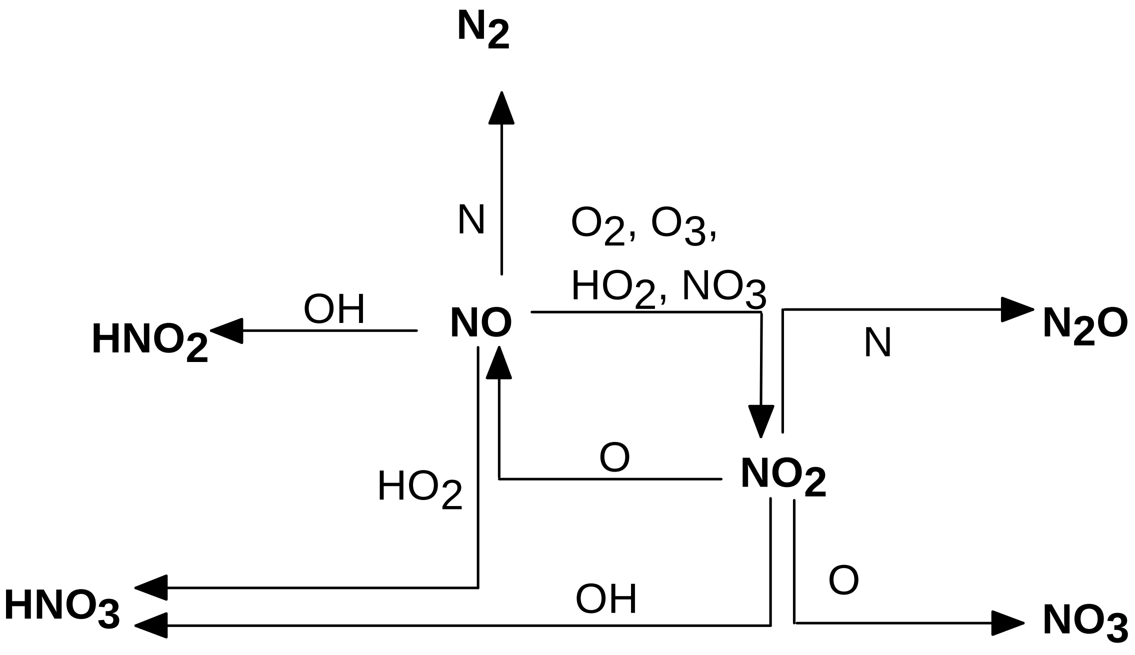

Fig. 3.1 Simplified reaction mechanism for NO_x in the absence of propene

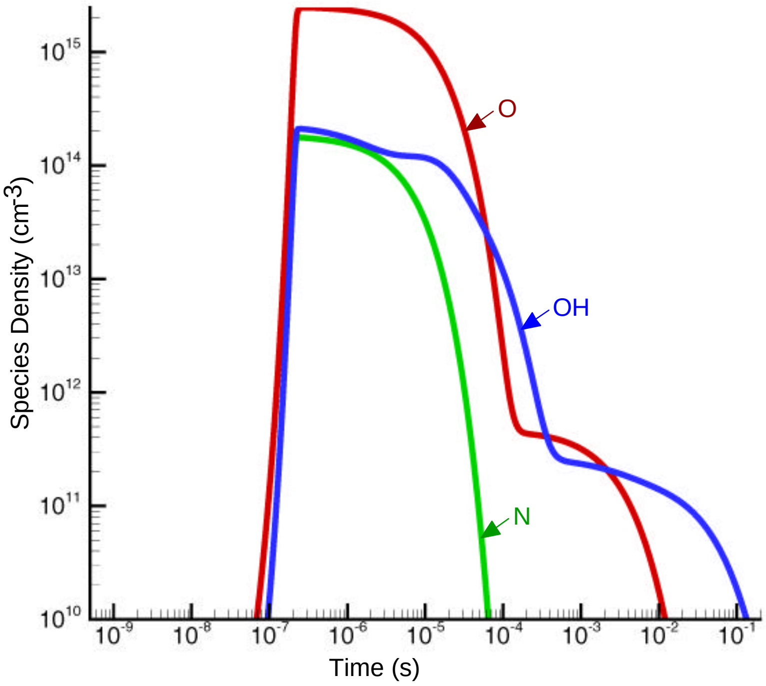

Fig. 3.2 Time evolution of O, OH and N during the DBD processing of NO_x

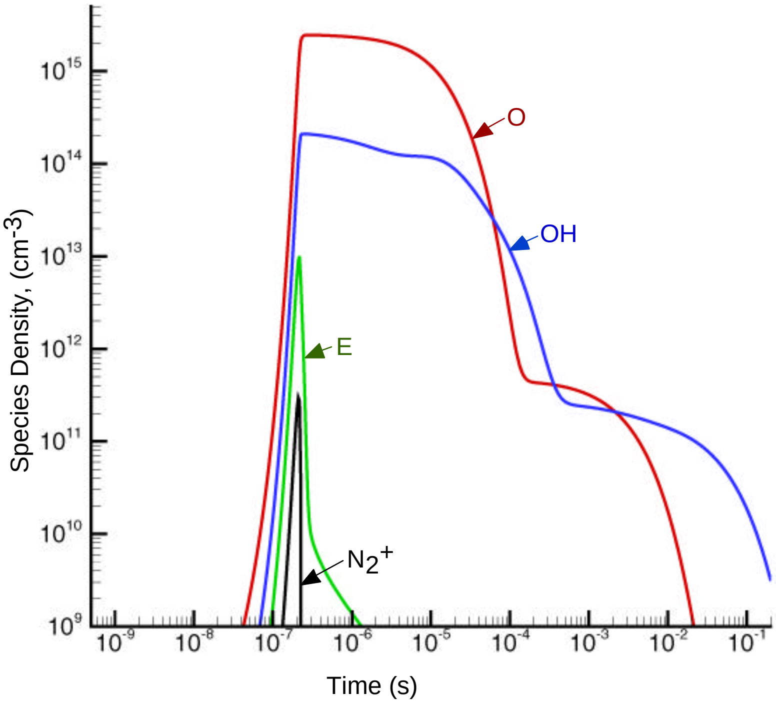

Fig. 3.3 Time evolution of e, N_2^+, O and OH radicals during the DBD processing of NO_x

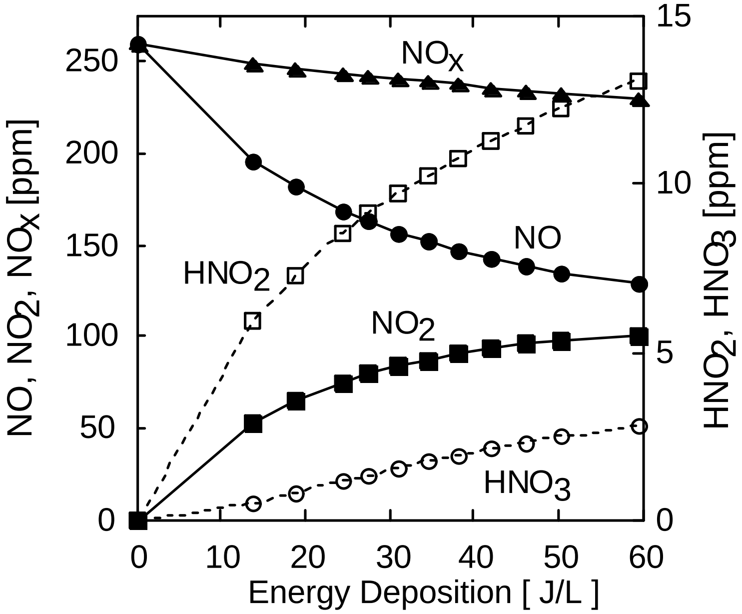

Fig. 3.4 NO, NO_2, NO_x, HNO_3, HNO_2 as a function of input energy density follwing 0.2 seconds

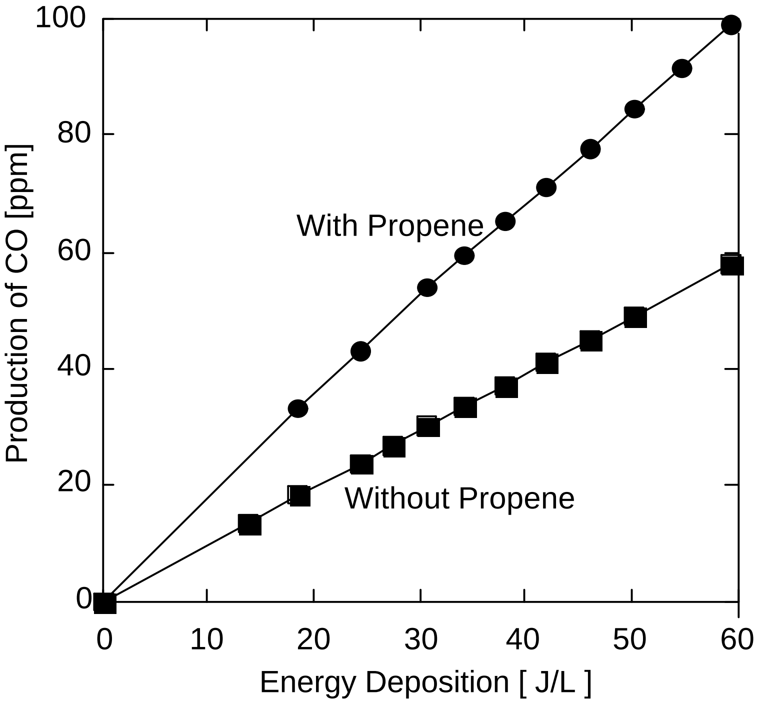

Fig. 3.5 CO production with and without propene as a function of input energy.

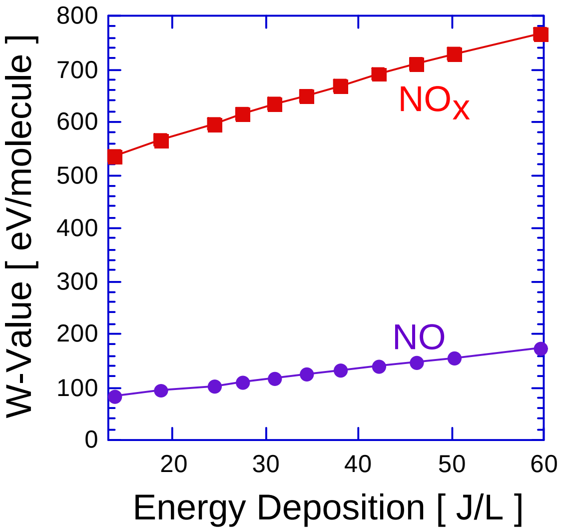

Fig. 3.6 W-Values for NO_x and NO removal in the absence of propene as a function of input energy density

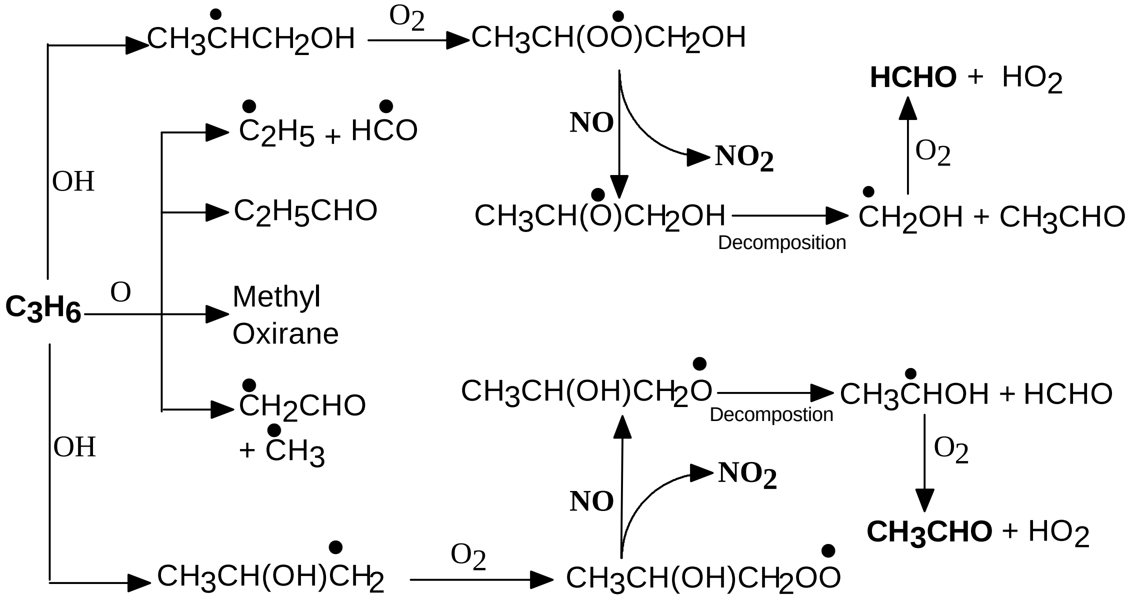

Fig. 3.7 Reaction mechanisms for NO_x in the presence of propene

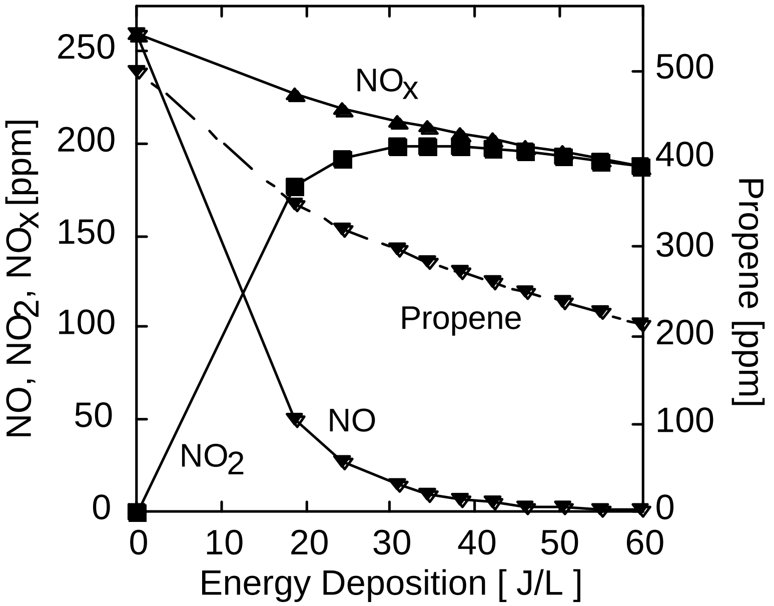

Fig. 3.8(a) Effect of varying energy deposition on NO, NO_2, NO_x and propene in the plasma processing of NO_x

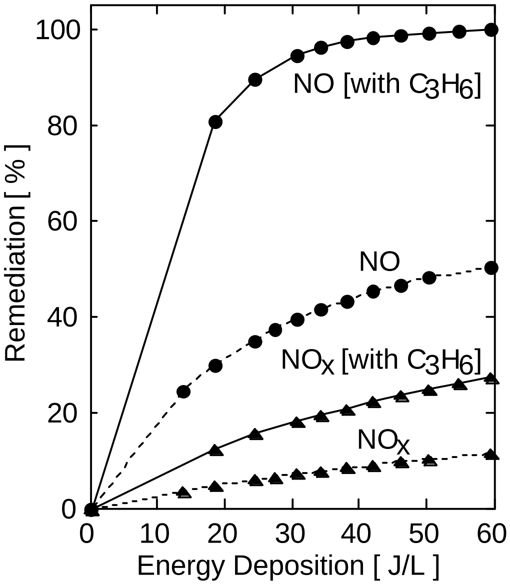

Fig.3.8(b) Comparison of NO and NO_x conversion levels with and without the introduction of propene in the inlet gas stream.

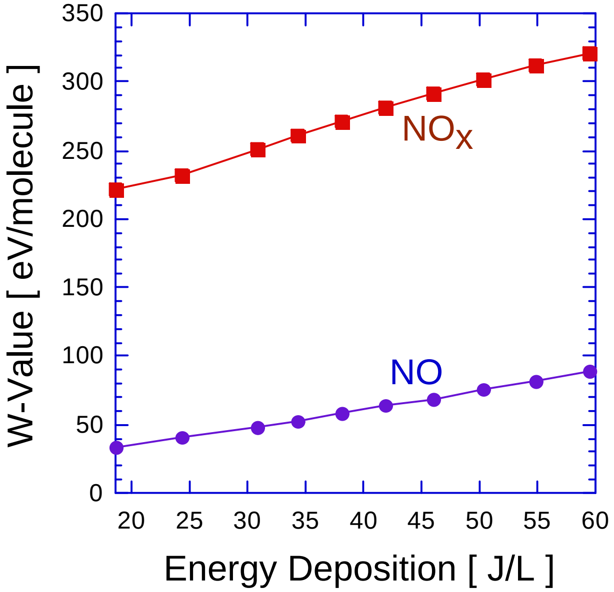

Fig. 3.9 Variation of W-Values for NO_x and NO as a function of input energy for the plasma remediation of NO_x in the presence of propene

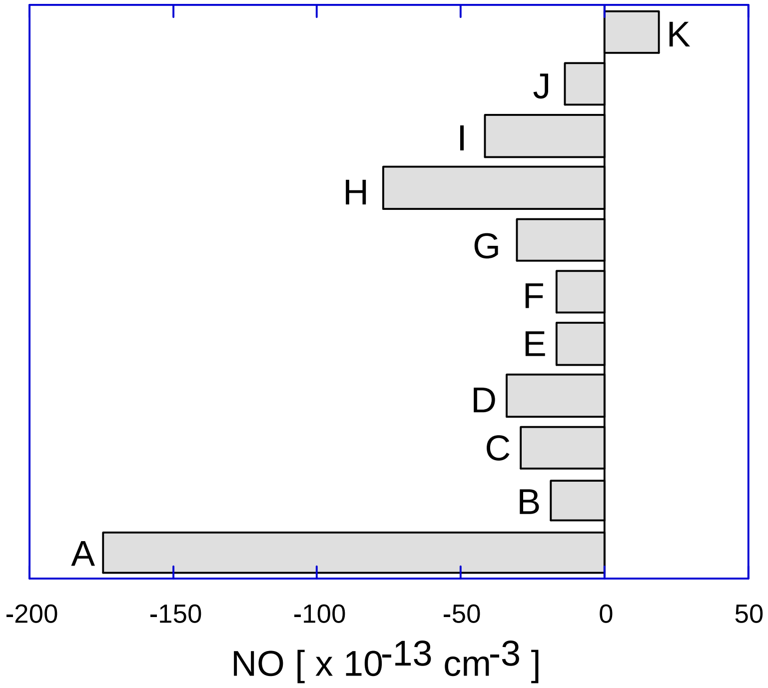

Fig. 3.10 Time integrated contribution of reactions for the generation and consumption of NO

A	$NO + HO_2 \rightarrow NO_2 + OH$
B	$NO + OH + M \rightarrow HNO_2 + M$
C	$NO + O_3 \rightarrow NO_2 + O_2$
D	$NO + N \rightarrow N_2 + O$
E	$O + NO + N_2 \rightarrow NO_2 + N_2$
F	$CH_3O_2 + NO \rightarrow CH_3O + NO_2$
G	$CH_3O + NO \rightarrow CH_3ONO$
H	$CH_3CH(OH)CH_2OO + NO \rightarrow CH_3CH(OH)CH_2O + NO_2$
I	$CH_3CH(OO)CH_2OH + NO \rightarrow CH_3CH(O)CH_2OH + NO_2$
J	$CH_2CHO + NO \rightarrow ONCH_2CHO$
K	$O + NO_2 \rightarrow NO + O_2$

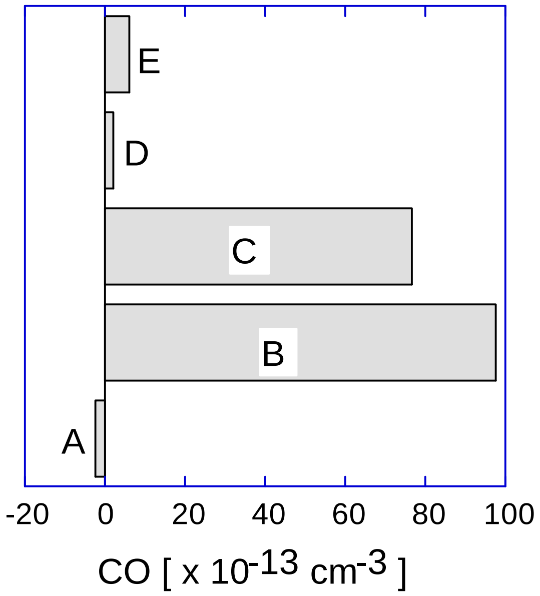

Fig. 3.11 Time integrated contributions from various reaction channels for the generation and consumption of CO

A	$OH + CO \rightarrow CO_2 + H$
B	$E + CO_2 \rightarrow CO + O + E$
C	$HCO + O_2 \rightarrow HO2 + CO$
D	$CO_2 + N \rightarrow CO + NO$
E	$CH_2CHO + O_2 \rightarrow HCHO + CO + OH$

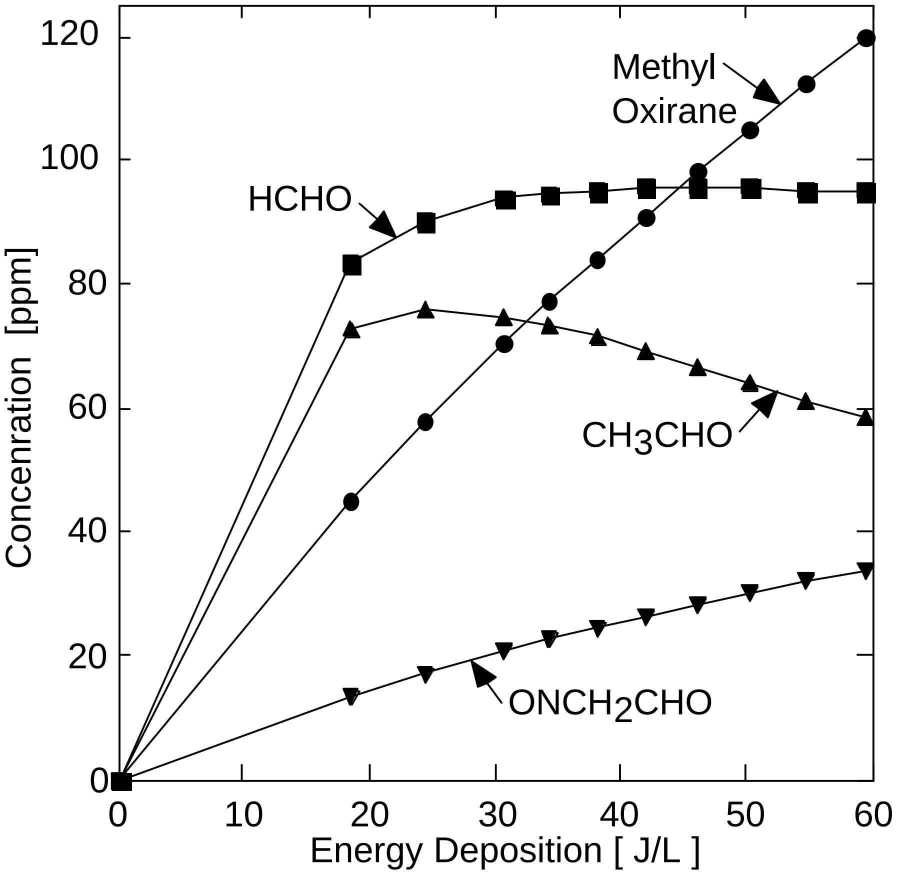

Fig. 3.12 End product profiles of the system with propene as a function of input energy deposition following 0.2 s

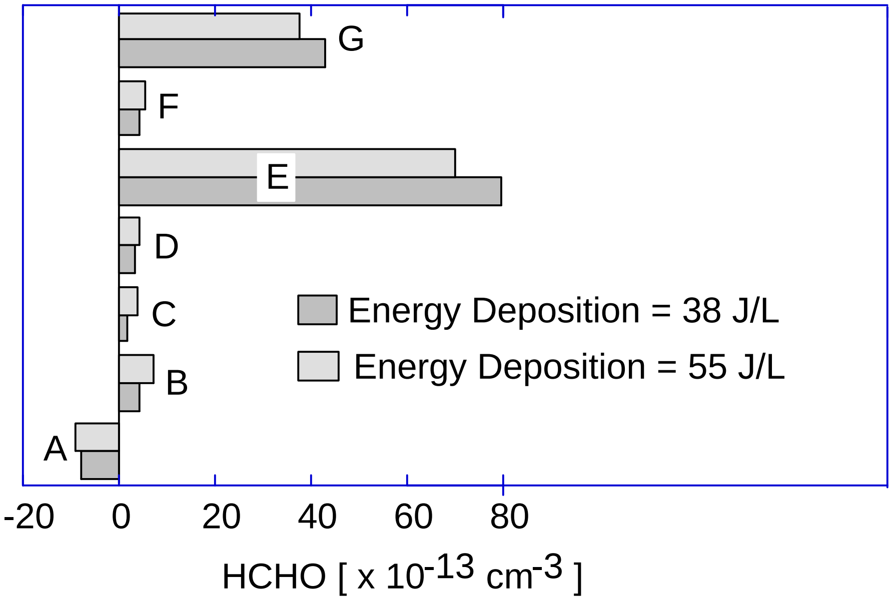

Fig. 3.13 Time integrated contribution from various reaction channels for the generation and consumption of HCHO.

A $HCHO + OH \rightarrow HCO + H_2O$
B $CH_3 + O \rightarrow HCHO + H$
C $CH_3O + O \rightarrow HCHO + OH$
D $CH_3O + NO \rightarrow HCHO + HNO$
E $CH_2OH + O_2 \rightarrow HCHO + HO_2$
F $CH_2CHO + O_2 \rightarrow HCHO + CO + OH$
G $CH_3CH(OH)CH_2O \rightarrow CH_3CHOH + HCHO$

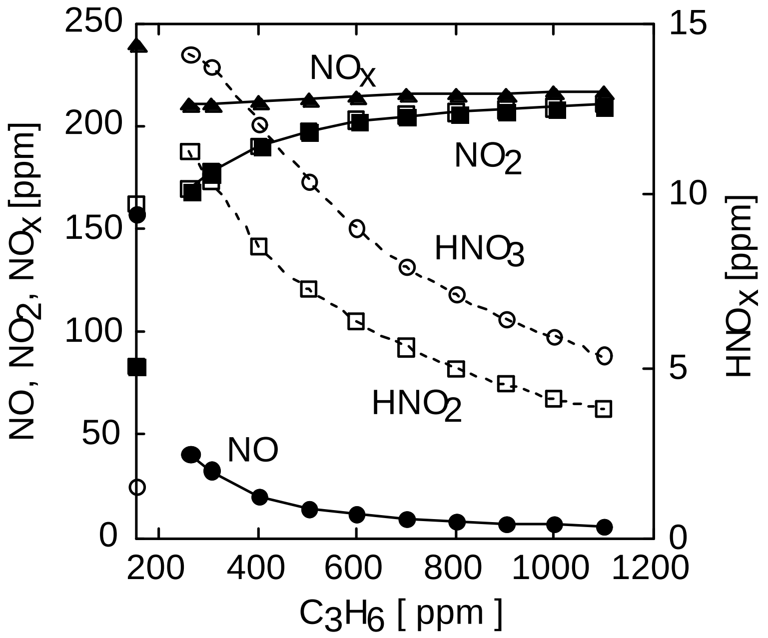

Fig. 3.14(a) Effect of propene variation on NO, NO_2, NO_x and HNO_x. All values correspond to an energy deposition of 18.7 J/L.

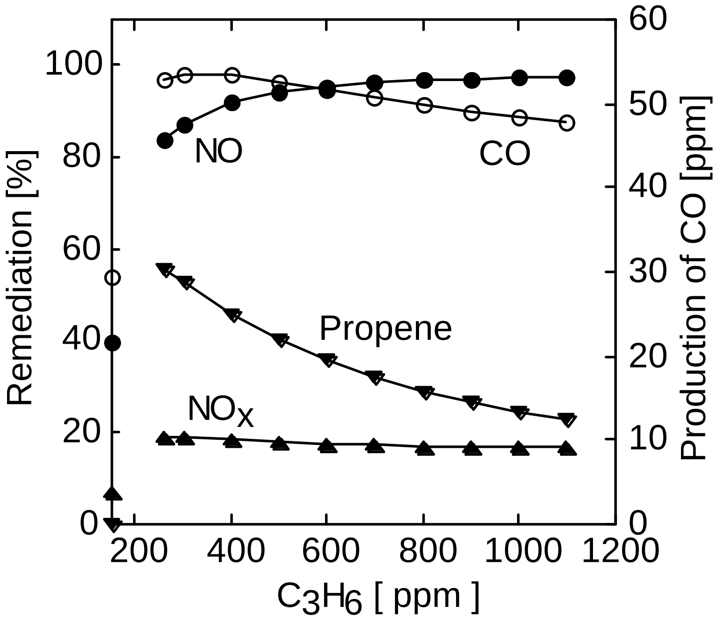

Fig. 3.14(b) Remediation percentages and CO production levels as a function of inlet propene concentration. All values correspond to an input energy of 18.7 J/L

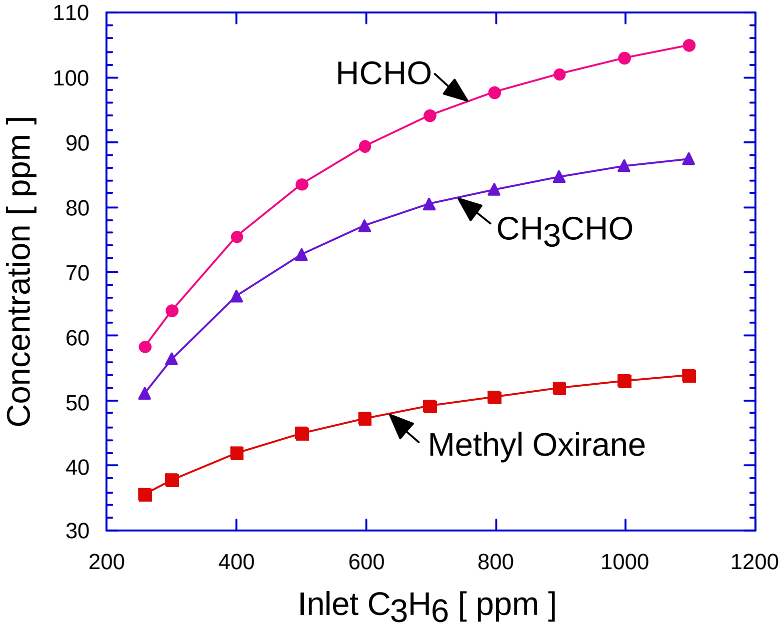

Fig. 3.15 Variation of end products with inlet propene for an energy deposition of 18.7 J/L. All concentrations correspond to values following 0.2 secs.

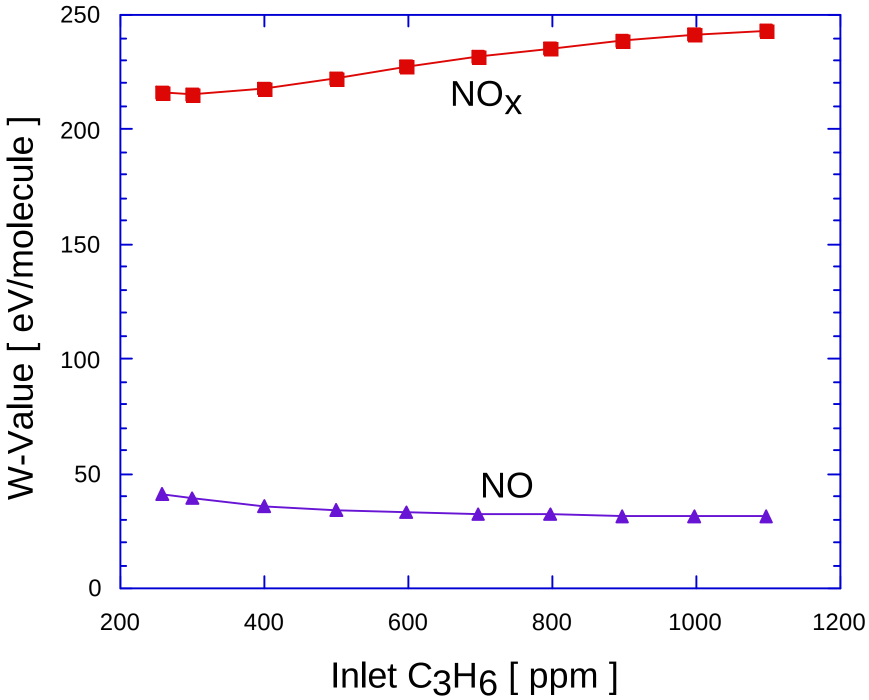

Fig. 3.16 Variation of W-Values for NO_x and NO as a function of inlet propene. All values are for an input energy of 18.7 J/L

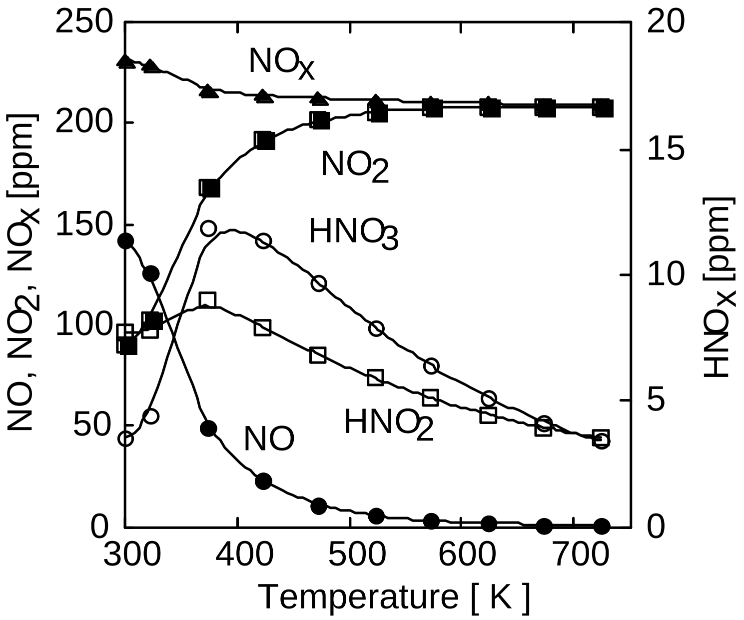

Fig. 3.17 Effect of reactor gas temperature on NO, NO_x, NO_2 and HNO_x production
Energy deposition = 30.86 J/L

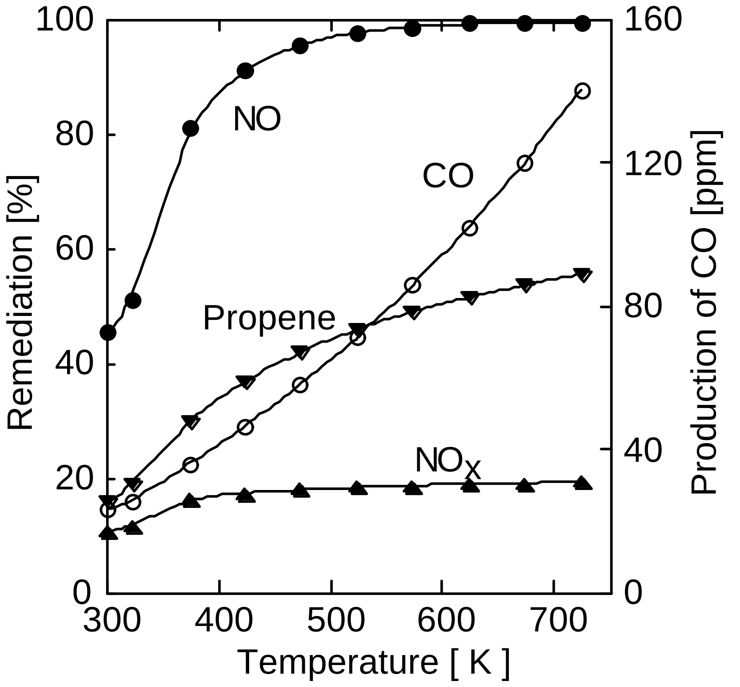

Fig. 3.18 Variation of NO_x, NO and propene conversion levels and production of CO as a function of gas temperature. Values correspond to E_{dep} of 30.86 J/L

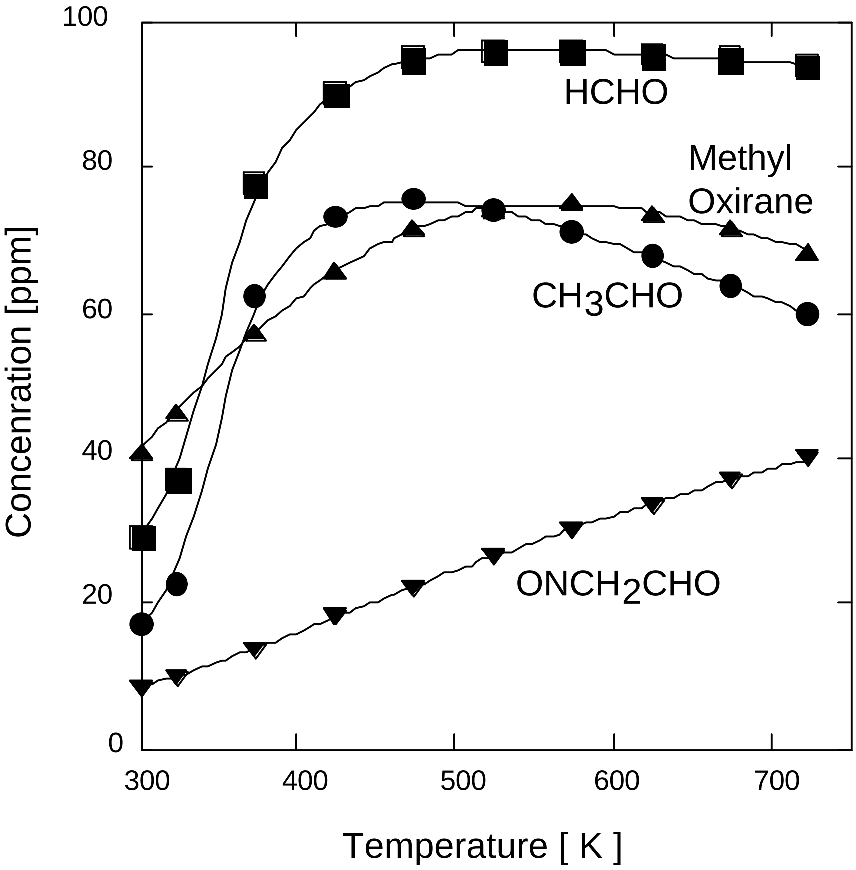

Fig. 3.19 Effect of temperature on the production levels of the end-products of the system with propene effects included. Input energy deposition = 30.86 J/L

3.9 References

1. Niessen, W., Wolf, O., Schruft, R. and Neiger, M., “The influence of ethene on the conversion of NO_x in a dielectric barrier discharge”, J. Phys. D:Appl. Phys., **31**, 1998, 542-550.
2. Atkinson, R., Tuazon, E.C., and Carter, W.P.L., “Effect of H-Atom Abstraction from the Reaction of the OH Radical with 1-Butene under Atmospheric Conditions”, *Int. J. Chem. Kinet.*, **17,** 725 (1985)
3. Niki, H., Maker, P.D., Savage, C.M., and Breitenbach, L.P., “Mechanism for Hydroxy Radical Initiated Oxidation of Olefin-Nitric Oxide Mixtures in Parts per Million Concentrations”, *J. Phys. Chem.*, **82,** 135 (1978).

4. EFFECT OF ADDITION OF PROPANE ON THE CONVERSION OF NO_x

4.1 Introduction

In the experiments that were conducted at Ford Research Labs, the gas stream also included propane (C_3H_8). In order to compare the results from GLOBAL_KIN with available data from experiments, propane was added to the reaction mechanism. This chapter contains results from GLOBAL_KIN, performed for the plasma processing of NO_x with the feed containing both propane and propene. The additional reaction mechanisms when adding propane are addressed in Section 4.2. The effects of input energy and reaction temperature are discussed in Section 4.3 and 4.4 respectively. Conclusions are provided in Section 4.5.

4.2 Reaction Mechanisms in NO_x Remediation in the Presence of C_3H_6 and C_3H_8

Propane adds to the reaction mechanism in almost the same way as propene does. There is, however, a significant difference in the values of the reaction rate coefficients of the underlying reactions. In contrast to propene, the initiating reactions with C_3H_8 are H-abstraction instead of addition reactions. The resulting alkyl radicals (i-C_3H_7 and n-C_3H_7) then quickly react with O_2 to form the peroxy radicals ($(CH_3)_2CHO_2$, $nC_3H_7O_2$) which further react with NO to form NO_2. The rate of reaction of OH with propene is higher than that with propane by at least two orders of magnitude at the temperatures, concentrations and pressures of interest. Hence, in a system with propane and propene, most of the initial OH reacts with propene instead of propane. Propene has higher reactivity compared to propane due to the presence of a double bond. The π electrons present in the double bond are more mobile compared to the σ bond and hence, the reactivity of propene is higher. This results in effectively reducing the participation of propane in the overall reaction chemistry.

The by-product of the reaction of the peroxy radicals with NO, the alkoxy radicals ($(CH_3)_2CHO$, C_3H_7O), then react with O_2 to generate propionaldehyde (C_2H_5CHO) and acetone ($CH_3C(O)CH_3$). The peroxy radicals could also produce nitrates in the reactions with NO. The reaction mechanism for propane-NO_x system is summarized in Fig. 4.1. To quantify these trends, simulations were performed under various initial conditions and input energy densities with added propane.

4.3 Effect of Input Energy Density on the Remediation of NO_x in the Presence of Propane and Propene

To investigate the effect of input energy density with propane, 175 ppm of propane with 500 ppm of C_3H_6 was added to the gas mixture in Table 3.1. The effect of increasing energy density on NO and NO_2 conversion is shown in Fig. 4.2(a). As a baseline for isolating the effect of addition of propane, the case with propene alone has been included. The addition of propane has a small, though not a negligible effect. Comparison of the modeling results with experiments shows close agreement with respect to [NO], but a noticeable deviation in [NO_2] and hence [NO_x]. The model prediction of NO_2 deviates from the experimental values by about 35 ppm. The conversion percentages for propene in the presence and absence of propane are shown in Fig. 4.2(b). With propane, the radicals that were previously available to propene are now competed for by propane and hence one sees a decrease in the conversion levels for propene. However, since the reactivity of propane compared with propene is small, the effect is not pronounced. The conversion levels for propane reach a high of 6% at the higher energy levels [60 J/L]. The conversion of propene in the presence of propane agrees reasonably well with the experiments.

At higher energy inputs, propane does have a noticeable effect on the CO production levels as is shown in Fig. 4.3(a). The variation of the end product concentrations with energy deposition is shown in Fig. 4.3(b). Typical end products include formaldehyde (HCHO), methyl oxirane, propionaldehyde (C_2H_5CHO), glyoxal (CHO-CHO), methyl nitrite (CH_3ONO) and 2-nitroso ethanal ($ONCH_2CHO$). Glyoxal is produced by the reaction of O_2 with vinoxy radical (CH_2CHO).

$$CH_2CHO + O_2 \rightarrow CHO\text{-}CHO + OH \qquad [\ 4.1\ ]$$

Experimental data was available only for HCHO and at 30 J/L. The model and the experiment agree well for that energy deposition.

4.4 Effect of Reactor Temperature on NO_x Conversion with Inlet Gas containing Propane and Propene

As described in the last chapter, temperature plays the important role of altering the reaction rate coefficients and thus the overall process output. The effect of temperature on NO_x remediation was analyzed with 500 ppm of propene and 175 ppm of propane. The results of the analysis are shown in Figs. 4.4(a) and 4.4(b). Propene, propane, CO and NO conversion increased with increasing temperature, though the NO_x conversion remained at an almost fixed level. The increase in the conversion levels for propene, CO and NO can be explained along the same lines as described in Chapter 3. The degradation of propane occurs mainly by the following mechanisms.

$$C_3H_8 + OH \rightarrow i\text{-}C_3H_7 + H_2O, \quad k = 7.95\times10^{-13}\left(\frac{T}{300}\right)^{2.0}\exp\left(-\frac{227}{T}\right)cm^3s^{-1} \quad [\ 4.2\ ]$$

$$C_3H_8 + OH \rightarrow n\text{-}C_3H_7 + H_2O, \quad k = 1.44\times10^{-12}\left(\frac{T}{300}\right)^{1.0}\exp\left(-\frac{130}{T}\right)cm^3s^{-1} \quad [\ 4.3\ ]$$

The reaction rate constants for the initial attack of propane by OH increase with increasing temperature and hence, more propane is converted at higher temperatures. There is no appreciable change in NO_x conversion with temperature. The maximum conversion of propane was around 10% at the maximum temperature. The effects of temperature on the production of HCHO, propionaldehyde and methyl oxirane are shown in Fig. 4.4(b). As is the case for propene alone, an increase in temperature produced an increase in the final end products mainly owing to the increase in the reaction rate coefficients of the underlying reactions with the increase in temperature.

4.5 Concluding Remarks

In general, the addition of propane did not affect the overall product output distribution significantly. The presence of propane actually produced a decreased conversion of propene, since the initiator radicals are consumed by propane also. Increasing energy inputs with propane produced almost the same outputs as with propene alone. This was because of the high reactivity of propene as compared to propane. Varying reactor temperature followed the same trends with propene alone. Higher temperatures lead to more NO conversion. NO_x conversion, however, remained almost unaffected by increasing gas temperatures.

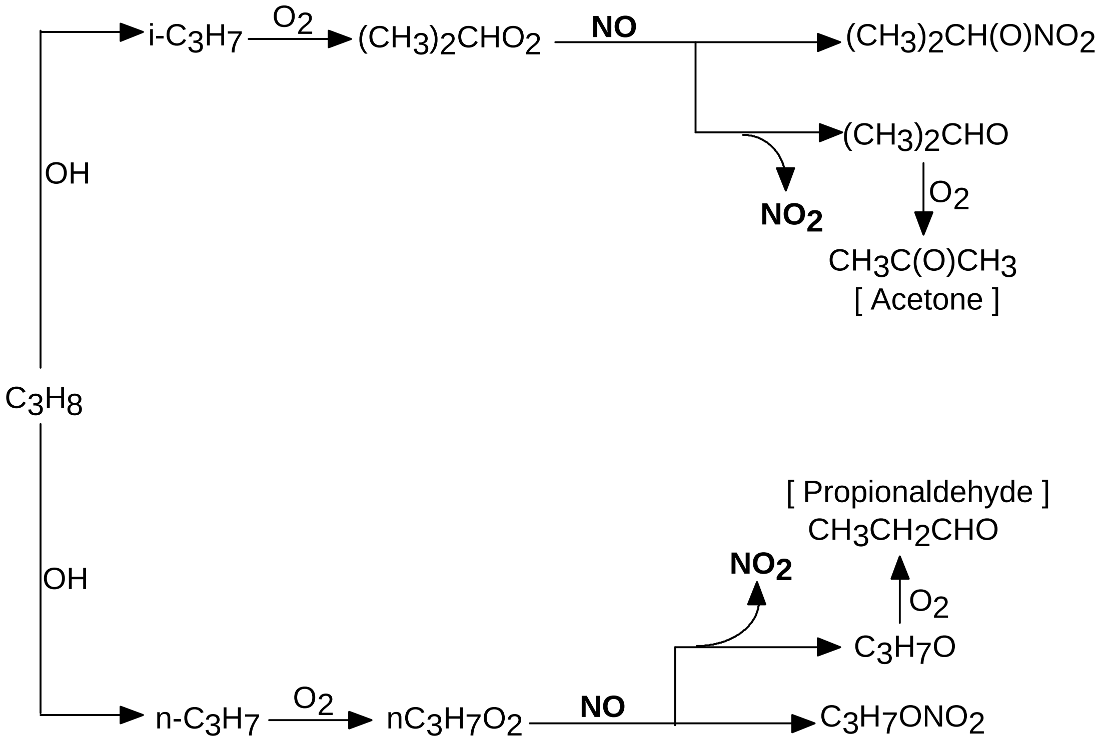

Fig. 4.1 Reaction mechanism for NO_x in the presence of propane

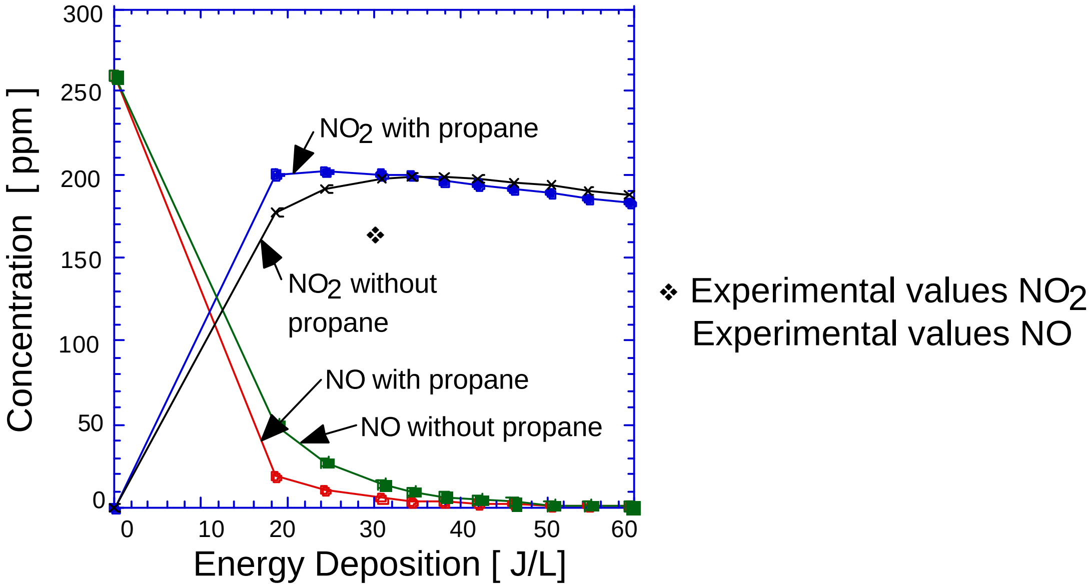

Fig. 4.2(a) Comparison of NO and NO_2 conversion levels with and without the addition of propane. All values correspond to a reactor residence time of 0.2 s.

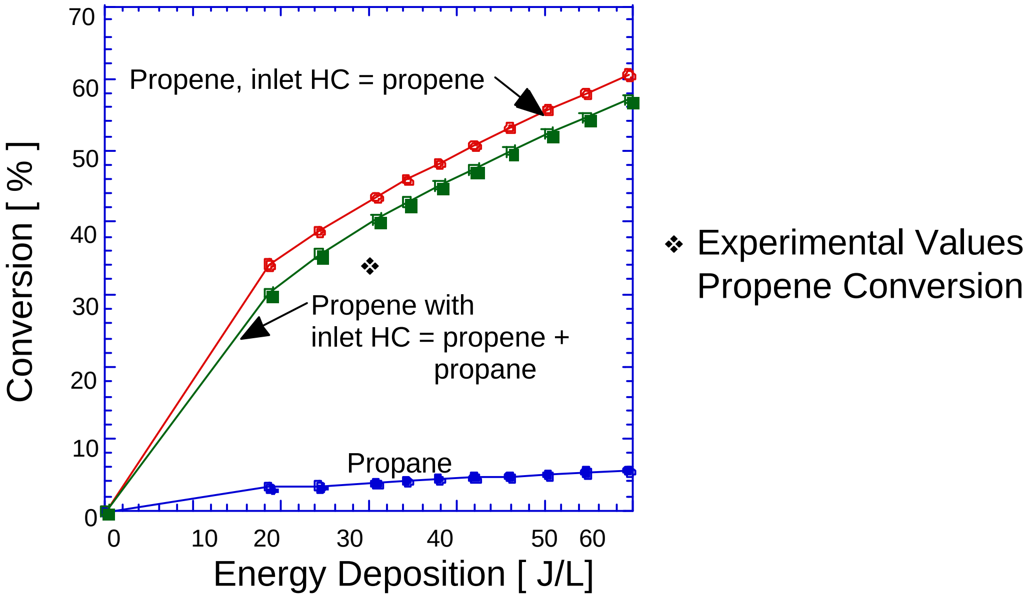

Fig. 4.2(b) Comparison of percentage conversion levels for propene with and without the addition of propane, following 0.2 s.

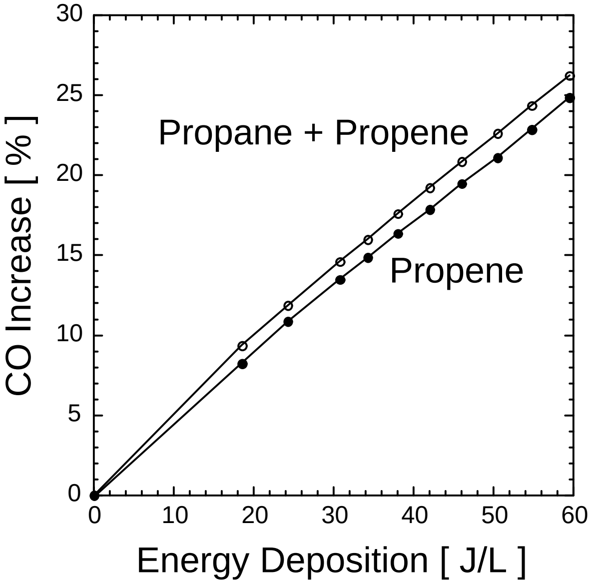

Fig. 4.3(a) Effect of energy deposition on the production level of CO in the presence of propane. All values are for a residence time of 0.2 s.

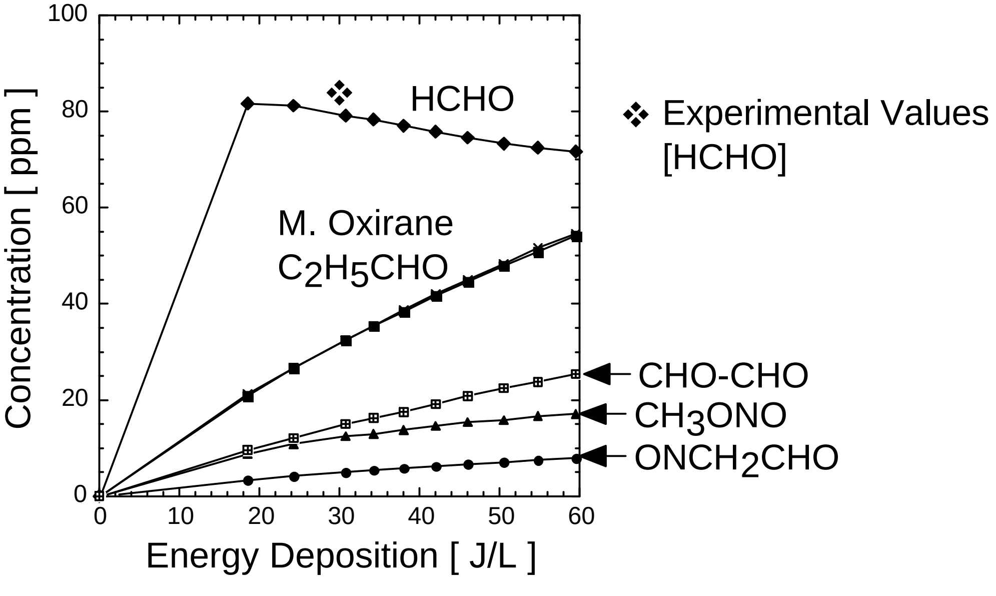

Fig. 4.3(b) Effect of energy deposition on the production level of end products with the addition of propane. Values correspond to a residence time of 0.2 s.

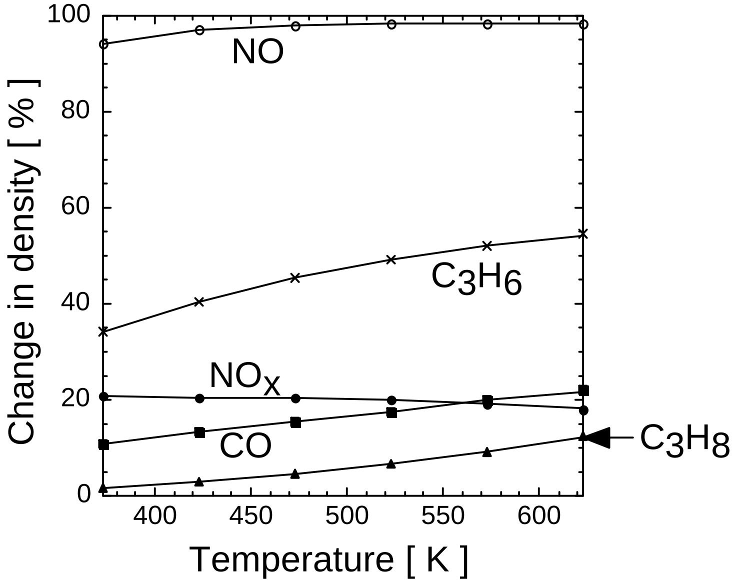

Fig. 4.4(a) Change in species densities with reactor temperature for a system containing propane and propene. Values are for an energy deposition of 30 J/L and a residence time of 0.2 s.

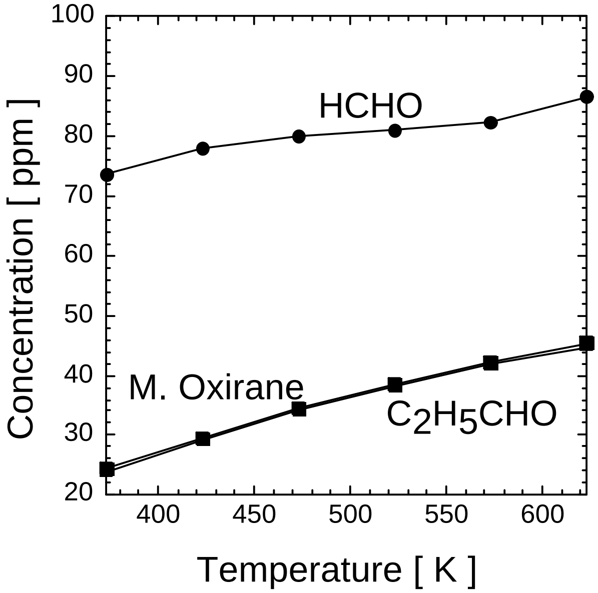

Fig. 4.4(b) Final product concentrations as a function of reactor temperature following 0.2 s, with the system containing propane in addition to propene. Values correspond to an energy deposition of 30 J/L.

5. EFFECT OF MULTIPLE PULSES ON NO_x PROCESSING

5.1 Introduction

Comparison of the results from GLOBAL_KIN with experiments performed at Ford Research Laboratory showed that methyl nitrate (CH_3ONO_2) was experimentally produced (approx. 12 ppm) whereas only 1 ppm was predicted by the model. Simulations predicted the formation of significant amounts of methyl oxirane and methyl nitrite (CH_3ONO), whereas these species were not found in the experiments by mass spectroscopy. These differences motivated us to analyze the effects that multiple discharge pulsing might have on the overall plasma chemistry. The role of multiple pulses in the plasma chemistry is discussed in Section 5.2. The time evolution of species during multiple pulsing is discussed in Section 5.3. Comparison of the effects of single and multiple pulse formats on the overall reaction mechanism is given in Section 5.4. Simulations were performed with varying propane in the inlet with multiple pulse inputs and these results are summarized and discussed in Section 5.5. Simulations were performed at different reactor temperatures with the multiple pulse format and these results are given in Section 5.6. Finally, concluding remarks are in Section 5.7.

5.2 Role of Multiple Pulses in Affecting the Overall Plasma Chemistry

CH_3ONO_2 (methyl nitrate) was formed in significant amounts in the DBD processing experiments conducted at Ford Research Laboratories (approx. 12 ppm) with the gas mixture given in Table 3.2 while it was not formed in our simulations using a single pulse format. CH_3ONO_2 could be produced by,

$$CH_3O + NO_2 + M \rightarrow CH_3ONO_2 + M, \qquad k = 1.5\times10^{-11}\left(\frac{T}{300}\right)^{0.5} cm^3 s^{-1} \qquad [\,5.1\,]$$

Reaction 5.1 implies that CH_3O radicals and NO_2 have to be present in significant quantities at the same time for the production of methyl nitrate. Since the feed does not contain NO_2, for reaction 5.1 to occur at significant rates, CH_3O and NO_2 must both be produced in significant quantities. There are other pathways for consumption of the CH_3O radical.

$$CH_3O + NO \rightarrow CH_3ONO, \qquad k = 2.0\times10^{-11}\left(\frac{T}{300}\right)^{0.5} cm^3 s^{-1} \qquad [\,5.2\,]$$

$$CH_3O + O_2 \rightarrow HCHO + HO_2, \qquad k = 1.13\times10^{-13}\exp\left(-\frac{1310}{T}\right) cm^3 s^{-1} \qquad [\,5.3\,]$$

$$CH_3O + OH \rightarrow HCHO + H_2O, \qquad k = 3.0\times10^{-11}\left(\frac{T}{300}\right)^{0.5} cm^3 s^{-1} \qquad [\,5.4\,]$$

$$CH_3O + CH_3O \rightarrow HCHO + CH_3OH, \qquad k = 1.0\times10^{-10}\left(\frac{T}{300}\right)^{0.5} cm^3 s^{-1} \qquad [\,5.5\,]$$

When the rates of the reactions 5.2 – 5.5 at 453 K are compared, it is found that reaction 5.2 dominates by at least two orders of magnitude. The rates of reactions 5.1 and 5.2 can be written as

$$r_{5.1} = -\frac{dN_{CH_3O}}{dt} = k_{5.1}[CH_3O][NO_2] \qquad [\,5.6\,]$$

$$r_{5.2} = -\frac{dN_{CH_3O}}{dt} = k_{5.2}[CH_3O][NO] \qquad [\,5.7\,]$$

The rate constants being almost equal, the ratio of the rates are approximately the ratios of the concentrations of NO_2 and NO. The time evolution of CH_3O radical, NO and NO_2

are shown in Fig. 5.1. Since the concentration of NO is always greater than NO_2 at high values of CH_3O, one always expects more of methyl nitrite to be formed.

In order for the production of methyl nitrate in the model to match experiments, the concentration of NO_2 should be greater than NO when the concentration of CH_3O is maximum. With multiple discharge pulses, the concentration of NO is gradually reduced and that of NO_2 is gradually increased. CH_3O radicals are produced during each pulse. Hence there will eventually be a time when the concentration of NO_2 exceeds that of NO at which time one would expect the formation of CH_3ONO_2.

5.3 Time Evolution of Species Densities during the Multiple Pulsing of Gas Mixtures containing NO_x

The effect of varying input voltage with multiple pulsing at a repetition rate of 75 s^{-1} with an energy input of 76 J/L was investigated. The variations in the NO, NO_2 and NO_x concentrations with time are shown in Fig. 5.2. Each of the points in the plots correspond to a density just prior to the next pulse. At the end of the processing time, almost 110 ppm of NO_x is removed resulting in about 42% NO_x conversion. After 0.12 s, $[NO_2]$ decreases due to the formation of CH_3ONO_2, HNO_3 and HNO_2 during each of the pulse periods. The NO concentration does not decrease to zero as was seen in the case of a single pulse input due to the regeneration of NO, primarily from NO_2.

$$O + NO_2 \rightarrow NO + O_2 \qquad [\ 5.8\ ]$$

This is shown in Fig. 5.3. Initially NO is removed, but at longer times, NO is regenerated. The variation of the N-containing products and energy deposition as a function of time are shown in Fig. 5.4. The multiple pulse format has resulted in the production of CH_3ONO_2. The final products with propene are shown in Fig. 5.5 and include methyl oxirane, propionaldehyde, acetaldehyde and glyoxal (CHO-CHO). Methyl oxirane, acetaldehyde and glyoxal are mainly produced by reactions 3.33, 3.34 and 3.12 respectively. Propionaldehyde is produced by the reaction of O with C_3H_6.

$$O + C_3H_6 \rightarrow C_2H_5CHO \qquad [\ 5.9\ ]$$

5.4 Comparison of Single and Multiple Pulse Inputs

The use of multiple pulse formats significantly affects the reaction chemistry. For example, in single pulse formats, one could neglect reaction [5.1] since the rate of this reaction at any point of time is much less when compared to reaction [5.2]. However, in the case of multiple pulse formats, the products generated from previous pulses are important in the reaction mechanism. A comparison between the products with a single pulse and multiple pulses is shown in Fig. 5.6 for the same total energy deposition. The NO_2 produced for the multiple pulse format is at least 40 ppm less than the NO_2 for a single pulse. The overall NO_x reduction differs by about 35 ppm, in the favor of multiple pulse format. The acids HNO_2 and HNO_3 are produced in more amounts with multiple pulses. Production of methyl nitrate increases by a factor of 13 when using a multiple pulse format over a single pulse input. There is a however only a small difference in the production of CH_3ONO.

The differences in the concentration of the C end products between single pulse and multiple pulse formats are shown in Fig. 5.7. With multiple pulses, propene conversion increases (for the same input energy) by 12%. The concentration of other products such as CHO-CHO, CH_3CHO, C_2H_5CHO and CO remain almost unchanged.

5.4 Combined Effect of Multiple Pulsing and Varying Propane Concentration on NO_x Remediation

The effect of multiple pulsing with propane was investigated with the gas mixture in Table 3.1 with 500 ppm of propene and varying propane. The total number of pulses was fixed at 15 and the pulses were equally spaced over a period of 0.2 s. The total energy deposited was approximately 76 J/L.

With multiple pulsing, the results were not much different when compared with single pulsed inputs. The variation of [NO], [NO_2] and [C_3H_6] as a function of propane is shown in Fig. 5.8. NO concentrations remained virtually a constant for different propane concentrations. Though small, propene conversion did decrease with increasing propane concentration. This is due to the increased competition for the radicals available for propene by propane. [NO_2] also remained unaffected with propane. The final concentrations of the end products as a function of inlet propane concentration are shown in Fig. 5.9. With increasing propane, the concentrations of HCHO, C_2H_5CHO, methyl oxirane, glyoxal, methyl nitrate and methyl nitrite remained unaffected. However, CH_3CHO decreased from 92 ppm to 76 ppm.

Thus, even with multiple pulse formats, propane does not affect the reactor outputs much, thereby implying that the contribution of propane to a secondary reaction chemistry is quite minimal.

5.5 Effect of Reactor Temperature on the Remediation of NO_x with the Inclusion of Multiple Pulses

The combined effects of multiple pulses and reactor temperature were studied with the gas mixture in Table 3.1 with 500 ppm of propene and 175 ppm of propane. The total residence time of gas was fixed at 0.2 s and during this period, 15 equally spaced pulses were applied. The total energy deposition was approximately 76 J/L.

The trends in the temporal evolution of NO and NO_2 for varying reactor temperatures are shown in Fig. 5.10. With increasing reactor temperature, [NO] decreased and $[NO_2]$ increased at intermediate points in time. However, at longer times, the concentrations of NO and NO_2 approached a finite asymptotic value. At 0.1 s, the $[NO]_{T=360\ K}$ was greater than $[NO]_{T=500\ K}$ by 33 ppm and $[NO_2]_{T=360\ K}$ was less than $[NO_2]_{T=500\ K}$ by the same amount, whereas at 0.2 s, $[NO_2]_{T=500\ K}$ differed from $[NO_2]_{T=360K}$ only by 6 ppm and $[NO]_{T=360\ K} \approx [NO]_{T=500\ K}$.

The variation of the end products as a function of time is shown in Fig. 5.11. The solid line in the graphs represent results at T_{GAS}=500 K while the dashed line corresponds to T_{GAS}=360 K. Formaldehyde was produced more rapidly at higher temperatures but the rate of production decreased at longer times. At 0.2 s, there was almost no difference in the final [HCHO] between T_{GAS}=360 K and T_{GAS}=500 K. Acetaldehyde production increased with increase in temperature. There was almost a linear increase in glyoxal concentration with time, with higher temperatures resulting in it's increased rates of production.

The effects of temperature on the production of methyl nitrate and methyl nitrite are shown in Fig. 5.12. At lower temperatures, equal amounts of CH_3ONO and

CH_3ONO_2 are produced. This difference becomes larger at higher temperatures. The concentrations of HNO_3 and HNO_2 as a function of time are shown in Fig. 5.13. Unlike other end products, $[HNO_2]$ decreases with increase in temperature. $[HNO_3]$ on the other hand, increased with increase in temperature.

The variation of methyl oxirane with time for various reactor temperatures is shown in Fig. 5.14. As the temperature is increased, the rate of the reaction increases due to the positive energy of activation.

$$C_3H_6 + O \rightarrow \text{Methyl Oxirane}, \qquad k = 9.051\times10^{-12}\exp\left(-\frac{609.9}{T}\right)cm^3s^{-1} \qquad [\ 5.10\ ]$$

Temperature increases from 360 K to 500 K increased the final concentrations of methyl oxirane by 21 ppm. The time evolution of propane and propene for 360 K and 500 K are shown in Fig. 5.15. Increasing temperature increased the conversion of propene and propane. C_3H_6 showed a change in conversion from 57.2% at 360 K to 84.8% at 500 K. Propane conversion increased from 2.85% at 360 K to 15.42% at 500 K. This is expected since propene is more reactive than propane due to the presence of a double bond. Finally, CO production as a function of time for different gas temperatures is shown in Fig. 5.16. More CO is formed at higher temperatures indicating that the production channels for CO dominate over consumption channels at higher temperatures. The difference in the concentration of CO between the two temperatures is approximately 75 ppm. Thus, while considering the rise in temperature for improving the performance, one should also take into account the production of CO and other pollutants that might be produced in higher quantities.

5.6 Concluding Remarks

The effect of multiple discharge pulses on the plasma remediation of NO_x in the presence of hydrocarbons was studied. When using multiple pulses, new reactions occur in the latter pulses due to the reaction products from previous pulses. CH_3ONO_2, which was not produced in noticeable quantities with single pulse format, was produced in significant amounts with multiple pulsing. Comparison of the products of single and multiple pulse discharges showed marked differences in final concentrations of NO_2, HNO_x, C_3H_6 and CO. The effect of varying hydrocarbon (propane) concentration with multiple pulsing was investigated and results showed that propane's contribution to NO_x remediation did not increase with multiple pulse formats. Parameterizations of reactor temperature with multiple discharge formats indicated an increase in the conversion of NO, C_3H_6 and C_3H_8 with increase in temperatures. All end products except HNO_2 were produced in increasing amounts with increases in temperature. CO was also produced in higher quantities at higher temperatures and this should always be considered in varying the operating temperature for improving NO_x remediation.

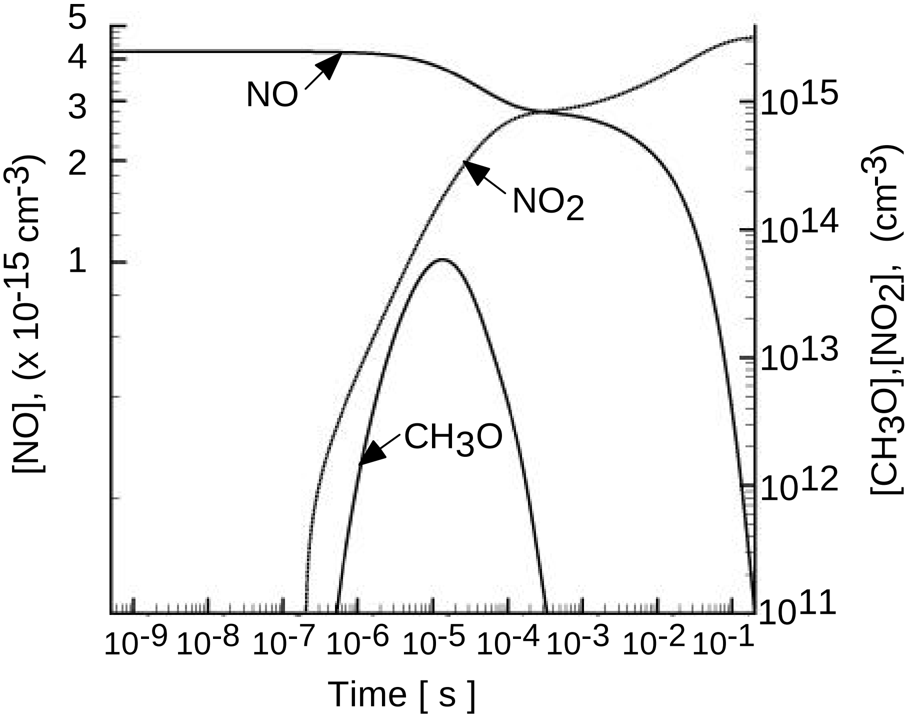

Fig. 5.1 Temporal evolution of NO, NO_2 and CH_3O radical during the plasma processing of NO_x with a single discharge pulse

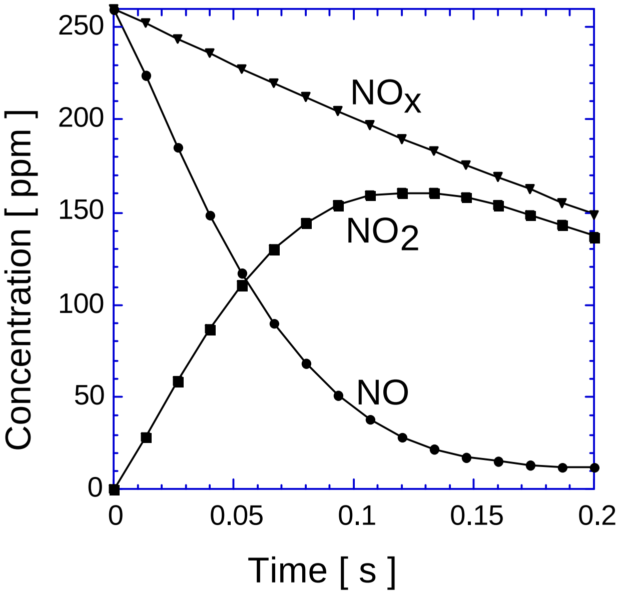

Fig. 5.2 : Variation of NO, NO_2 and NO_x with time for a multiply pulsed discharge processing of NO_x in a DBD.

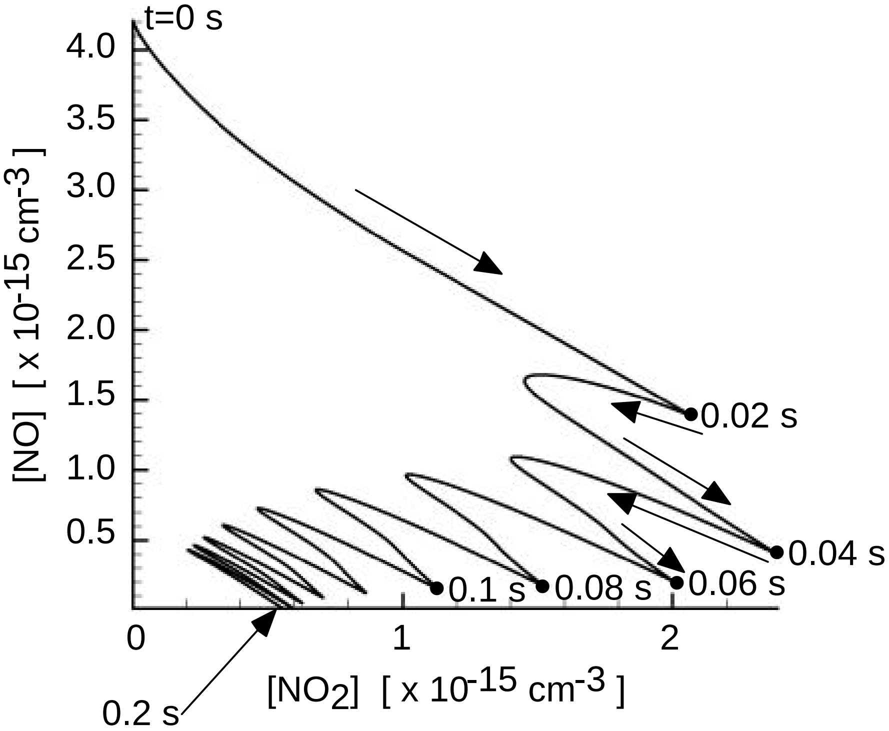

Fig. 5.3 Variation of NO with NO_2. The curve corresponds to marching along a time line.

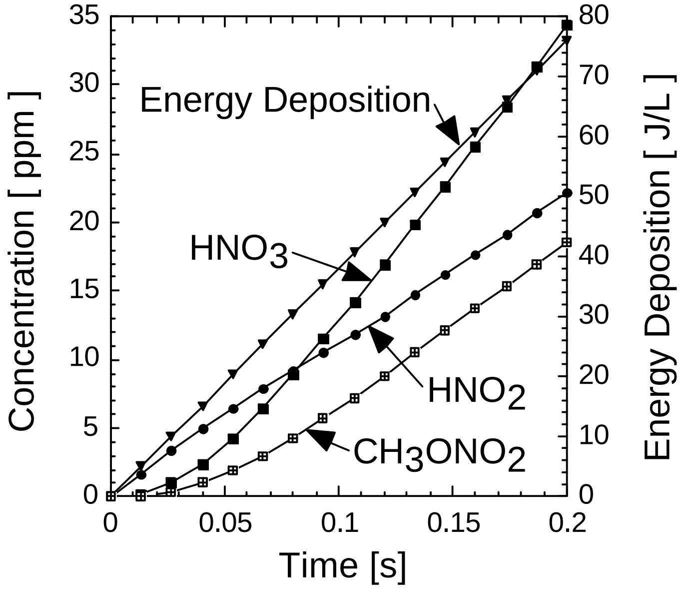

Fig. 5.4 : Variation of HNO_3, HNO_2, CH_3ONO_2 and energy deposition as a function of time during the multiply pulsed discharge processing of NO_x in the presence of propene.

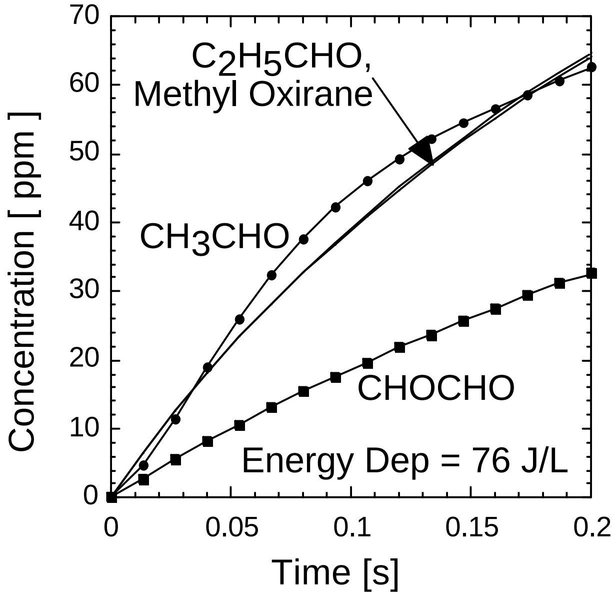

Fig. 5.5 : Production levels of the typical end-products encountered in the plasma processing of NO_x in the presence of propene as a function of time. Each of the symbols in the lines correspond to a pulsing at that point in time.

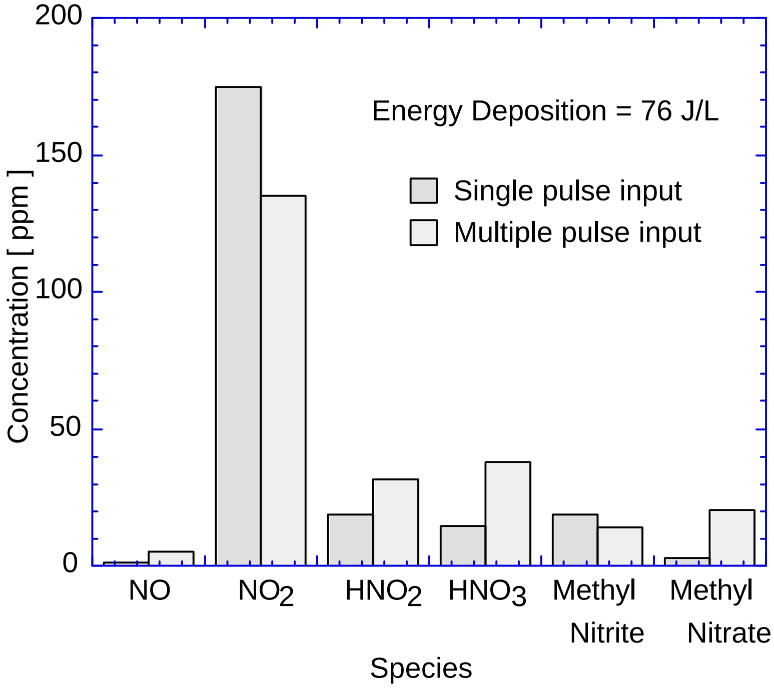

Fig. 5.6 Comparison of the exit level concentrations of various species after the plasma processing of NO_x with single and multiple pulsed discharges.

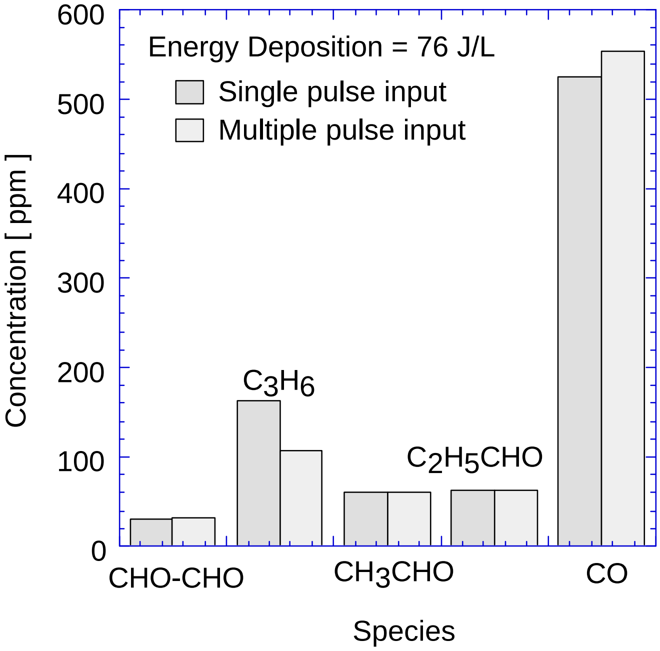

Fig. 5.7 Comparison of concentrations of the end-products of plasma processing of Nox with single and multiple pulse inputs.

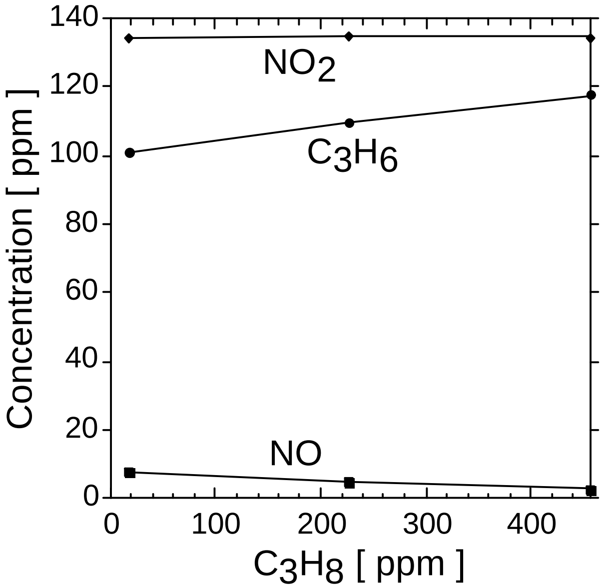

Fig. 5.8 Outlet concentrations of NO, NO_2 and C_3H_6 as a function of inlet propane concentration for the multiple pulsed plasma processing of NO_x in the presence of propane and propene.

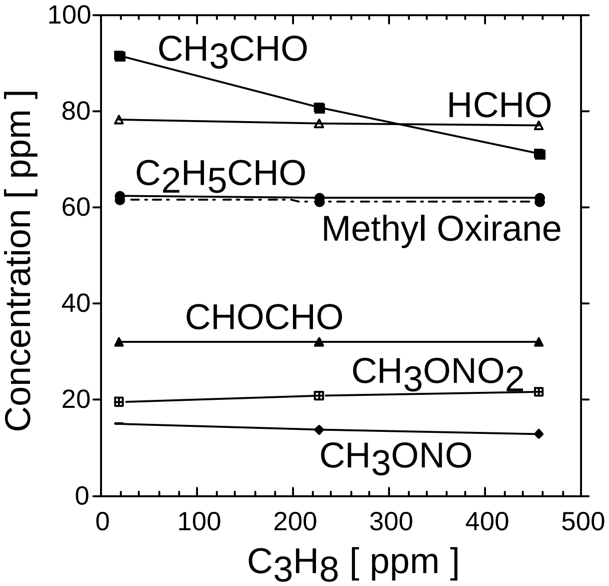

Fig. 5.9 Production levels of typical end-products of the plasma processing of NO_x with the variation in the inlet propane concentration. All values correspond to an energy deposition of 76 J/L and for a 15 pulse input.

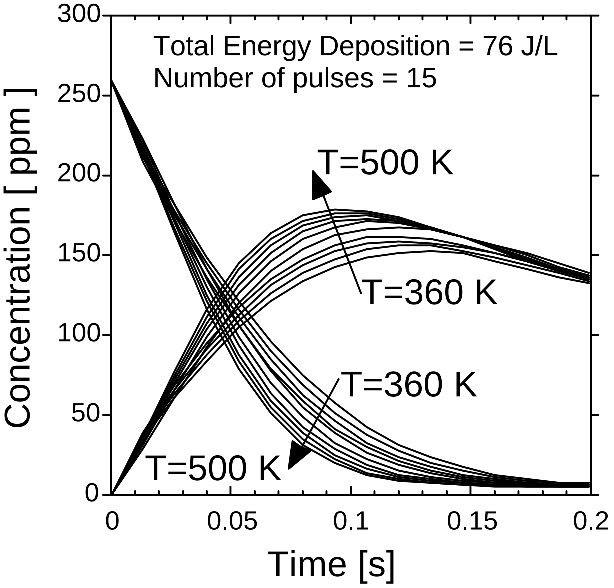

Fig. 5.10 Variation of NO and NO_2 with time for varying reactor temperatures.

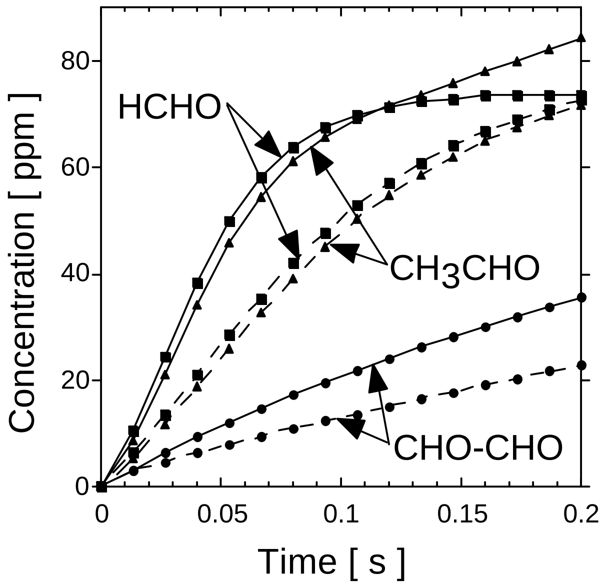

Fig. 5.11 Temporal evolution of end-products of the multiply pulsed plasma processing of NO_x in a DBD. Solid lines represent operating conditions at 500 K and dashed lines correspond to reactor temperatures of 360 K.

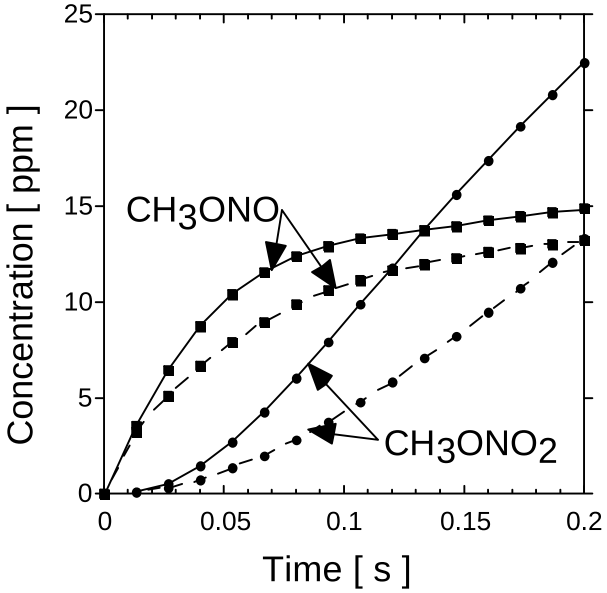

Fig. 5.12 Variation of methyl nitrate and methyl nitrite as a function of time for two different reactor temperatures. Solid lines represent T_{GAS}=500 K while dashed lines correspond to T_{GAS}=360 K.

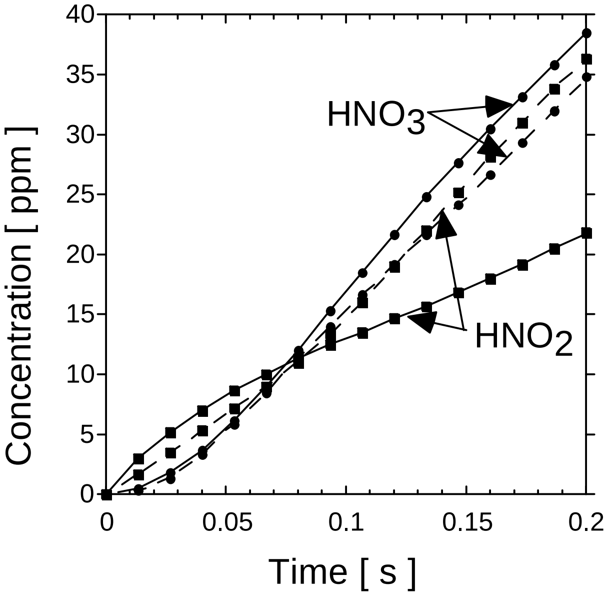

Fig. 5.13 HNO_2 and HNO_3 profiles as a function of time for T_{GAS}=360 K (dashed lines) and T_{GAS}=500 K.

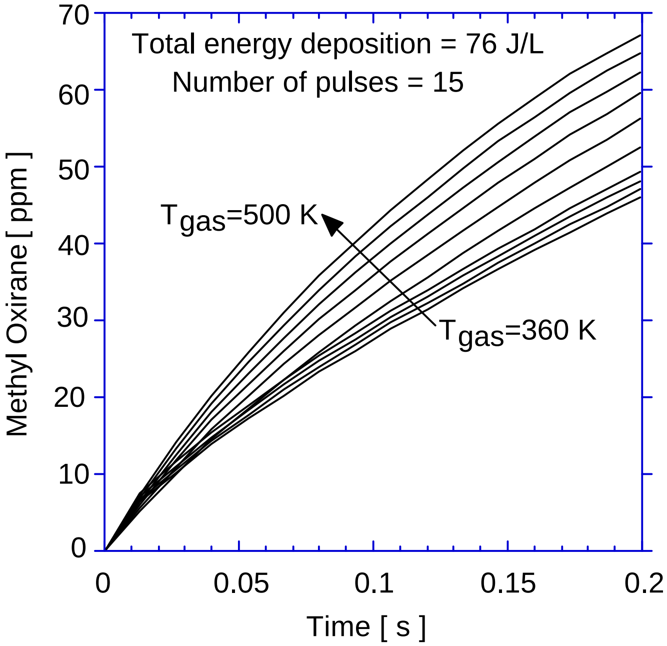

Fig. 5.14 Methyl Oxirane variation as a function of time for different reactor gas gas temperatures for the multiply pulsed plasma processing of NO_x in the presence of propane and propene.

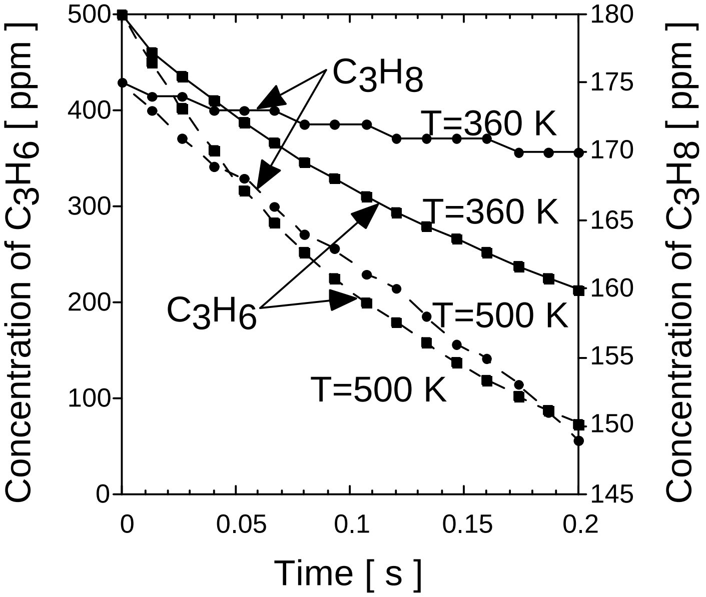

Fig. 5.15 Variation of conversion levels of C_3H_6 and C_3H_8 as a function of time for different cases of gas temperatures : 360 K (dashed lines) and 500 K (solid lines).

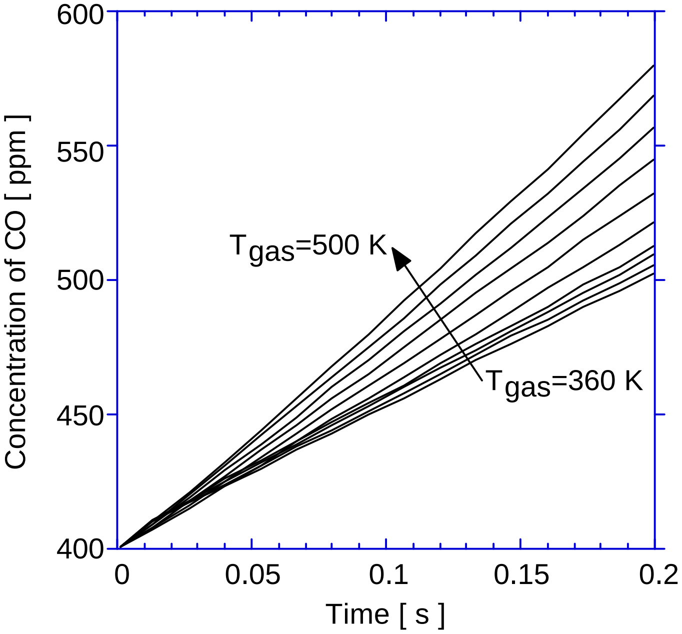

Fig. 5.16 Production levels of CO during the multiply pulsed plasma processing of NO_x in the presence of propane and propene.

6. CONCLUSIONS

We have used a zero-dimensional model, called GLOBAL_KIN, to investigate the dielectric barrier discharge (DBD) remediation of NO_x in simulated diesel exhausts at atmospheric pressure. The model is capable of analyzing detailed reaction chemistries in the DBDs. Ultimately, the aim of the analysis is to obtain a set of operating conditions/ranges in which maximal and energy-efficient remediation of NO_x is obtained.

Plasma remediation of NO_x in the presence of hydrocarbons has been investigated. The results indicate that hydrocarbons play a significant role in the overall reaction chemistry of NO_x. With hydrocarbons, the energy efficiency of the process is found to improve. Increasing energy deposition through the application of higher voltages led to higher NO_x remediation. Variation of temperature did not significantly affect the net NO_x remediation. Alkanes, propane in particular, were analyzed to determine their role in NO_x remediation. Alkanes being less reactive compared to alkenes, did not appreciably affect the process outputs.

Industrial systems for plasma remediation employ higher repetition rate discharges. Multiple discharge formats were implemented in GLOBAL_KIN. New reactions occur during the latter pulses due to the reaction products from previous pulses. Single and multiple pulse discharge processing of NO_x were compared. The results obtained using the multiple pulse formats agreed more closely with the experiments.

One of the underlying assumptions of GLOBAL_KIN is the homogeneity of the gas mixture in the reactor. This is not the case in real time systems wherein spatial dependencies exist. Future improvements will account for these spatial dependencies.

Another improvement to the model will include heterogeneous reaction chemistries and particulate formation.

APPENDIX A : LIST OF SPECIES USED IN THE REMEDIATION OF NO_X IN $N_2/O_2/H_2O/CO_2/CO/H_2/C_3H_6/C_3H_8$

E
O_2^+
$O(^1D)$
N_2
N_2^+
H_2O
HCO
NO
H^-
H_2
CO
CO_2^+
H_2O_2
H_2O^+
NO^+
NO_3-
N_4^+
H_2NO^+
NH_3^+
$H_3O^+\cdot(H_2O)_2$
C_2O
C_3H_8
C_3H_7CHO
$(CH_3)_2CHO_2$
C_3H_6
C_2H_5
C_2H_5NO
C_2H_5O
C_2H_3
C_2H_3O
C_2HO
C_2
CH_3CHCH
$CH_3CHOHCH_2(OO)$
$CH_3CHOHCH_2O$
CH_3CO
CH_3NO_2
CH_3OH
CH_2CCH_3
CH_2CHCHO
CH_2CHCO

O_2
O_2^-
O^+
$N_2(A)$
N
O_3
HO_2
HNO_2
HNO
N_2O
CO^+
HNO_3
N_2O_5
H_3O^+
NO_2^+
NO^+*O_2
$O_2^+\cdot H_2O$
NH_3
NH_4^+
$H_3O^+\cdot(H_2O)_3$
IC_3H_7
NC_3H_7OH
NC_3H_7O
C_3H_5
$C_2H_5COCH_3$
$C_2H_5O_2$
C_2H_4
C_2H_3CHO
C_2H_2
$CHOCHO$
C_2HCO
CH_3CHCH_2OH
$CH_3CH(OO)CH_2OH$
CH_3CHCO
CH_3COCHO
CH_3ONO
CH_3OCH_3
CH_2CCH_2
CH_2CHCH_2
CH_2CO
CH

O_2
O
O^-
$N(^2D)$
OH
NO_2
H
NO_3
C
CO_2
HO_2NO_2
NH
N_3^+
NO_2-
N^+
$H_3O^+\cdot H_2O$
NH_2
$NO^+\cdot H_2O$
CCN
$C_2H_5OONO_2$
CH_3COO
CH_2OHNO
CH_3NCH_3
$CH_3CO_3NO_2$
$HOCH_2NO_2$
$HCOO$
$NC_3H_7ONO_2$
C_2H_2OH
C_2H
CH_3CHO
$CH_3CHOHCH_2$
$CH_3CH(O)CH_2OH$
CH_3COO_2
CH_3COCH_3
CH_3ONO_2
CH_3OOH
CH_2CHO
CH_2CHCH_2O
CH_2OH
$HCHO$
$C_2H_5ONO_2$

N_2O_4
H_3O
H_2NO
H_2CN
CH_3O_2
CN
$NCCN$
N_3
CH_4
CH_3O
H_2^+
HCN
$HOCN$
CNN
N_4
CH_3
C_2H_6
$HCOOH$
NCO
$HNCO$
NC_3H_7
$NC_3H_7O_2$
$(CH_3)_2CHO$
C_3H_3
C_2H_5CHO
C_2H_5OH
C_2H_4OH
C_2H_3CO
CH_3CONO
NC_3H_7OOH
$(CH_3)_2CHONO_2$
$(CH_3)_2CHOOH$
C_2H_5ONO
$ONCH_2CHO$
$CONH_2$
CH_3CHOH
CH_2
Methyl Oxirane

APPENDIX B. LIST OF REACTIONS USED IN THE REMEDIATION OF NOx

Electron impact reactions resulting in the production of new species

Reaction	Rate Coefficient [a]	Ref.
$e + N_2 \rightarrow N_2^+ + e + e$	6.664×10^{-11}	1
$e + N_2 \rightarrow N_2(A) + e$	8.524×10^{-9}	1
$e + N_2 \rightarrow N + N + e$	7.05×10^{-10}	1
$e + O_2 \rightarrow O^- + O$	5.276×10^{-11}	1
$e + O_2 \rightarrow O_2^+ + e + e$	1.961×10^{-10}	2
$e + O_2 \rightarrow O + O + e$	1.434×10^{-9}	2
$e + O_2 \rightarrow O(^1D) + O + e$	4.8×10^{-9}	2
$e + N_2^+ \rightarrow N(^2D) + N$	$2 \times 10^{-7} Te^{-0.5}$	34
$e + H_2O \rightarrow H_2O^+ + e + e$	6.525×10^{-11}	3
$e + H_2O \rightarrow H + OH + e$	5.322×10^{-11}	3
$e + H_2O \rightarrow H^- + OH$	2.512×10^{-10}	3
$e + N_3^+ \rightarrow N + N_2$	$2 \times 10^{-7} Te^{-0.5}$	b
$e + H_3O^+ \cdot (H_2O)_2 \rightarrow H + (H_2O)_3$	$2 \times 10^{-7} Te^{-0.5}$	b
$e + NO_2^+ \rightarrow NO + O$	$2 \times 10^{-7} Te^{-0.5}$	b
$e + NO_2^+ \rightarrow NO + O(^1D)$	$2 \times 10^{-7} Te^{-0.5}$	4
$e + H_2NO^+ \rightarrow H_2O + N$	$2 \times 10^{-7} Te^{-0.5}$	b
$e + NO^+ \rightarrow N(^2D) + O$	$2 \times 10^{-7} Te^{-0.5}$	4
$e + NO^+ \rightarrow N + O(^1D)$	$2 \times 10^{-7} Te^{-0.5}$	34
$e + O_2 + M \rightarrow O_2^- + M$	$1 \times 10^{-31} Te^{-0.5}$	4
$e + NO^+ \cdot O_2 \rightarrow NO + O_2$	$2 \times 10^{-7} Te^{-0.5}$	b
$e + NO_2 \rightarrow NO_2^-$	4×10^{-11}	4
$e + N_4^+ \rightarrow N_2 + N_2$	$2 \times 10^{-7} Te^{-0.5}$	b
$e + NO^+ \cdot (H_2O)_2 \rightarrow NO + H_2O + H_2O$	$2 \times 10^{-7} Te^{-0.5}$	b

$e + H_2O^+ \rightarrow OH + H$	$6.6x10^{-6}Te^{-0.5}$	5
$e + H_2O^+ \rightarrow O + H + H$	$2.88x10^{-6}Te^{-0.5}$	5
$e + H_2O^+ \rightarrow O + H_2$	$2.52x10^{-6}Te^{-0.5}$	5
$e + H_3O^+ \rightarrow H_2O + H$	$2x10^{-7}Te^{-0.5}$	b
$e + O_2^+ \rightarrow O(^1D) + O$	$2x10^{-7}Te^{-0.5}$	b
$e + H_2^+ \rightarrow H_2$	$2x10^{-7}Te^{-0.5}$	b
$e + O_2^+ \cdot H_2O \rightarrow O_2 + H_2O$	$2x10^{-7}Te^{-0.5}$	b
$e + H_3O^+ \cdot H_2O \rightarrow H + H_2O + H_2O$	$2x10^{-7}Te^{-0.5}$	b
$e + NH_3^+ \rightarrow NH_2 + H$	$2x10^{-7}Te^{-0.5}$	b
$e + NH_4^+ \rightarrow NH_3 + H$	$2x10^{-7}Te^{-0.5}$	b
$e + NO^+ \cdot H_2O \rightarrow NO + H_2O$	$2x10^{-7}Te^{-0.5}$	b
$e + NO^+ \cdot (H_2O)_3 \rightarrow NO + H_2O + H_2O + H_2O$	$2x10^{-7}Te^{-0.5}$	b
$e + N_2(A) \rightarrow N_2^+ + e + e$	$2.2x10^{-7}$ x $(\exp(-9.33/Te)/(Te^{-0.5}(1+9.33)/Te))$ x $((20+9.33/Te)^{-1} + \log(1.25(1+Te/9.33)))$	35
$e + O_3 \rightarrow e + O_2 + O(^1D)$	$5x10^{-10}$	b
$e + CO_2 \rightarrow O + CO + e$	$1.195x10^{-9}$	6
$e + CO_2 \rightarrow CO_2^+ + e + e$	$1.693x10^{-10}$	6
$e + CO_2 \rightarrow O^- + CO$	$6.565x10^{-12}$	6
$e + CO_2^+ \rightarrow CO + O$	$2x10^{-7}Te^{-0.5}$	b
$e + C^+ \rightarrow C$	$2x10^{-7}Te^{-0.5}$	34

Reactions of $N_2/O_2/H_2O/NO$

Reaction	Rate Coefficient [c]	Ref.
$O + O_2 + M \rightarrow O_3 + M$	$6.9x10^{-34}(T/300)^{-1.25}$	30
$H + OH + M \rightarrow H_2O + M$	$4.3x10^{-31}$	4
$N_2O_5 \rightarrow NO_2 + NO_3$	$5.49x10^{14}T^{0.1}\exp(-11080/T)$	30

$NO + O_2 + NO \rightarrow NO_2 + NO_2$	$1.4\text{x}10^{-38}$	b
$NO + HO_2 \rightarrow NO_2 + OH$	$3.7\text{x}10^{-12}\exp(240/T)$	11
$N(^2D) + N_2 \rightarrow N + N_2$	$2.4\text{x}10^{-14}$	4
$NO + O + O_2 \rightarrow NO_2 + O_2$	$2.44\text{x}10^{-27}T^{-1.8}$	11
$N(^2D) + O_2 \rightarrow NO + O$	$6.8\text{x}10^{-12}$	4
$NO + OH + M \rightarrow HNO_2 + M$	$7.4\text{x}10^{-31}(T/300)^{-2.4}$	11
$N(^2D) + NO \rightarrow N_2 + O$	$6.3\text{x}10^{-11}$	4
$NO + H + M \rightarrow HNO + M$	$3.4\text{x}10^{-32}$	4
$N(^2D) + N_2O \rightarrow NO + N_2$	$2.6\text{x}10^{-12}$	4
$NO + NO_3 \rightarrow NO_2 + NO_2$	$1.6\text{x}10^{-11}\exp(150/T)$	11
$HO_2 + NO + M \rightarrow HNO_3 + M$	$5.6\text{x}10^{-33}$	b
$HO_2 + NO \rightarrow O_2 + HNO$	$9.0\text{x}10^{-19}\exp(2819/T)$	12
$N(^2D) + NO_2 \rightarrow N_2O + O$	$1.5\text{x}10^{-12}$	4
$NO + O_3 \rightarrow NO_2 + O_2$	$2.0\text{x}10^{-12}\exp(-1400/T)$	13
$N(^2D) + NO_2 \rightarrow NO + NO$	$1.5\text{x}10^{-12}$	4
$NO + N \rightarrow N_2 + O$	$3.1\text{x}10^{-11}$	4
$H + O_2 + M \rightarrow HO_2 + M$	$5.64\text{x}10^{-28}T^{-1.6}$	14
$H + H + M \rightarrow H_2 + M$	$4.8\text{x}10^{-33}$	4
$H + NO_2 \rightarrow OH + NO$	$8\text{x}10^{-11}$	4
$H + HO_2 \rightarrow OH + OH$	$2.8\text{x}10^{-10}\exp(-440/T)$	15
$N_2(A) + N_2 \rightarrow N_2 + N_2$	$1.9\text{x}10^{-13}$	36
$H + O_3 \rightarrow OH + O_2$	$1.4\text{x}10^{-10}\exp(-480/T)$	11
$N_2(A) + NO \rightarrow NO + N_2$	$3.6\text{x}10^{-10}$	36
$H + HNO \rightarrow H_2 + NO$	$1\text{x}10^{-11}$	4
$N_2(A) + O_2 \rightarrow O + O + N_2$	$1.5\text{x}10^{-12}$	36
$N + NO_2 \rightarrow N_2O + O$	$2.4\text{x}10^{-12}$	4
$N_2(A) + O_2 \rightarrow O_2 + N_2$	$2.8\text{x}10^{-11}$	36

$N + NO_2 \rightarrow NO + NO$	$6x10^{-13}$	4
$N_2(A) + N_2O \rightarrow N_2 + N_2 + O$	$1.4x10^{-11}$	36
$N_2(A) + N_2O \rightarrow N_2 + N_2O$	$1.7x10^{-10}$	36
$N + N + M \rightarrow N_2 + M$	$3.9x10^{-33}$	4
$N_2(A) + NO_2 \rightarrow NO + O + N_2$	$1x10^{-12}$	36
$N_2(A) + H_2 \rightarrow N_2 + H_2$	$2.6x10^{-11}$	36
$N + OH \rightarrow NO + H$	$3.8x10^{-11}exp(85/T)$	11
$O(^1D) + N_2 \rightarrow O + N_2$	$1.8x10^{-11}exp(107/T)$	11
$N + O + M \rightarrow NO + M$	$5.46x10^{-33}exp(155/T)$	16
$O(^1D) + O_2 \rightarrow O + O_2$	$3.8x10^{-11}$	4
$N + O_2 \rightarrow NO + O$	$4.4x10^{-12}exp(-3220/T)$	11
$N + O_3 \rightarrow NO + O_2$	$5x10^{-16}$	4
$O(^1D) + H_2O \rightarrow O + H_2O$	$1.2x10^{-11}$	4
$O(^1D) + H_2O \rightarrow OH + OH$	$2.2x10^{-10}$	4
$O + HO_2 \rightarrow OH + O_2$	$2.9x10^{-11}exp(200/T)$	11
$O + O3 \rightarrow O2 + O2$	$8.0x10^{-12}exp(-2060/T)$	11
$O + NO_2 + M \rightarrow NO_3 + M$	$9.0x10^{-32}(T/300)^{-2.0}$	11
$NO_3 + NO_3 \rightarrow$ $NO_2 + NO_2 + O_2$	$1.2x10^{-15}$	4
$OH + OH \rightarrow O + H_2O$	$3.5x10^{-16}T^{1.4}exp(200/T)$	15
$N_2O_5 + H_2O \rightarrow$ $HNO_3 + HNO_3$	$5x10^{-21}$	4
$NH + NO \rightarrow N_2O + H$	$1.3x10^{-12}$	4
$OH + NO_2 + N_2 \rightarrow$ $HNO_3 + N_2$	$2.2x10^{-30}exp(T/300)^{-2.9}$	11
$NH + O_2 \rightarrow HNO + O$	$2.3x10^{-13}$	4
$OH + HNO_3 \rightarrow NO_3 + H_2O$	$1.5x10^{-14}exp(650/T)$	24
$OH + HNO \rightarrow H_2O + NO$	$2.15x10^{-17}T^{1.88}exp(481/T)$	21

$OH + HO_2 \rightarrow H_2O + O_2$	$8x10^{-11}$	b
$H_2O^+ + H_2O \rightarrow H_3O^+ + OH$	$1.7x10^{-9}$	4
$OH + HNO_2 \rightarrow NO_2 + H_2O$	$1.8x10^{-11}exp(-390/T)$	11
$H_2O^+ + O_2 \rightarrow O_2^+ + H_2O$	$4.3x10^{-10}$	4
$OH + O_3 \rightarrow HO_2 + O_2$	$1.9x10^{-12}exp(-1000/T)$	24
$N_3^+ + O_2 \rightarrow NO^+ + N_2O$	$3.6x10^{-11}$	4
$OH + N_2O \rightarrow HNO + NO$	$3.8x10^{-17}$	4
$N_3^+ + O_2 \rightarrow NO_2^+ + N_2$	$1.5x10^{-11}$	4
$HO_2 + NO_2 + N_2 \rightarrow$ $HO_2NO_2 + N_2$	$1.5x10^{-31}(T/300)^{-3.2}$	11
$N_3^+ + NO \rightarrow NO^+ + N + N_2$	$1.4x10^{-10}$	4
$HO_2 + O_3 \rightarrow OH + O_2 + O_2$	$1.4x10^{-14}exp(-600/T)$	24
$N_3^+ + NO_2 \rightarrow NO^+ + NO + N_2$	$7x10^{-11}$	4
$NO_2 + O_3 \rightarrow NO_3 + O_2$	$1.2x10^{-13}exp(-2450/T)$	11
$N_3^+ + NO_2 \rightarrow NO_2^+ + N + N_2$	$7x10^{-11}$	4
$N_3^+ + N_2O \rightarrow NO^+ + N_2 + N_2$	$5x10^{-11}$	4
$O + NO_2 \rightarrow NO + O_2$	$6.5x10^{-12}exp(120/T)$	11
$O + NO_3 \rightarrow O_2 + NO_2$	$1x10^{-11}$	4
$N_3^+ + NO_2^- \rightarrow N + N_2 + NO_2$	$2x10^{-6}(T/300)^{-0.5}$	4
$O + OH \rightarrow H + O_2$	$2.3x10^{-11}exp(110/T)$	15
$O^+ + N_2 \rightarrow NO^+ + N$	$1.2x10^{-12}$	4
$OH + OH + O_2 \rightarrow H_2O_2 + O_2$	$6.9x10^{-31}(T/300)^{-0.8}$	11
$O^+ + NO \rightarrow NO^+ + O$	$1.7x10^{-12}$	4
$OH + H_2O_2 \rightarrow H_2O + HO_2$	$2.9x10^{-12}exp(-160/T)$	24
$O^+ + O_2 \rightarrow O_2^+ + O$	$1.9x10^{-11}$	4
$H + HO_2 \rightarrow H_2 + O_2$	$1.1x10^{-10}exp(-1070/T)$	15
$O^+ + NO_2 \rightarrow NO_2^+ + O$	$1.6x10^{-9}$	4

$HO_2NO_2 + O_2 \rightarrow HO_2 + NO_2 + O_2$	$3.6\times10^{-6}\exp(-10000/T)$	24
$O^+ + NO_2^- \rightarrow O + NO_2$	$2\times10^{-6}(T/300)^{-0.5}$	4
$O_2^+ + NO \rightarrow NO^+ + O_2$	4.4×10^{-10}	4
$O_2^+ + NO_2 \rightarrow NO_2^+ + O_2$	8.8×10^{-9}	4
$O_2^+\cdot H_2O + H_2O \rightarrow H_3O^+ + OH + O_2$	1.2×10^{-9}	4
$H_3O^+ + H_2O + M \rightarrow H_3O^+\cdot H_2O + M$	5×10^{-27}	4
$O_2^+ + NO_2^- \rightarrow O_2 + NO_2$	$2\times10^{-6}(T/300)^{-0.5}$	4
$H_3O^+\cdot H_2O + H_2O \rightarrow H_3O^+\cdot(H_2O)_2$	1×10^{-9}	4
$NO_2^+ + NO \rightarrow NO^+ + NO_2$	2.9×10^{-10}	4
$H_3O^+\cdot(H_2O)_2 + NO_2^- \rightarrow H + (H_2O)_3 + NO_2$	$2\times10^{-7}(T/300)^{-0.5}$	4
$H_3O^+\cdot(H_2O)_2 + NO_3^- \rightarrow H + (H_2O)_3 + NO_3$	$2\times10^{-7}(T/300)^{-0.5}$	4
$NO_2^+ + NO_2^- \rightarrow NO_2 + NO_2$	$3\times10^{-6}(T/300)^{-0.5}$	4
$NO_2^+ + NO_3^- \rightarrow NO_2 + NO_3$	$3\times10^{-6}(T/300)^{-0.5}$	4
$N_2^+ + NO \rightarrow NO^+ + N_2$	3.3×10^{-10}	4
$N_3^+ + H_2O \rightarrow H_2NO^+ + N_2$	3.3×10^{-10}	4
$N_2^+ + NO_2 \rightarrow NO_2^+ + N_2$	3.3×10^{-10}	4
$N_2^+ + NO_2 \rightarrow NO^+ + N_2O$	5.0×10^{-11}	4
$H_2NO^+ + NO_2^- \rightarrow H_2O + N + NO_2$	$2\times10^{-6}(T/300)^{-0.5}$	4
$H_2NO^+ + NO_3^- \rightarrow H_2O + N + NO_3$	$2\times10^{-6}(T/300)^{-0.5}$	4
$NO_2^- + HNO_3 \rightarrow NO_3^- + HNO_2$	1.6×10^{-9}	4
$N_2^+ + NO_2^- \rightarrow N_2 + NO_2$	$3\times10^{-6}(T/300)^{-0.5}$	4

$NO_2^- + NO_2 \rightarrow NO_3^- + NO$	$1x10^{-13}$	4
$N_2^+ + NO_3^- \rightarrow N_2 + NO_3$	$3x10^{-6}(T/300)^{-0.5}$	4
$NO_2^- + N_2O \rightarrow NO_3^- + N_2$	$5x10^{-13}$	4
$NO_2^- + N_2O_5 \rightarrow NO_3^- + NO_2 + NO_2$	$7x10^{-10}$	4
$NO_2^- + O_3 \rightarrow NO_3^- + O_2$	$1.2x10^{-10}$	4
$NO_3^- + NO \rightarrow NO_2^- + NO_2$	$5x10^{-13}$	4
$NO^+ + NO_2^- \rightarrow NO + NO_2$	$3x10^{-6}(T/300)^{-0.5}$	4
$NO^+ + NO_3^- \rightarrow NO + NO_3$	$3x10^{-6}(T/300)^{-0.5}$	4
$O_2^- + NO_2 \rightarrow NO_2^- + O_2$	$7x10^{-10}$	4
$NO^+ + O_2 + M \rightarrow NO^+{\cdot}O_2 + M$	$3x10^{-31}$	26
$O_2^- + N_2^+ \rightarrow N_2 + O_2$	$2x10^{-6}(T/300)^{-0.5}$	4
$NO^+{\cdot}O_2 + NO_2^- \rightarrow NO + O_2 + NO_2$	$3x10^{-6}(T/300)^{-0.5}$	4
$N(^2D) + NH_3 \rightarrow NH + NH_2$	$5x10^{-11}$	4
$NO^+{\cdot}O_2 + NO_2^- \rightarrow NO_3 + NO_2$	$2x10^{-7}(T/300)^{-0.5}$	4
$NO^+{\cdot}O_2 + NO_3^- \rightarrow NO + O_2 + NO_3$	$3x10^{-6}(T/300)^{-0.5}$	4
$OH + NH_3 \rightarrow NH_2 + H_2O$	$3.5x10^{-12}exp(-925/T)$	11
$O(^1D) + NH_3 \rightarrow NH_2 + OH$	$2.5x10^{-10}$	4
$NH_2 + NO \rightarrow N_2 + H_2O$	$1.6x10^{-11}(T/300)^{-1.5}$	11
$N^+ + N_2 + M \rightarrow N_3^+ + M$	$5.2x10^{-30}$	4
$NH_2 + NO_2 \rightarrow N_2O + H_2O$	$1.9x10^{-11}(T/300)^{-2.2}$	11
$N^+ + O_2 \rightarrow NO^+ + O$	$2.6x10^{-10}$	4
$O_2^+ + NH_3 \rightarrow NH_3^+ + O_2$	$1x10^{-9}$	26
$N^+ + O_2 \rightarrow O_2^+ + N$	$3.1x10^{-10}$	4
$NH_3^+ + NH_3 \rightarrow NH_4^+ + NH_2$	$2.2x10^{-9}$	4
$N^+ + O_2 \rightarrow O^+ + NO$	$3.6x10^{-11}$	4

$H_3O^+ + NH_3 \rightarrow NH_4^+ + H_2O$	2.5×10^{-9}	4
$N^+ + NO \rightarrow NO^+ + N$	9×10^{-10}	4
$N^+ + NH_3 \rightarrow NH_3^+ + N$	2.4×10^{-9}	4
$N_2^+ + N_2 + M \rightarrow N_4^+ + M$	1.1×10^{-29}	4
$N_3^+ + NH_3 \rightarrow NH_3^+ + N + N_2$	2.1×10^{-9}	4
$N_2^+ + O_2 \rightarrow O_2^+ + N_2$	5.1×10^{-11}	4
$N_2^+ + NH_3 \rightarrow NH_3^+ + N_2$	1.9×10^{-9}	4
$N_4^+ + NO \rightarrow NO^+ + N_2 + N_2$	1.8×10^{-9}	4
$N_4^+ + NO_2 \rightarrow NO_2^+ + N_2 + N_2$	2.5×10^{-10}	4
$NH_3^+ + NO_3^- \rightarrow NH_3 + NO_3$	$5\times10^{-6}(T/300)^{-0.5}$	b
$N_4^+ + NO_2 \rightarrow NO^+ + N_2O + N_2$	5×10^{-11}	4
$NH_4^+ + NO_3^- \rightarrow$ $NH_3 + H + NO_3$	$3\times10^{-6}(T/300)^{-0.5}$	4
$N_4^+ + O_2 \rightarrow O_2^+ + N_2 + N_2$	2.5×10^{-10}	4
$NO^+ + H_2O + M \rightarrow$ $NO^+\cdot H_2O + M$	1.6×10^{-28}	4
$NO^+\cdot H_2O + H_2O + M \rightarrow$ $NO^+\cdot(H_2O)_2 + M$	1×10^{-27}	4
$N_4^+ + NO_2^- \rightarrow NO_2 + N_2 + N_2$	$3\times10^{-6}(T/300)^{-0.5}$	4
$NO^+\cdot(H_2O)_2 + M \rightarrow$ $NO^+\cdot H_2O + H_2O + M$	1.3×10^{-12}	4
$N_4^+ + NO_3^- \rightarrow NO_3 + N_2 + N_2$	$3\times10^{-6}(T/300)^{-0.5}$	4
$NO^+\cdot(H_2O)_2 + H_2O \rightarrow NO^+\cdot(H_2O)_3$	1×10^{-9}	4
$O_2^+ + H_2O + M \rightarrow O_2^+\cdot H_2O + M$	2.5×10^{-28}	4
$NO^+\cdot(H_2O)_3 + H_2O \rightarrow$ $H_3O^+\cdot(H_2O)_2 + HNO_2$	8×10^{-11}	4
$NH_2 + O \rightarrow NH + OH$	1.2×10^{-11}	26
$NH_2 + O \rightarrow HNO + H$	7.6×10^{-11}	26

$HO_2NO_2 + N_2 \rightarrow HO_2 + NO_2 + N_2$	$5x10^{-6}exp(-10000/T)$	11
$OH + NO_2 + O_2 \rightarrow HNO_3 + O_2$	$2.6x10^{-30}(T/300)^{-2.9}$	11
$OH + H_2 \rightarrow H_2O + H$	$7.7x10^{-12}exp(-2100/T)$	15
$O(^1D) + H_2O \rightarrow H_2 + O_2$	$2.3x10^{-12}$	24
$O(^1D) + H_2 \rightarrow OH + H$	$1.1x10^{-10}$	24
$O + H_2O_2 \rightarrow OH + HO_2$	$1.4x10^{-12}exp(-2000/T)$	15
$O+ H_2 \rightarrow OH + H$	$1.6x10^{-11}exp(-4570/T)$	24
$H + HO_2 \rightarrow H_2O + O$	$9.4x10^{-13}$	24
$O + O_2 + N_2 \rightarrow O_2 + O + N_2$	$6.2x10^{-34}(T/300)^{-2.0}$	30[b]
$HO_2 + HO_2 + M \rightarrow H_2O_2 + O_2 + M$	$1.9x10^{-33}exp(980/T)$	11
$O + NO + N_2 \rightarrow NO_2 + N_2$	$9.1x10^{-28}T^{-1.6}$	11
$NO_2 + NO_3 + M \rightarrow N_2O_5 + M$	$2.7x10^{-30}(T/300)^{-3.4}$	11
$N^+ + H_2O \rightarrow H_2O^+ + N$	$5.55x10^{-8}T^{-0.52}$	5
$H_2O^+ + NO_2^- \rightarrow H_2O + NO_2$	$2x10^{-6}(T/300)^{-0.5}$	32
$H_2O^+ + NO_3^- \rightarrow H_2O + NO_3$	$2x10^{-6}(T/300)^{-0.5}$	32
$H_2O^+ + O_2^- \rightarrow H_2O + O_2$	$2x10^{-6}(T/300)^{-0.5}$	32
$H_3O^+ + NO_2^- \rightarrow H_2O + H + NO_2$	$2x10^{-6}(T/300)^{-0.5}$	32
$H_3O^+ + NO_3^- \rightarrow H_2O + H + NO_3$	$2x10^{-6}(T/300)^{-0.5}$	32
$H_3O^+ + O_2^- \rightarrow H_2O + H + O_2$	$2x10^{-6}(T/300)^{-0.5}$	32
$O_2^+ + NO_3^- \rightarrow O_2 + NO_3$	$2x10^{-6}(T/300)^{-0.5}$	32
$O_2^+ + O_2^- \rightarrow O_2 + O_2$	$2x10^{-6}(T/300)^{-0.5}$	32
$N_3^+ + NO_3^- \rightarrow N_2 + N + NO_3$	$2x10^{-6}(T/300)^{-0.5}$	b
$N_3^+ + O_2^- \rightarrow N_2 + N + O_2$	$2x10^{-6}(T/300)^{-0.5}$	b
$NO^+ + O_2^- \rightarrow NO + O_2$	$2x10^{-6}(T/300)^{-0.5}$	32
$NO_2^+ + O_2^- \rightarrow NO_2 + O_2$	$2x10^{-6}(T/300)^{-0.5}$	32

$O^+ + NO_3^- \rightarrow O + NO_3$	$2x10^{-6}(T/300)^{-0.5}$	32
$O^+ + O_2^- \rightarrow O + O_2$	$2x10^{-6}(T/300)^{-0.5}$	32
$NO^+ \cdot O_2 + O_2^- \rightarrow NO + O_2 + O_2$	$2x10^{-6}(T/300)^{-0.5}$	b
$N^+ + O_2^- \rightarrow N + O_2$	$2x10^{-6}(T/300)^{-0.5}$	32
$N^+ + NO_2^- \rightarrow N + NO_2$	$2x10^{-6}(T/300)^{-0.5}$	32
$N^+ + NO_3^- \rightarrow N + NO_3$	$2x10^{-6}(T/300)^{-0.5}$	32
$N_4^+ + O_2^- \rightarrow N_2 + N_2 + O_2$	$2x10^{-6}(T/300)^{-0.5}$	b
$O_2^+ \cdot H_2O + O_2^- \rightarrow O_2 + O_2 + H_2O$	$2x10^{-6}(T/300)^{-0.5}$	b
$O_2^+ \cdot H_2O + NO_3^- \rightarrow O_2 + NO_3 + H_2O$	$2x10^{-6}(T/300)^{-0.5}$	b
$O_2^+ \cdot H_2O + NO_2^- \rightarrow O_2 + H_2O + NO_2$	$2x10^{-6}(T/300)^{-0.5}$	b
$H_3O^+ \cdot H_2O + NO_2^- \rightarrow H + H_2O + H_2O + NO_2$	$2x10^{-6}(T/300)^{-0.5}$	b
$H_3O^+ \cdot H_2O + NO_3^- \rightarrow H + H_2O + H_2O + NO_3$	$2x10^{-6}(T/300)^{-0.5}$	b
$H_3O^+ \cdot H_2O + O_2^- \rightarrow H + H_2O + H_2O + O_2$	$2x10^{-6}(T/300)^{-0.5}$	b
$H_3O^+ \cdot (H_2O)_2 + O_2^- \rightarrow H + (H_2O)_3 + O_2$	$2x10^{-6}(T/300)^{-0.5}$	b
$H_2NO^+ + O_2^- \rightarrow H_2O + N + O_2$	$2x10^{-6}(T/300)^{-0.5}$	b
$NH_3^+ + NO_2^- \rightarrow NH_3 + NO_2$	$2x10^{-6}(T/300)^{-0.5}$	32
$NH_3^+ + O_2^- \rightarrow NH_3 + O_2$	$2x10^{-6}(T/300)^{-0.5}$	32
$NH_4^+ + NO_2^- \rightarrow NH_3 + H + NO_2$	$2x10^{-6}(T/300)^{-0.5}$	b
$NH_4^+ + NO_3^- \rightarrow NH_3 + H + NO_3$	$2x10^{-6}(T/300)^{-0.5}$	b
$NH_4^+ + O_2^- \rightarrow NH_3 + H + O_2$	$2x10^{-6}(T/300)^{-0.5}$	b
$NO^+ \cdot H_2O + NO_2^- \rightarrow$	$2x10^{-6}(T/300)^{-0.5}$	b

$NO + H_2O + NO_2$		
$NO^+\cdot H_2O + NO_3^- \rightarrow NO + H_2O + NO_3$	$2x10^{-6}(T/300)^{-0.5}$	b
$NO^+\cdot H_2O + O_2^- \rightarrow NO + H_2O + O_2$	$2x10^{-6}(T/300)^{-0.5}$	b
$NO^+\cdot (H_2O)_2 + NO_3^- \rightarrow NO + H_2O + H_2O + NO_3$	$2x10^{-6}(T/300)^{-0.5}$	b
$NO^+\cdot (H_2O)_3 + NO_3^- \rightarrow NO + H_2O + H_2O + H_2O + NO_3$	$2x10^{-6}(T/300)^{-0.5}$	b
$NO^+\cdot (H_2O)_2 + NO_2^- \rightarrow NO + H_2O + H_2O + NO_2$	$2x10^{-6}(T/300)^{-0.5}$	b
$NO^+\cdot (H_2O)_3 + NO_2^- \rightarrow NO + H_2O + H_2O + H_2O + NO_2$	$2x10^{-6}(T/300)^{-0.5}$	b
$NO^+\cdot (H_2O)_2 + O_2^- \rightarrow NO + H_2O + H_2O + O_2$	$2x10^{-6}(T/300)^{-0.5}$	b
$NO^+\cdot (H_2O)_3 + O_2^- \rightarrow NO + H_2O + H_2O + H_2O + O_2$	$2.00x10^{-6}(T/300)^{-0.5}$	b
$O + H + M \rightarrow OH + M$	$1.62x10^{-32}$	28
$H + H_2O_2 \rightarrow H_2O + OH$	$4x10^{-11}exp(-2000/T)$	15
$NO_2 + NO_2 + N_2 \rightarrow N_2O_4 + N_2$	$1.4x10^{-33}(T/300)^{-3.8}$	17
$N_2O_4 + N_2 \rightarrow NO_2 + NO_2 + N_2$	$1.29x10^{-5}(T/300)^{-3.8} * exp(-6460/T)$	17
$NH_2 + H_2 \rightarrow NH_3 + H$	$5.98x10^{-12}exp(-2290/T)$	27
$NH_3 + H \rightarrow NH_2 + H_2$	$1.35x10^{-10}exp(-3660/T)$	27
$OH + NO_3 \rightarrow HO_2 + NO_2$	$2.6x10^{-11}$	29
$HO_2 + NO_3 \rightarrow OH + NO_2 + O_2$	$3.6x10^{-12}$	29
$HO_2 + NO_3 \rightarrow HNO_3 + O_2$	$9.2x10^{-13}$	29
$H + H_2O_2 \rightarrow HO_2 + H_2$	$8x10^{-11}exp(-4000/T)$	15
$HNO_3 + NO \rightarrow HNO_2 + NO_2$	$7.37x10^{-21}$	25

$H_2 + O_2 \rightarrow H + HO_2$	$2.4x10^{-10}exp(-28500/T)$	15
$H + O_2 \rightarrow OH + O$	$2.8x10^{-7}T^{-0.9}exp(-8750/T)$	15
$OH + M \rightarrow O + H + M$	$4x10^{-9}exp(-50000/T)$	15
$OH + O_2 \rightarrow O + HO_2$	$3.7x10^{-11}exp(-26500/T)$	15
$OH + H \rightarrow O + H_2$	$1.14x10^{-12}T^{0.67}exp(-518/T)$	5
$HO_2 + M \rightarrow H + O_2 + M$	$2x10^{-5}T^{-1.18}exp(-24363/T)$	15
$HO_2 + H_2 \rightarrow H_2O_2 + H$	$5x10^{-11}exp(-13100/T)$	15
$H_2O_2 + O_2 \rightarrow HO_2 + HO_2$	$9x10^{-11}exp(-20000/T)$	15
$H_2O + H \rightarrow H_2 + OH$	$1.03x10^{-16}T^{1.9}exp(-9265/T)$	15
$H_2O + O \rightarrow OH + OH$	$7.6x10^{-15}T^{1.3}exp(-8605/T)$	15
$H^- + N_2^+ \rightarrow H + N_2$	$3x10^{-6}(T/300)^{-0.5}$	b
$O^- + N_2^+ \rightarrow O + N_2$	$3x10^{-6}(T/300)^{-0.5}$	b
$O^- + H_2^+ \rightarrow O + H_2$	$3x10^{-6}(T/300)^{-0.5}$	32
$O_2^- + H_2^+ \rightarrow O_2 + H_2$	$3x10^{-6}(T/300)^{-0.5}$	32
$H^- + H_2^+ \rightarrow H + H_2$	$3x10^{-6}(T/300)^{-0.5}$	32
$H^- + H_2O^+ \rightarrow H + H_2O$	$3x10^{-6}(T/300)^{-0.5}$	32
$O^- + H_2O^+ \rightarrow O + H_2O$	$3x10^{-6}(T/300)^{-0.5}$	32
$H^- + H_3O^+ \rightarrow H_2 + H_2O$	$3x10^{-6}(T/300)^{-0.5}$	b
$O^- + H_3O^+ \rightarrow OH + H_2O$	$3x10^{-6}(T/300)^{-0.5}$	b
$H^- + O_2^+ + M \rightarrow H_2O + M$	$1.2x10^{-25}$	b
$O^- + O_2^+ \rightarrow O + O_2$	$3x10^{-6}(T/300)^{-0.5}$	32
$H^- + N_3^+ \rightarrow NH + N_2$	$3x10^{-6}(T/300)^{-0.5}$	b
$O^- + N_3^+ \rightarrow NO + N_2$	$3x10^{-6}(T/300)^{-0.5}$	b
$H^- + NO^+ + M \rightarrow HNO + M$	$1.2x10^{-25}$	b
$O^- + NO^+ \rightarrow NO + O$	$3x10^{-6}(T/300)^{-0.5}$	b
$H^- + NO_2^+ + M \rightarrow HNO_2 + M$	$1.2x10^{-25}$	b
$O^- + NO_2^+ \rightarrow NO_2 + O$	$3x10^{-6}(T/300)^{-0.5}$	32

$H^- + O^+ + M \rightarrow OH + M$	1.2×10^{-25}	b
$O^- + O^+ + M \rightarrow O_2 + M$	1.2×10^{-25}	b
$H^- + NO^+\cdot O_2 \rightarrow HNO + O_2$	$3\times10^{-6}(T/300)^{-0.5}$	b
$O^- + NO^+\cdot O_2 \rightarrow NO_2 + O_2$	$3\times10^{-6}(T/300)^{-0.5}$	b
$H^- + N^+ + M \rightarrow NH + M$	1.2×10^{-25}	b
$O^- + N^+ + M \rightarrow NO + M$	1.2×10^{-25}	b
$H^- + N_4^+ \rightarrow H + N_2 + N_2$	$3\times10^{-6}(T/300)^{-0.5}$	b
$O^- + N_4^+ \rightarrow O + N_2 + N_2$	$3\times10^{-6}(T/300)^{-0.5}$	b
$H^- + O_2^+\cdot H_2O \rightarrow HO_2 + H_2O$	$3\times10^{-6}(T/300)^{-0.5}$	b
$O^- + O_2^+\cdot H_2O \rightarrow O + O_2 + H_2O$	$3\times10^{-6}(T/300)^{-0.5}$	b
$H^- + H_3O^+\cdot H_2O \rightarrow H_2 + H_2O + H_2O$	$3\times10^{-6}(T/300)^{-0.5}$	b
$O^- + H_3O^+\cdot H_2O \rightarrow OH + H_2O + H_2O$	$3\times10^{-6}(T/300)^{-0.5}$	b
$H^- + H_3O^+\cdot(H_2O)_2 \rightarrow H_2 + (H_2O)_3$	$3\times10^{-6}(T/300)^{-0.5}$	b
$O^- + H_3O^+\cdot(H_2O)_2 \rightarrow OH + (H_2O)_3$	$3\times10^{-6}(T/300)^{-0.5}$	b
$H^- + H_2NO^+ \rightarrow H_2 + HNO$	$3\times10^{-6}(T/300)^{-0.5}$	b
$O^- + H_2NO^+ \rightarrow OH + HNO$	$3\times10^{-6}(T/300)^{-0.5}$	b
$H^- + NH_3^+ \rightarrow H + NH_3$	$3\times10^{-6}(T/300)^{-0.5}$	b
$O^- + NH_3^+ \rightarrow O + NH_3$	$3\times10^{-6}(T/300)^{-0.5}$	b
$H^- + NH_4^+ \rightarrow H_2 + NH_3$	$3\times10^{-6}(T/300)^{-0.5}$	b
$O^- + NH_4^+ \rightarrow OH + NH_3$	$3\times10^{-6}(T/300)^{-0.5}$	b
$H^- + NO^+\cdot H_2O \rightarrow H + NO + H_2O$	$3\times10^{-6}(T/300)^{-0.5}$	b
$O^- + NO^+\cdot H_2O \rightarrow O + NO + H_2O$	$3\times10^{-6}(T/300)^{-0.5}$	b
$H^- + NO^+\cdot(H_2O)_2 \rightarrow HNO + H_2O + H_2O$	$3\times10^{-6}(T/300)^{-0.5}$	b
$O^- + NO^+\cdot(H_2O)_2 \rightarrow NO_2 + H_2O + H_2O$	$3\times10^{-6}(T/300)^{-0.5}$	b

$H^- + NO^+\cdot(H_2O)_3 \rightarrow HNO + H_2O + H_2O + H_2O$	$3\text{x}10^{-6}(T/300)^{-0.5}$	b
$O^- + NO^+\cdot(H_2O)_3 \rightarrow NO_2 + H_2O + H_2O + H_2O$	$3\text{x}10^{-6}(T/300)^{-0.5}$	b
$(H_2O)_3 \rightarrow H_2O + H_2O + H_2O$	$1\text{x}10^{-7}$	b
$OH + NO_2 + H_2O \rightarrow HNO_3 + H_2O$	$2.2\text{x}10^{-30}(T/300)^{-2.9}$	30
$N_2^+ + H_2O \rightarrow H_2O^+ + N_2$	$2\text{x}10^{-9}$	b
$O + OH + M \rightarrow HO_2 + M$	$2.76\text{x}10^{-31}$	30
$O(^1D) + O_3 \rightarrow O_2 + O + O$	$1.2\text{x}10^{-10}$	31
$O(^1D) + NO \rightarrow O_2 + N$	$8.5\text{x}10^{-11}$	31
$NH + NO \rightarrow N_2 + OH$	$4.5\text{x}10^{-11}$	31
$N_3 + NO \rightarrow N_2O + N_2$	$1.19\text{x}10^{-12}$	31
$NH_2 + O \rightarrow H_2 + NO$	$8.3\text{x}10^{-12}$	31
$OH + NO_2 \rightarrow HO_2 + NO$	$3.03\text{x}10^{-11}\exp(-3360/T)$	31
$NO_3 + NO_2 \rightarrow NO + NO_2 + O_2$	$8.21\text{x}10^{-14}\exp(-1480/T)$	31
$O(^1D) + NO_2 \rightarrow O_2 + NO$	$2.5\text{x}10^{-10}$	31
$O(^1D) + N_2O \rightarrow NO + NO$	$6.7\text{x}10^{-11}$	31
$NO_2 + O_3 \rightarrow O_2 + O_2 + NO$	$1.0\text{x}10^{-18}$	22
$O + N_3 \rightarrow NO + N_2$	$1.12\text{x}10^{-11}$	31
$O + HNO \rightarrow OH + NO$	$1.82\text{x}10^{-11}$	31
$HNO + O_2 \rightarrow NO + HO_2$	$5.25\text{x}10^{-12}\exp(-1510/T)$	23
$O + O + M \rightarrow O_2 + M$	$5.21\text{x}10^{-35}\exp(900/T)$	31

Additional reactions of $N_2/O_2/H_2O/CO_2$

Reaction	Rate Coefficient [c]	Ref.
$N_2(A) + CO_2 \rightarrow N_2 + CO_2$	$2.5\text{x}10^{-11}$	36
$N_2(A) + CO \rightarrow N_2 + CO$	$1.1\text{x}10^{-10}$	36
$O(^1D) + CO_2 \rightarrow O + CO_2$	$7.4\text{x}10^{-11}$	b

$OH + CO \rightarrow CO_2 + H$	$1.12\text{x}10^{-13}\exp(-9.1\text{x}10^{-4}\text{ x }T)$	15
$CO_2^+ + NO \rightarrow NO^+ + CO_2$	$1.2\text{x}10^{-10}$	4
$CO_2^+ + O_2 \rightarrow O_2^+ + CO_2$	$5.6\text{x}10^{-11}$	4
$CO_2^+ + NO_2^- \rightarrow CO_2 + NO_2$	$2\text{x}10^{-6}(T/300)^{-0.5}$	32
$CO_2^+ + NO_3^- \rightarrow CO_2 + NO_3$	$2\text{x}10^{-6}(T/300)^{-0.5}$	32
$CO_2^+ + O_2^- \rightarrow CO_2 + O_2$	$2\text{x}10^{-6}(T/300)^{-0.5}$	32
$OH + CO \rightarrow HOCO^*$	$1.55\text{x}10^{-13}$	b
$CO_2 + H \rightarrow CO + OH$	$2.5\text{x}10^{-10}\exp(-13300/T)$	15
$CO_2 + O \rightarrow CO + O_2$	$2.8\text{x}10^{-11}\exp(-26500/T)$	15
$CO + O_2 \rightarrow CO_2 + O$	$4.2\text{x}10^{-12}\exp(-24000/T)$	15
$CO + O + M \rightarrow CO_2 + M$	$1.7\text{x}10^{-33}\exp(-1510/T)$	15
$CO + HO_2 \rightarrow OH + CO_2$	$2.5\text{x}10^{-10}\exp(-11900/T)$	15
$HCO + M \rightarrow H + CO + M$	$8.5\text{x}10^{-3}T^{-2.14}\exp(-10278/T)$	15
$HCO + H_2 \rightarrow CH_2O + H$	$3\text{x}10^{-18}T^{2.0}\exp(-8972/T)$	15
$HCO + O_2 \rightarrow HO_2 + CO$	$8.5\text{x}10^{-11}\exp(-850/T)$	15
$HCO + H \rightarrow H_2 + CO$	$2\text{x}10^{-10}$	15
$HCO + O \rightarrow H + CO_2$	$5\text{x}10^{-11}$	15
$HCO + O \rightarrow OH + CO$	$5\text{x}10^{-11}$	15
$HCO + OH \rightarrow H_2O + CO$	$5\text{x}10^{-11}$	15
$HCO + HO_2 \rightarrow OH + H + CO_2$	$5\text{x}10^{-11}$	15
$HCO + H_2O_2 \rightarrow CH_2O + HO_2$	$1.7\text{x}10^{-13}\exp(-3486/T)$	15
$HCO + H_2O \rightarrow CH_2O + OH$	$3.9\text{x}10^{-16}T^{1.35}\exp(-13146/T)$	15
$HCO + HCO \rightarrow CH_2O + CO$	$3\text{x}10^{-11}$	15
$HCO + HCO \rightarrow H_2 + CO + CO$	$5\text{x}10^{-12}$	15
$H^- + CO_2^+ \rightarrow H + CO_2$	$3\text{x}10^{-6}(T/300)^{-0.5}$	b
$O^- + CO_2^+ \rightarrow O + CO_2$	$3\text{x}10^{-6}(T/300)^{-0.5}$	b
$CH_2O + OH \rightarrow H + HCOOH$	$2\text{x}10^{-13}$	31

$HCOOH + OH \rightarrow$ $H_2O + CO_2 + H$	$4.8x10^{-13}$	31
$CN + O \rightarrow CO + N$	$1.7x10^{-11}$	31
$CN + N \rightarrow N_2 + C$	$3x10^{-10}$	b
$CN + N + M \rightarrow CNN + M$	$2.76x10^{-32}$	31
$CN + NO \rightarrow N_2 + CO$	$1.2x10^{-13}$	31
$CN + N_2O \rightarrow CNN + NO$	$6.40x10^{-21}T^{2.6}exp(-1860/T)$	31
$CN + HCN \rightarrow NCCN + H$	$6.31x10^{-17}T^{1.57}exp(-50/T)$	31
$CN + H_2O \rightarrow HCN + OH$	$1.33x10^{-11}exp(-3752/T)$	31
$CN + H_2 \rightarrow HCN + H$	$1.13x10^{-10}exp(-2700/T)$	31
$CN + O_2 \rightarrow NCO + O$	$1.1x10^{-11}exp(205/T)$	31
$CN + CO_2 \rightarrow NCO + CO$	$2x10^{-15}$	31
$HCN + O \rightarrow OH + CN$	$4.5x10^{-15}T^{1.58}exp(-13386/T)$	31
$HCN + O \rightarrow H + NCO$	$3.3x10^{-16}T^{1.47}exp(-3774/T)$	31
$HCN + O \rightarrow CO + NH$	$9.0x10^{-16}T^{1.21}exp(-3824/T)$	31
$HCN + OH \rightarrow H_2O+ CN$	$1.28x10^{-11}exp(-4161/T)$	31
$HCN + OH \rightarrow HOCN + H$	$2.01x10^{-11}exp(-8516/T)$	31
$HCN + OH \rightarrow HNCO + H$	$2.84x10^{-13}exp(-4397/T)$	31
$HCN + OH \rightarrow NH_2 + CO$	$1.07x10^{-13}exp(-5892/T)$	31
$HCN + H \rightarrow CN + H_2$	$6.31x10^{-10}exp(-12400/T)$	31
$NCO + H_2 \rightarrow H + HNCO$	$1.26x10^{-21}T^{3}exp(-2012/T)$	31
$NCO + O \rightarrow NO + CO$	$1.48x10^{-11}$	31
$NCO + O_2 \rightarrow NO + CO_2$	$1.32x10^{-12}$	31
$NCO + NO \rightarrow CO + N_2 + O$	$7.61x10^{-12}$	31
$NCO + NO \rightarrow CO_2 + N_2$	$1.45x10^{-11}$	31
$NCO + NO \rightarrow N_2O + CO$	$1.09x10^{-11}$	31
$NCCN + O \rightarrow CN + NCO$	$4.15x10^{-11}exp(-5500/T)$	31

NCCN + H $\rightarrow$ NCN + CN	$8.59\text{x}10^{-16}$	31
CO + H + M $\rightarrow$ HCO + M	$1.99\text{x}10^{-33}\text{exp}(-842/T)$	31
CO + NO_2 $\rightarrow$ CO_2 + NO	$1.48\text{x}10^{-10}\text{exp}(-17009/T)$	31
CO + O_3 $\rightarrow$ O_2 + CO_2	$4\text{x}10^{-25}$	31
C + CO + M $\rightarrow$ C_2O + M	$6.3\text{x}10^{-32}$	31
C_2O + O $\rightarrow$ CO + CO	$9.51\text{x}10^{-11}$	31
C_2O + O_2 $\rightarrow$ C_2O + CO	$3.3\text{x}10^{-13}$	31
C_2O + N $\rightarrow$ CO + CN	$5.5\text{x}10^{-10}$	31
C + N + M $\rightarrow$ CN + M	$9.41\text{x}10^{-33}$	31
C + NCCN $\rightarrow$ CN + CCN	$3\text{x}10^{-11}$	31
C + NO $\rightarrow$ CN + O	$4.8\text{x}10^{-11}$	31
C + N_2 + M $\rightarrow$ CNN + M	$3.1\text{x}10^{-33}$	31
C + N_3 $\rightarrow$ CN + N_2	$1.10\text{x}10^{-10}$	31
C + O_2 $\rightarrow$ CO + O	$2.6\text{x}10^{-11}$	31
CCN+ O $\rightarrow$ CO + CN	$6\text{x}10^{-12}$	31
CCN+ N $\rightarrow$ CN + CN	$1\text{x}10^{-10}$	31
CO_2 + N $\rightarrow$ CO + NO	$3.2\text{x}10^{-13}\text{exp}(-1710/T)$	31
C^+ + H^- $\rightarrow$ C + H	$5\text{x}10^{-8}\ (T/300)^{-0.5}$	32
C^+ + O^- $\rightarrow$ C + O	$5\text{x}10^{-8}\ (T/300)^{-0.5}$	32
C^+ + O_2^- $\rightarrow$ C + O_2	$5\text{x}10^{-8}\ (T/300)^{-0.5}$	32

Additional reactions due to the presence of C_3H_6/C_3H_8

Reaction	k^a	n	E_a (K)	Ref
$C_3H_8 + H \rightarrow n\text{-}C_3H_7 + H_2$	4.31×10^{-12}	2.54	$3.40\times10^{+03}$	7
$C_3H_8 + H \rightarrow i\text{-}C_3H_7 + H_2$	1.90×10^{-12}	2.4	$2.25\times10^{+03}$	7
$C_3H_8 + O \rightarrow n\text{-}C_3H_7 + OH$	1.39×10^{-12}	2.68	$1.87\times10^{+03}$	7
$C_3H_8 + O \rightarrow i\text{-}C_3H_7 + OH$	4.08×10^{-13}	2.71	$1.06\times10^{+03}$	7
$C_3H_8 + C_2H_5 \rightarrow n\text{-}C_3H_7 + C_2H_6$	1.65×10^{-15}	3.65	$4.60\times10^{+03}$	7
$C_3H_8 + C_2H_5 \rightarrow i\text{-}C_3H_7 + C_2H_6$	9.31×10^{-16}	3.46	$3.76\times10^{+03}$	7
$C_3H_8 + CH_3 \rightarrow n\text{-}C_3H_7 + CH_4$	1.65×10^{-15}	3.65	$3.60\times10^{+03}$	7
$C_3H_8 + CH_3 \rightarrow i\text{-}C_3H_7 + CH_4$	9.31×10^{-16}	3.46	$2.76\times10^{+03}$	7
$C_3H_8 + OH \rightarrow n\text{-}C_3H_7 + H_2O$	7.95×10^{-13}	2	$2.27\times10^{+02}$	7
$C_3H_8 + OH \rightarrow i\text{-}C_3H_7 + H_2O$	1.44×10^{-12}	1	$1.30\times10^{+02}$	7
$n\text{-}C_3H_7 + O_2 \rightarrow n\text{-}C_3H_7O_2$	5.64×10^{-12}	-2.7		7
$i\text{-}C_3H_7 + O_2 \rightarrow (CH_3)_2CHO_2$	1.50×10^{-11}			7
$n\text{-}C_3H_7O_2 + NO \rightarrow n\text{-}C_3H_7O + NO_2$	8.69×10^{-12}			18
$n\text{-}C_3H_7O_2 + NO \rightarrow n\text{-}C_3H_7ONO_2$	1.80×10^{-13}			18
$(CH_3)_2CHO_2 + NO \rightarrow (CH_3)_2CHO + NO_2$	2.70×10^{-12}		$-3.60\times10^{+02}$	18
$(CH_3)_2CHO_2 + NO \rightarrow (CH_3)_2CHONO_2$	3.80×10^{-13}			18
$n\text{-}C_3H_7O_2 + HO_2 \rightarrow n\text{-}C_3H_7OOH + O_2$	1.90×10^{-13}		$-1.30\times10^{+03}$	18
$(CH_3)_2CHO_2 + HO_2 \rightarrow (CH_3)_2CHOOH + O_2$	1.90×10^{-13}		$-1.30\times10^{+03}$	33
$n\text{-}C_3H_7O + O_2 \rightarrow C_2H_5CHO + HO_2$	6.00×10^{-14}		$5.50\times10^{+02}$	18
$(CH_3)_2CHO + O_2 \rightarrow CH_3COCH_3 + HO_2$	1.50×10^{-14}		$2.00\times10^{+02}$	18
$n\text{-}C_3H_7 \rightarrow C_2H_4 + CH_3$	$1.20\times10^{+13}$		$1.53\times10^{+04}$	7
$n\text{-}C_3H_7 \rightarrow C_3H_6 + H$	$1.09\times10^{+13}$		$1.78\times10^{+04}$	7

$n\text{-}C_3H_7 + H_2 \rightarrow C_3H_8 + H$	3.25×10^{-14}	2.84	$4.60\times10^{+03}$	7
$n\text{-}C_3H_7 + H \rightarrow C_3H_6 + H_2$	3.00×10^{-12}			7
$n\text{-}C_3H_7 + OH \rightarrow C_3H_6 + H_2O$	4.00×10^{-11}			7
$n\text{-}C_3H_7 + OH \rightarrow n\text{-}C_3H_7OH$	4.00×10^{-11}			7
$n\text{-}C_3H_7 + HO_2 \rightarrow C_2H_5 + OH + HCHO$	4.00×10^{-11}			7
$n\text{-}C_3H_7 + H_2O_2 \rightarrow HO_2 + C_3H_8$	5.23×10^{-15}	2.11	$1.29\times10^{+03}$	7
$n\text{-}C_3H_7 + CH_4 \rightarrow C_3H_8 + CH_3$	3.63×10^{-16}	4. 2	$5.47\times10^{+03}$	7
$n\text{-}C_3H_7 + C_2H_6 \rightarrow C_3H_8 + C_2H_5$	1.22×10^{-15}	3.82	$4.55\times10^{+03}$	7
$n\text{-}C_3H_7 + HCHO \rightarrow C_3H_8 + HCO$	7.63×10^{-14}	2.9	$2.95\times10^{+03}$	7
$n\text{-}C_3H_7 + HCO \rightarrow C_3H_8 + CO$	1.00×10^{-10}			7
$n\text{-}C_3H_7 + HCO \rightarrow C_3H_7CHO$	2.00×10^{-11}			7
$n\text{-}C_3H_7 + CH_3 \rightarrow CH_4 + C_3H_6$	3.06×10^{-12}	-0.32		7
$n\text{-}C_3H_7 + C_2H_5 \rightarrow C_3H_6 + C_2H_6$	2.40×10^{-12}			7
$n\text{-}C_3H_7 + C_2H_5 \rightarrow C_3H_8 + C_2H_4$	1.90×10^{-12}			7
$n\text{-}C_3H_7 + C_3H_8 \rightarrow C_3H_8 + i\text{-}C_3H_7$	1.13×10^{-17}	4	$2.38\times10^{+03}$	7
$n\text{-}C_3H_7 + n\text{-}C_3H_7 \rightarrow C_3H_6 + C_3H_8$	2.80×10^{-12}			7
$n\text{-}C_3H_7O \rightarrow C_2H_5 + HCHO$	$5.01\times10^{+13}$		$7.85\times10^{+03}$	7
$i\text{-}C_3H_7 \rightarrow C_3H_6 + H$	$1.60\times10^{+13}$		$1.80\times10^{+04}$	7
$i\text{-}C_3H_7 + H_2 \rightarrow C_3H_8 + H$	7.73×10^{-14}	3.28	$4.36\times10^{+03}$	7
$i\text{-}C_3H_7 + H \rightarrow C_3H_6 + H_2$	6.00×10^{-12}			7
$i\text{-}C_3H_7 + OH \rightarrow C_3H_6 + H_2O$	4.00×10^{-11}			7
$i\text{-}C_3H_7 + HO_2 \rightarrow CH_3CHO + CH_3 + OH$	4.00×10^{-11}			7
$i\text{-}C_3H_7 + H_2O_2 \rightarrow C_3H_8 + HO_2$	4.92×10^{-15}	2.83	$2.04\times10^{+03}$	7
$i\text{-}C_3H_7 + C_2H_6 \rightarrow C_3H_8 + C_2H_5$	3.55×10^{-16}	4.2	$4.39\times10^{+03}$	7
$i\text{-}C_3H_7 + HCHO \rightarrow C_3H_8 + HCO$	1.80×10^{-13}		$3.50\times10^{+03}$	7
$i\text{-}C_3H_7 + HCO \rightarrow C_3H_8 + CO$	2.00×10^{-10}			7
$i\text{-}C_3H_7 + HCO \rightarrow C_3H_7CHO$	3.00×10^{-11}			7

$i\text{-}C_3H_7 + CH_3 \rightarrow CH_4 + C_3H_6$	7.52×10^{-12}	-0.68		7
$i\text{-}C_3H_7 + C_2H_5 \rightarrow C_3H_8 + C_2H_4$	4.16×10^{-12}	-0.35		7
$i\text{-}C_3H_7 + C_2H_5 \rightarrow C_3H_6 + C_2H_6$	5.20×10^{-12}	-0.35		7
$i\text{-}C_3H_7 + C_2H_4 \rightarrow C_3H_6 + C_2H_5$	4.40×10^{-14}		$3.32\times10^{+03}$	7
$i\text{-}C_3H_7 + C_3H_8 \rightarrow C_3H_8 + n\text{-}C_3H_7$	3.55×10^{-16}	4.2	$4.39\times10^{+03}$	7
$i\text{-}C_3H_7 + n\text{-}C_3H_7 \rightarrow C_3H_6 + C_3H_8$	1.16×10^{-11}	-0.35		7
$i\text{-}C_3H_7 + i\text{-}C_3H_7 \rightarrow C_3H_6 + C_3H_8$	6.50×10^{-12}	-0.7		7
$CH_4 + H \rightarrow CH_3 + H_2$	1.01×10^{-12}	3	$4.41\times10^{+03}$	19
$CH_4 + HO_2 \rightarrow CH_3 + H_2O_2$	3.00×10^{-13}	0	$9.35\times10^{+03}$	19
$C_2H_6 + H \rightarrow C_2H_5 + H_2$	4.03×10^{-12}	2.1	$3.51\times10^{+03}$	19
$C_2H_6 + O \rightarrow C_2H_5 + OH$	2.91×10^{-12}	2.25	$2.52\times10^{+03}$	19
$C_2H_6 + OH \rightarrow C_2H_5 + H_2O$	1.62×10^{-12}	1.81	$5.33\times10^{+02}$	19
$C_2H_6 + HO_2 \rightarrow H_2O_2 + C_2H_5$	4.90×10^{-13}		$7.52\times10^{+03}$	19
$HCHO + HO_2 \rightarrow H_2O_2 + HCO$	3.30×10^{-12}		$5.87\times10^{+03}$	19
$HCHO + NO_2 \rightarrow HCO + HNO_2$	8.29×10^{-16}	3.67	$6.10\times10^{+03}$	18
$HCHO + NO_3 \rightarrow HCO + HNO_3$	5.80×10^{-16}			18
$CO_2 + N \rightarrow CO + NO$	3.20×10^{-13}		$1.71\times10^{+03}$	18
$CH_3 + H_2 \rightarrow CH_4 + H$	2.61×10^{-14}	2.77	$3.99\times10^{+03}$	19
$CH_3 + O_2 \rightarrow HCHO + OH$	1.60×10^{-15}	2.5	$1.11\times10^{+03}$	19
$CH_3 + OH \rightarrow CH_3OH$	1.15×10^{-08}	-4.4	$1.26\times10^{+03}$	19
$CH_3 + OH \rightarrow CH_2OH + H$	1.25×10^{-05}	-5.03	$8.26\times10^{+03}$	19
$CH_3 + H_2O_2 \rightarrow CH_4 + HO_2$	2.00×10^{-14}		$-3.00\times10^{+02}$	19
$CH_3 + C_2H_6 \rightarrow CH_4 + C_2H_5$	9.79×10^{-17}	5.64	$2.83\times10^{+03}$	19
$CH_3 + HCHO \rightarrow CH_4 + HCO$	1.87×10^{-15}	4.85	$1.75\times10^{+03}$	19
$CH_3 + CO \rightarrow CH_3CO$	1.98×10^{-10}	-8.35	$5.27\times10^{+03}$	19
$CH_3 + HCO \rightarrow CH_4 + CO$	2.00×10^{-10}			19
$CH_3 + HCO \rightarrow CH_3CHO$	3.00×10^{-11}			19

$CH_3 + N \rightarrow H + H + HCN$	3.32×10^{-13}			18
$CH_3 + N \rightarrow HCN + H_2$	8.59×10^{-12}			18
$CH_3 + NO_2 \rightarrow CH_3NO_2$	3.44×10^{-11}	-0.6		18
$CH_3 + NO_2 \rightarrow HCHO + HNO$	5.39×10^{-12}			18
$CH_3 + NO_2 \rightarrow CH_3ONO$	1.16×10^{-13}			18
$CH_3 + NO_2 \rightarrow CH_3O + NO$	2.50×10^{-11}			18
$C_2H_5 \rightarrow C_2H_4 + H$	$4.44\times10^{+12}$	1.19	$1.87\times10^{+04}$	19
$C_2H_5 + H_2 \rightarrow C_2H_6 + H$	4.22×10^{-15}	3.6	$4.25\times10^{+03}$	19
$C_2H_5 + O_2 \rightarrow C_2H_4 + HO_2$	1.40×10^{-12}		$1.95\times10^{+03}$	19
$C_2H_5 + O_2 \rightarrow C_2H_5O_2$	7.66×10^{-10}	-5.12	$1.49\times10^{+03}$	19
$C_2H_5 + O_2 \rightarrow CH_3CHO + OH$	1.14×10^{-13}	-0.12	$4.28\times10^{+03}$	19
$C_2H_5 + H \rightarrow C_2H_6$	1.66×10^{-10}	0		19
$C_2H_5 + H \rightarrow CH_3 + CH_3$	6.05×10^{-10}	-1.4	$6.59\times10^{+02}$	19
$C_2H_5 + H \rightarrow C_2H_4 + H_2$	3.00×10^{-12}			19
$C_2H_5 + O \rightarrow CH_3CHO + H$	1.33×10^{-10}			19
$C_2H_5 + O \rightarrow HCHO + CH_3$	2.67×10^{-11}			19
$C_2H_5 + OH \rightarrow C_2H_4 + H_2O$	4.00×10^{-11}			19
$C_2H_5 + OH \rightarrow CH_3 + H + HCHO$	4.00×10^{-11}			19
$C_2H_5 + HO_2 \rightarrow CH_3 + HCHO + OH$	4.00×10^{-11}			19
$C_2H_5 + HO_2 \rightarrow C_2H_6 + O_2$	5.00×10^{-13}			19
$C_2H_5 + HO_2 \rightarrow C_2H_4 + H_2O_2$	5.00×10^{-13}			19
$C_2H_5 + H_2O_2 \rightarrow C_2H_6 + HO_2$	1.45×10^{-14}		$4.90\times10^{+02}$	19
$C_2H_5 + HCHO \rightarrow C_2H_6 + HCO$	8.33×10^{-14}	2.81	$2.95\times10^{+03}$	19
$C_2H_5 + HCO \rightarrow C_2H_6 + CO$	2.00×10^{-10}			19
$C_2H_5 + HCO \rightarrow C_2H_5CHO$	3.00×10^{-11}			19
$C_2H_5 + CH_3 \rightarrow C_3H_8$	4.70×10^{-11}	-0.5		19
$C_2H_5 + CH_3 \rightarrow CH_4 + C_2H_4$	1.88×10^{-12}	-0.5		19

$C_2H_5 + C_2H_5 \rightarrow C_2H_4 + C_2H_6$	2.30×10^{-12}			19
$C_2H_4 + H \rightarrow C_2H_5$	6.87×10^{-12}	1.49	$4.99\times10^{+02}$	19
$C_2H_4 + H \rightarrow C_2H_3 + H_2$	4.07×10^{-12}	2.53	$6.16\times10^{+03}$	19
$C_2H_4 + O \rightarrow CH_3 + HCO$	1.52×10^{-12}	1.55	$2.15\times10^{+02}$	19
$C_2H_4 + O \rightarrow CH_2CHO + H$	6.24×10^{-13}			19
$C_2H_4 + O \rightarrow CH_2CO + H_2$	3.81×10^{-14}			19
$C_2H_4 + O \rightarrow C_2H_3 + OH$	1.33×10^{-12}	1.91	$1.88\times10^{+03}$	19
$C_2H_4 + OH \rightarrow C_2H_3 + H_2O$	1.69×10^{-13}	2.75	$2.10\times10^{+03}$	19
$C_2H_4 + OH \rightarrow C_2H_4OH$	9.00×10^{-12}			19
$C_2H_4 + HO_2 \rightarrow CH_3CHO + OH$	1.00×10^{-14}		$4.00\times10^{+03}$	19
$C_2H_3 + H_2 \rightarrow C_2H_4 + H$	1.64×10^{-13}	2.63	$4.30\times10^{+03}$	19
$C_2H_3 + O_2 \rightarrow C_2H_2 + HO_2$	2.00×10^{-13}			19
$C_2H_3 + H \rightarrow C_2H_2 + H_2$	1.60×10^{-10}			19
$C_2H_3 + O \rightarrow CH_2CO + H$	1.60×10^{-10}			19
$C_2H_3 + OH \rightarrow H_2O + C_2H_2$	5.00×10^{-11}			19
$C_2H_3 + OH \rightarrow CH_3CHO$	5.00×10^{-11}			19
$C_2H_3 + HO_2 \rightarrow OH + CH_3 + CO$	5.00×10^{-11}			19
$C_2H_3 + H_2O_2 \rightarrow C_2H_4 + HO_2$	2.00×10^{-14}		$3.00\times10^{+02}$	19
$C_2H_3 + CH4 \rightarrow C_2H_4 + CH_3$	2.18×10^{-14}	4.02	$2.75\times10^{+03}$	19
$C_2H_3 + C_2H_6 \rightarrow C_2H_4 + C_2H_5$	1.50×10^{-13}	3.3	$5.29\times10^{+03}$	19
$C_2H_3 + HCHO \rightarrow C_2H_4 + HCO$	8.22×10^{-14}	2.81	$2.95\times10^{+03}$	19
$C_2H_3 + CO \rightarrow C_2H_3CO$	2.50×10^{-13}		$2.42\times10^{+03}$	19
$C_2H_3 + HCO \rightarrow C_2H_4 + CO$	1.50×10^{-10}			19
$C_2H_3 + HCO \rightarrow C_2H_3CHO$	3.00×10^{-11}			19
$C_2H_3 + CH_3 \rightarrow C_2H_2 + CH_4$	3.40×10^{-11}			19
$C_2H_3 + CH_3 \rightarrow C_3H_6$	1.20×10^{-10}			19
$C_2H_3 + C_2H_5 \rightarrow C_2H4 + C_2H_4$	8.00×10^{-13}			19

$C_2H_3 + C_2H_5 \rightarrow C_2H_2 + C_2H_6$	8.00×10^{-13}			19
$C_2H_3 + C_2H_3 \rightarrow C_2H_4 + C_2H_2$	1.60×10^{-12}			19
$C_2H_2 + O \rightarrow CH_2 + CO$	5.15×10^{-12}	1.17	$1.07\times10^{+03}$	19
$C_2H_2 + O \rightarrow C_2HO + H$	1.50×10^{-11}		$2.29\times10^{+03}$	19
$C_2H_2 + OH \rightarrow C_2H + H_2O$	1.04×10^{-13}	2.68	$6.06\times10^{+03}$	19
$C_2H_2 + HO_2 \rightarrow CH_2CO + OH$	1.00×10^{-14}		$4.00\times10^{+03}$	19
$C_2H_2 + CH_3 \rightarrow C_3H_5$	1.00×10^{-12}		$3.88\times10^{+03}$	19
$C_2H_2 + OH \rightarrow C_2H_2OH$	8.50×10^{-12}		$7.05\times10^{+02}$	19
$C_2H + H_2 \rightarrow C_2H_2 + H$	1.90×10^{-11}		$1.45\times10^{+03}$	19
$C_2H + O_2 \rightarrow CO + HCO$	4.00×10^{-12}			19
$C_2H + O_2 \rightarrow C_2HO + O$	1.00×10^{-12}			19
$C_2H + H \rightarrow C_2H_2$	3.00×10^{-10}			19
$C_2H + O \rightarrow CH + CO$	3.00×10^{-11}			19
$C_2H + OH \rightarrow C_2H_2 + O$	3.00×10^{-11}			19
$C_2H + OH \rightarrow CH_2 + CO$	3.00×10^{-11}			19
$C_2H + HO_2 \rightarrow C_2H_2 + O_2$	3.00×10^{-11}			19
$C_2H + HO_2 \rightarrow C_2HO + OH$	3.00×10^{-11}			19
$C_2H + CH_4 \rightarrow C_2H_2 + CH_3$	3.00×10^{-12}		$2.50\times10^{+02}$	19
$C_2H + C_2H_6 \rightarrow C_2H_2 + C_2H_5$	6.00×10^{-12}			19
$C_2H + CO \rightarrow C_2HCO$	2.50×10^{-13}		$2.42\times10^{+03}$	19
$C_2H + HCO \rightarrow C_2H_2 + CO$	1.00×10^{-10}			19
$C_2H + CH_3 \rightarrow C_3H_3 + H$	4.00×10^{-11}			19
$C_2H + C_2H_5 \rightarrow C_2H_2 + C_2H_4$	3.00×10^{-12}			19
$C_2H + C_2H_5 \rightarrow C_3H_3 + CH_3$	3.00×10^{-11}			19
$C_2H + C_2H_3 \rightarrow C_2H_2 + C_2H_2$	1.60×10^{-12}			19
$C_2H + C_2H \rightarrow C_2H_2 + C_2$	3.00×10^{-12}			19
$CH_3CO + M \rightarrow CH_3 + CO + M$	6.44×10^{-03}	-8.62	$1.13\times10^{+04}$	19

$CH_3CO + O_2 \rightarrow CH_3COO_2$	3.00×10^{-12}			19
$CH_3CO + H \rightarrow CH_3 + HCO$	1.60×10^{-10}			19
$CH_3CO + O \rightarrow CH_3 + CO_2$	1.60×10^{-11}			19
$CH_3CO + OH \rightarrow CH_2CO + H_2O$	2.00×10^{-11}			19
$CH_3CO + OH \rightarrow CH_3 + CO + OH$	5.00×10^{-11}			19
$CH_3CO + HO_2 \rightarrow CH_3 + CO_2 + OH$	5.00×10^{-11}			19
$CH_3CO + H_2O_2 \rightarrow CH_3CHO + HO_2$	3.00×10^{-13}		$4.14\times10^{+03}$	19
$CH_3CO + HCO \rightarrow CH_3CHO + CO$	1.50×10^{-11}			19
$CH_3CO + HCO \rightarrow CH_3COCHO$	3.00×10^{-11}			19
$CH_3CO + CH_3 \rightarrow CH_3COCH_3$	6.70×10^{-09}	-0.8		19
$CH_3CO + C_2H_5 \rightarrow C_2H_5COCH_3$	5.19×10^{-10}			19
$CH_3CO + C_2H_3 \rightarrow CH_3 + CH_2CHCO$	3.00×10^{-11}			19
$CH_3CO + C_2H \rightarrow C_2HCO + CH_3$	3.00×10^{-11}			19
$CH_3O_2 + H \rightarrow CH_3O + OH$	1.60×10^{-10}			19
$CH_3O_2 + O \rightarrow CH_3O + O_2$	6.00×10^{-11}			19
$CH_3O_2 + OH \rightarrow CH_3OH + O_2$	1.00×10^{-10}			19
$CH_3O_2 + HO_2 \rightarrow CH_3OOH + OH$	7.70×10^{-14}		$-1.30\times10^{+03}$	19
$CH_3O_2 + H_2O_2 \rightarrow CH_3OOH + HO_2$	4.00×10^{-12}		$5.00\times10^{+03}$	19
$CH_3O_2 + HCO \rightarrow CH_3O + H + CO_2$	5.00×10^{-11}			19
$CH_3O_2 + CH_3 \rightarrow CH_3O + CH_3O$	4.00×10^{-11}			19
$CH_3O_2 + C_2H_5 \rightarrow CH_3O + C_2H_5O$	4.00×10^{-11}			19
$CH_3O_2 + C_2H_3 \rightarrow CH_3O + C_2H_3O$	4.00×10^{-11}			19
$CH_3O_2 + C_2H \rightarrow CH_3O + C_2HO$	4.00×10^{-11}			19
$CH_3O_2 + CH_3CO \rightarrow CH_3 + CO_2 + CH_3O$	4.00×10^{-11}			19
$CH_3O_2 + CH_3O_2 \rightarrow CH_3O + CH_3O + O_2$	1.30×10^{-13}			19
$CH_3O_2 + CH_3O_2 \rightarrow CH_3OH + HCHO + O_2$	2.10×10^{-13}			19
$CH_3O_2 + NO \rightarrow CH_3O + NO_2$	4.20×10^{-12}		$-1.80\times10^{+02}$	19

$CH_3O + O_2 \rightarrow HCHO + HO_2$	1.10×10^{-13}		$1.31\times10^{+03}$	19
$CH_3O + H \rightarrow HCHO + H_2$	3.30×10^{-11}			19
$CH_3O + O \rightarrow HCHO + OH$	1.00×10^{-11}			19
$CH_3O + OH \rightarrow HCHO + OH$	3.00×10^{-11}			19
$CH_3O + HO_2 \rightarrow HCHO + H_2O_2$	5.00×10^{-13}			19
$CH_3O + CH_4 \rightarrow CH_3OH + CH_3$	2.60×10^{-13}		$4.45\times10^{+03}$	19
$CH_3O + C_2H_6 \rightarrow CH_3OH + C_2H_5$	4.00×10^{-13}		$3.57\times10^{+03}$	19
$CH_3O + HCHO \rightarrow CH_3OH + HCO$	1.70×10^{-13}		$1.50\times10^{+03}$	19
$CH_3O + CO \rightarrow CH_3 + CO_2$	2.60×10^{-11}		$5.94\times10^{+03}$	19
$CH_3O + HCO \rightarrow CH_3OH + CO$	1.50×10^{-10}			19
$CH_3O + CH_3 \rightarrow HCHO + CH_4$	4.00×10^{-11}			19
$CH_3O + CH_3 \rightarrow CH_3OCH_3$	2.00×10^{-11}			19
$CH_3O + C_2H_5 \rightarrow HCHO + C_2H_6$	4.00×10^{-11}			19
$CH_3O + C_2H_3 \rightarrow HCHO + C_2H_4$	4.00×10^{-11}			19
$CH_3O + C_2H \rightarrow HCHO + C_2H_2$	4.00×10^{-11}			19
$CH_3O + CH_3CO \rightarrow CH_3OH + CH_2CO$	1.00×10^{-11}			19
$CH_3O + CH_3CO \rightarrow HCHO + CH_3CHO$	1.00×10^{-11}			19
$CH_3O + CH_3O_2 \rightarrow HCHO + CH_3OOH$	5.00×10^{-13}			19
$CH_3O + CH_3O \rightarrow CH_3OH + HCHO$	1.00×10^{-10}			19
$CH_3O + NO_2 \rightarrow CH_3ONO_2$	1.50×10^{-11}			18
$CH_3O + NO_2 \rightarrow HCHO + HNO_2$	3.00×10^{-13}			18
$CH_3O + NO \rightarrow CH_3ONO$	2.00×10^{-11}			18
$CH_3O + NO \rightarrow HCHO + HNO$	4.00×10^{-12}	-0.7		18
$CH_3OH + O \rightarrow CH_2OH + OH$	4.63×10^{-14}	3.77	$3.40\times10^{+02}$	20
$CH_3OH + O \rightarrow CH_3O + OH$	7.08×10^{-13}	1.54	$1.00\times10^{+03}$	20
$CH_3OH + OH \rightarrow H_2O + CH_2OH$	8.79×10^{-13}			20
$CH_3OH + OH \rightarrow H_2O + CH_3O$	1.66×10^{-11}		$8.54\times10^{+02}$	20

$CH_3OH + H \rightarrow CH_2OH + H_2$	1.39×10^{-11}			20
$CH_3OH + H \rightarrow CH_3O + H_2$	6.64×10^{-11}		$3.07\times10^{+03}$	20
$C_2H_5 + NO \rightarrow C_2H_5NO$	6.49×10^{-11}	-3.37	$1.74\times10^{+03}$	18
$C_3H_6 + O \rightarrow$ Methyl Oxirane	9.05×10^{-12}		$6.10\times10^{+02}$	33
$C_3H_6 + O \rightarrow C_2H_5CHO$	9.05×10^{-12}		$6.10\times10^{+02}$	33
$C_3H_6 + O \rightarrow CH_2CHO + CH_3$	6.03×10^{-12}		$6.10\times10^{+02}$	33
$C_3H_6 + O \rightarrow C_2H_5 + HCO$	6.03×10^{-12}		$6.10\times10^{+02}$	33
$C_3H_6 + OH \rightarrow CH_3CHCH_2OH$	6.56×10^{-11}	-1.48	$3.61\times10^{+02}$	33
$C_3H_6 + OH \rightarrow CH_3CHOHCH_2$	3.53×10^{-11}	-1.48	$3.61\times10^{+02}$	33
$C_3H_6 + H \rightarrow CH_3 + C_2H_4$	1.20×10^{-11}		$6.55\times10^{+02}$	34
$C_3H_6 + H \rightarrow i\text{-}C_3H_7$	1.00×10^{-11}	0.25	$5.93\times10^{+02}$	34
$CH_3CH(OH)CH_2 + O_2 \rightarrow CH_3CH(OH)CH_2OO$	3.90×10^{-12}			33
$CH_3CHCH_2OH + O_2 \rightarrow CH_3CH(OO)CH_2OH$	1.16×10^{-11}			33
$CH_3CH(OH)CH_2OO + NO \rightarrow NO_2 + CH_3CH(OH)CH_2O$	1.00×10^{-14}			33
$CH_3CH(OO)CH_2OH + NO \rightarrow NO_2 + CH_3CH(O)CH_2OH$	1.00×10^{-14}			33
$CH_3CH(OH)CH_2O \rightarrow HCHO + CH_3CHOH$	$7.94\times10^{+13}$		$1.05\times10^{+04}$	33
$CH_3CH(O)CH_2OH + M \rightarrow CH_3CHO + CH_2OH + M$	1.00×10^{-11}			33
$CH_3CHOH + O_2 \rightarrow CH_3CHO + HO_2$	1.00×10^{-11}			33
$CH_2OH + O_2 \rightarrow HCHO + HO_2$	1.06×10^{-10}	-1.58	$8.01\times10^{+02}$	33
$CH_2CHO + NO \rightarrow ONCH_2CHO$	2.51×10^{-11}			37
$CH_2CHO + O_2 \rightarrow CHOCHO + OH$	2.20×10^{-13}			37
$CH_2CHO + O_2 \rightarrow HCHO + CO + OH$	3.00×10^{-14}			37

$CH_2CHCHO + OH \rightarrow H_2O + CH_2CHCO$	2.66×10^{-11}			37
Methyl Oxirane + OH $\rightarrow$ H_2O + Products	4.95×10^{-13}			18
$C_2H_6 + N \rightarrow CH_3NCH_3$	4.00×10^{-16}			18
$C_2H_5O_2 + NO \rightarrow C_2H_5O + NO_2$	8.90×10^{-12}			18
$C_2H_5O_2 + NO \rightarrow C_2H_5ONO_2$	1.30×10^{-13}			18
$C_2H_5O_2 + NO_2 \rightarrow C_2H_5OONO_2$	2.59×10^{-10}	-3.74	$1.03\times10^{+03}$	18
$C_2H_5O_2 \rightarrow C_2H_4 + HO_2$	$2.69\times10^{+36}$			18
$C_2H_5O + NO \rightarrow C_2H_5ONO$	2.63×10^{-11}			18
$C_2H_5O + NO \rightarrow CH_3CHO + HNO$	1.30×10^{-11}			18
$C_2H_5O + NO_2 \rightarrow C_2H_5ONO_2$	2.80×10^{-11}			18
$C_2H_5O + NO_2 \rightarrow CH_3CHO + HNO_2$	6.61×10^{-12}			18
$C_2H4 + N \rightarrow HCN + CH_3$	2.46×10^{-12}	-3.28	$1.36\times10^{+03}$	18
$CH4 + N \rightarrow HCN + H_2 + H$	2.50×10^{-14}			18
$CH_3CHO + N \rightarrow HCN + H_2 + HCO$	1.99×10^{-14}			18
$CH_3CHO + NO_3 \rightarrow HNO_3 + CH_3CO$	2.73×10^{-15}			18
$CH_3COO_2 + NO \rightarrow CH_3 + CO_2 + NO_2$	2.00×10^{-11}			18
$CH_3COO_2 + NO \rightarrow CH_3COO + NO_2$	1.40×10^{-11}			18
$CH_3COO_2 + NO_2 \rightarrow CH_3CO_3NO_2$	1.75×10^{-12}		$-3.93\times10^{+02}$	18
$CH_3CO + NO \rightarrow CH_3CONO$	3.32×10^{-13}			18
$CH_3CO + NO_2 \rightarrow CH_3 + CO_2 + NO$	1.66×10^{-12}			18
$CH_3CO + NO_2 \rightarrow CH_3COO + NO$	2.50×10^{-11}			18
$CH_2OH + NO \rightarrow CH_2OHNO$	2.50×10^{-11}			18
$CH_2OH + NO_2 \rightarrow HOCH_2NO_2$	2.30×10^{-11}			18
$CH_2OH + O \rightarrow HCHO + OH$	1.50×10^{-10}			18
$CH_2OH + CH_3 \rightarrow CH_4 + HCHO$	4.00×10^{-12}			20
$CH_2OH + CH_3 \rightarrow C_2H_5OH$	2.00×10^{-11}			20
$CH_2CHO + NO_2 \rightarrow CH_2CO + HNO_2$	1.48×10^{-11}		$-8.00\times10^{+01}$	18

$CH_2 + NO \rightarrow CONH_2$	5.76×10^{-12}		$-1.90\times10^{+02}$	18
$CH_2CO + OH \rightarrow CH_2OH + CO$	1.08×10^{-11}			18
$CH_2CO + OH \rightarrow HCO + HCHO$	4.65×10^{-11}			18
$CH_2CO + H \rightarrow CH_3 + CO$	1.88×10^{-11}		$1.73\times10^{+03}$	18
$CH + NO \rightarrow CO + NH$	2.50×10^{-10}			18
$HCO + NO \rightarrow CO + HNO$	1.20×10^{-11}			18
$HCO + NO_2 \rightarrow H + CO_2 + NO$	1.95×10^{-10}	-0.75	$9.70\times10^{+02}$	18
$HCO + NO_2 \rightarrow HCOO + NO$	2.71×10^{-11}			18
$HCO + NO_2 \rightarrow CO + HNO_2$	8.73×10^{-11}		$3.19\times10^{+02}$	18
$CH_3ONO \rightarrow HCHO + HNO$	$3.98\times10^{+13}$		$1.94\times10^{+04}$	18
$HO_2 + NO_2 \rightarrow HNO_2 + O_2$	1.20×10^{-13}			18
$O + HNO_2 \rightarrow NO_2 + OH$	2.00×10^{-11}		$3.00\times10^{+03}$	18

[a] Rate coefficients have units of cm^3s^{-1}. Electron impact reactions without specific electron temperature dependencies are given for typical values of E/N.

[b] Estimated.

[c] Rate coefficients have units of s^{-1} for 1 body reaction, cm^3s^{-1} for 2 body reactions, and cm^6s^{-1} for 3 body reactions. Activation energies have equivalent units of K. T is the gas temperature. Two body reactions which do not have specific temperature dependencies were scaled by $(T/300)^{1/2}$ to account for changes in the reaction rate due to thermal speeds. Three body reactions were similarly scaled by $(T/300)^{-3/2}$.

[d] Estimated based on Lennard-Jones parameters. Value shown for T = 300K.

B.1 References

1. Y. Itikawa, M. Hayashi, A. Ichimura, K. Onda, K. Sakimoto, K. Takayanagi, M. Nakamura, H. Nishimura, and T. Takayanagi, “Cross Sections for Collisions of Electrons and Photons with Nitrogen Molecules” J. Phys. Chem. Ref. Data Reprint Number 299, **15** (3), 985 (1986).
2. A. V. Phelps, “Tabulations of Collision Cross Sections and Calculated Transport and Reaction Coefficients for Electron Collisions with O_2”, JILA Information Center Report Number 28, University of Colorado, Boulder, CO (1985).
3. M. Hayashi, “Electron Collision Cross Sections for Molecules Determined from Beam and Swarm Data” Nagoya Institute of Technology, Gokiso-Cho, Showa-Ku, Nagoya, 466, Japan. Printed in “Swarm Studies and Inelastic Electron-Molecular Collisions” Eds. L. C. Pitchford, B. V. McKoy, A. Chutjian, and S. Tratmar. Proceedings of the Meeting of the 4th International Swarm Seminar and the Inelastic Electron-Molecular Collision Symposium, July 19-23, 1985. Tahoe City, CA. Springer-Verlag, N.Y. 1987.
4. J. C. Person and D. O. Ham, Radiat. Phys. Chem., **31**, 1 (1988).
5. B. R. Rowe, F. Vallée, J. L. Queffelec, J. C. Gomet, and M. Morlais, J. Phys. Chem. **88**, 845 (1988).
6. J. J. Lowke, A. V. Phelps, and B. W. Irwin, J. Appl. Phys. **44**, 4664 (1973).
7. W. Tsang, J. Phys. Chem. Ref. Data **17**(2), 887 (1988).
8. K. Tachibana, Phys. Rev. A **34**, 1007 (1986).
9. D. Rapp and P. Englander-Golden, J. Chem. Phys. **43**, 1464 (1965).
10. M. Hayashi, “Recommended Values of Transport Cross Sections for Elastic Collision and Total Collision Cross Section for Electrons in Atomic and Molecular Gases”, Nagoya Institute of Technology Report No. IPPJ-AM-19, 1991.

11. R. Atkinson, D. L. Baulch, R. A. Cox, R. F. Hampson, Jr., J. A. Kerr, and J. Troe, “Evaluated Kinetic and Photochemical Data for Atmospheric Chemistry: Supplement III”, J. Phys. Chem, Ref. Data, 18, 881 (1989).
12. C. J. Howard, J. Chem. Phys. **71**, 2352 (1979).
13. W. B. DeMore, D. M. Golden, R. F. Hampson, C. J. Howard, M. J. Kurylo, M. J. Molina, A. R. Ravishankara, and S. P. Sander, “Chemical Kinetics and Photchemical Data for Use in Stratospheric Modeling: Evaluation Number 8”, JPL Publication 87-41, Jet Propulsion Laboratory, California Institute of Technology, Pasadena, California (1987).
14. R. Atkinson, D. L. Baulch, R. A. Cox, R. F. Hampson, Jr., J. A. Kerr, and J. Troe, “Evaluated Kinetic and Photochemical Data for Atmospheric Chemistry: Supplement IV”, J. Phys. Chem, Ref. Data, 21, 1125 (1992).
15. W. Tsang and R. F. Hampson, J. Phys. Chem. Ref. Data **15**, 1087 (1986).
16. I. M. Campbell and C. N. Gray, Chem. Phys. Lett. **18**, 607 (1973).
17. P. Borrell, C. J. Cobos, and K. Luther, J. Phys. Chem. **92**, 4377 (1988).
18. W.G. Mallard, F. Westley, J.T. Herron, and R.F. Hampson, “NIST Standard Reference Data (NIST Chemical Kinetics Database Version 6.0) (Giathesburg, MD:NIST) (1994).
19. W. Tsang and R. F. Hampson, J. Phys. Chem. Ref. Data **15**(3), 1087 (1986).
20. W. Tsang, J. Phys. Chem. Ref. Data **16**(3), 471 (1987).
21. M. R. Soto, M. Page, and M. L. McKee, Chem. Phys. **153**, 415 (1991).
22. J. Hjorth, J. Notholt, and G. Restelli, Int. J. Chem. Kin. **24**, 51 (1992).I
23. N. Fujii, H. Miyama, M. Koshi, T. Asuba, Symp. (Int.) Combust., [Proc.] **18**, 873 (1981).
24. S. Mukkavilli, C. K. Lee, K.Varghese, and L. L. Tavlarides, IEEE Trans. Plasma Sci. **16**, 652 (1988).
25. R. Svensson and E. Ljungström, Int. J. Chem. Kin. **20**, 857 (1988).

26. H. Mätzing, Radiat. Phys. Chem. **33**, 81 (1989).

27. W. Hack, P. Rouveirolles, and H. G. Wagner, J. Phys. Chem. **90**, 2505 (1986).

28. R. K. Bera and R. J. Hanrahan, J. Appl. Phys. **62**, 2523 (1987).

29. A. Mellouki, G. Le Bras, and G. Poulet, J. Phys. Chem. **92**, 2229 (1988).

30. F. Westley, J. T. Herron, R. J. Cvetanovic, R. F. Hampson, and W. G. Mallard, NIST Chemical Kinetics Database, NIST Standard Reference Database 17. National Institute of Standards and Technology, Standard Reference Data Program, Gaithersburg, MD 20899.

31. W. G. Mallard, F. Westley, J. T. Herron, and R. F. Hampson, NIST Chemical Kinetics Database - Version 6.0, NIST Standard Reference Database 17. National Institute of Standards and Technology, NIST Standard Reference Data, Gaithersburg, MD (1994).

32. R. E. Olson, J. R. Peterson, and J. Moseley, J. Chem. Phys. **53**, 3391 (1970).

33. R. Atkinson, “Gas-Phase Tropospheric Chemistry of Volatile Organic Compounds: 1. Alkanes and Alkenes”, J. Phys. Chem. Ref. Data, **26**(2), 215 (1997).

34. J. B. A. Mitchell, Phys. Rpts. **186**, 215 (1990).

35. C. Deutch, J. Appl. Phys. **44**, 1142 (1973).

36. L. G. Piper, J. Chem. Phys. **87**, 1625 (1987).

37. R. Atkinson, “Gas-Phase Tropospheric Chemistry of Organic Compounds”, J. Phys. Chem. Ref. Data. Monograph, **2**, 1 (1994).